The Pennsylvania State University

The Graduate School

Department of Chemical Engineering

FROM BACTERIAL ADHESION TO BIOFILM FORMATION: IMPACT OF HUMIC ACID AND QUORUM SENSING

A Thesis in

Chemical Engineering

by

Mary Elizabeth Parent

Submitted in Partial Fulfillment
of the Requirements
for the Degree of

Doctor of Philosophy

May 2007

The thesis of Mary Elizabeth Parent was reviewed and approved* by the following:

Darrell Velegol
Associate Professor of Chemical Engineering
Thesis Advisor
Chair of Committee

Costas Maranas
Donald B. Broughton Professor of Chemical Engineering

Michael Pishko
Professor of Chemical Engineering and Materials Science and Engineering

John M. Regan
Assistant Professor of Environmental Engineering

Andrew L. Zydney
Walter L. Robb Chair and Professor of Chemical Engineering
Head of the Department of Chemical Engineering

*Signatures are on file in the Graduate School

ABSTRACT

Biofilms are surface-associated bacterial populations prevalent in both engineered and natural settings. The influence of biofilms is far reaching; for example, they cause fouling on industrial equipment, infection of medical implants, and can be utilized in bioremediation. A better understanding of biofilm formation will generate more effective biofilm control strategies, which is the hope for the future of this work. Initial bacterial adhesion (the first stage of biofilm development) was studied in the presence of humic acid, a common soil component. It was determined that changes in the concentration of humic acid on silica do not affect *Escherichia coli* adhesion orientation, occurrence, nor force. Based on this evidence and other reports that showed bacterial adhesion is not strongly affected by external surface chemistries like humic acid, it was concluded that studying the events *following* bacterial adhesion could garner more insight into biofilm formation. For many species, such as *Pseudomonas aeruginosa,* quorum sensing is necessary for proper biofilm formation; thus the effect of the diffusion of signaling molecules from adhered cells on biofilm development was examined. Set-backs in creating engineered biofilms with tightly controlled size parameters and in measuring their adhesion forces prompted the investigation of the effect of signal diffusion on quorum sensing alone.

Quorum sensing is almost always regarded as a population density effect in three-dimensional bulk samples of bacteria. Two-dimensional samples of *Vibrio fischeri* cells adhered onto glass surfaces were created to examine the effect of *local* population densities on quorum sensing. This was done by measuring the luminescent response.

The 2-D bacterial populations allowed for the measurement of both time and distance effects on quorum sensing, which were previously very challenging to access in typical three-dimensional bulk samples. Thus, quorum sensing was considered in terms of signal diffusion. A diffusion model of quorum sensing signals guided the experiments and showed that for a given cell spacing (density) and diffusion time there exists a "true quorum"– a number of cells necessary for quorum sensing. The experiments showed that quorum sensing can occur locally in 2-D surface samples and is a function of cell population density as well as signal diffusion time.

With proof that quorum sensing occurs locally, engineered biofilm experiments were revisited. *P. aeruginosa* cells were localized on surfaces in either infinite or isolated arrays. Adhesion forces of infinite biofilms showed that populations contained 50-60% "sticky" cells that attached with greater than 70 pN (the maximum measurable force) regardless of adhesion time. However, time effects were still observed in that samples adhered for longer times contained more cells that were more strongly attached. The percentage of cells attached with greater than 10 pN in samples adhered for 150, 60, and 5 minutes were 86%, 81%, and 63%, respectively. Adhesion force measurements of small isolated biofilms served as preliminary tests of the "true quorum" concept. Diffusion in quorum sensing and that there exists a "true quorum" are important to consider for biofilm formation. Even small numbers of localized surface cells can act as "biofilm seeds".

TABLE OF CONTENTS

LIST OF FIGURES

LIST OF TABLES

ACKNOWLEDGEMENTS

The first to acknowledge is my wonderful advisor Darrell Velegol. Looking back on my career here at Penn State I realize how much I have learned and grown professionally, and I owe much of it to Darrell. He is one of the most brilliant and caring people I have met and I know the lab group will continue to succeed with his guidance.

The lab group, past and present, has been a huge support in my life. I thank my "big brothers and sister" Jason Feick, Aron Parekh, Gretchen Holtzer, Mike Salerno, and Joe Jones for showing me the ropes of grad school and I thank my "little sisters and brother" Allison Yake, Charles Snyder, Huda Jerri, and Nicole Blackman for their daily help. The only thing I ask of them is that summer rain rubber ducky races continue. Charles Snyder requires a special acknowledgement for his work on the diffusion modeling for his comprehensive project. I had the opportunity to work with the best undergrad ever, Nate Kopp, and I know he has a bright future ahead of him.

Don Lucas' skill as the department's engineering aid is much appreciated and was remembered each time one of his microscope stage plates was used. He has designed and fabricated two stage plates for me in a most amazingly timely fashion, and the lab still frequently uses them. Glassblower Doug Smith was instrumental in the redesign of the electrophoresis cell, which is also still in use by others in the lab. John McIntosh is acknowledged, for both his help in the Nanofabrication facility clean room as well as for the interesting conversations that ensued while bunny-suited.

I thank Patrick Cirino and Lane Weaver for their help in starting the fluorescent quorum sensing system and the subsequent time they spent sharing their expertise in

molecular biology over numerous conversations. I also thank the rest of my friends on the third floor for putting up with my pipet tip-stealing, plate reader-hogging, and freezer space-taking ways. A thank you goes to Penn State's Biochemistry and Molecular Biology Department in general, but specifically to Sarah Ades for her initial input on my project, Ken Keiler for the opportunity to present my work in their department seminar, and Ming Tien for his lab space.

To all my friends that I have had the pleasure of getting to know during my time here– thank you. Alisar Zhar, Kristin O'Neil, and Kelly McLaughlin were more than just great roommates and I know they will continue to be good friends of mine even as we move on to the next stages of our lives. Derek Triplett gets a special acknowledgement; grad school would not have been the same without his entertaining daily visits into the office. I thank Martin for his years of support. I thank Josh for serving as my cook, chauffer, editor, and everything over these last tumultuous months. Finally, I thank my loving family for their undying support.

The research conducted in this thesis was funded by the National Science Foundation through NSF CRAEMS grant CH3-0089156.

Material from the previously published work, "*E. coli* adhesion to silica in the presence of humic acid" (Parent and Velegol, 2004, Colloids and Surfaces B: Biointerfaces 39:45-51), appears in this thesis with permission from Elsevier. A copy of the permission letter is on the next page.

Dear Mary Parent,

We hereby grant you permission to reprint the aforementioned material at no charge in your thesis subject to the following conditions:

1. If any part of the material to be used (for example, figures) has appeared in our publication with credit or acknowledgement to another source, permission must also be sought from that source. If such permission is not obtained then that material may not be included in your publication/copies.

2. Suitable acknowledgment to the source must be made, either as a footnote or in a reference list at the end of your publication, as follows: "Reprinted from Publication title, Vol number, Author(s), Title of article, Pages No., Copyright (Year), with permission from Elsevier".

3. Your thesis may be submitted to your institution in either print or electronic form.

4. Reproduction of this material is confined to the purpose for which permission is hereby given.

5. This permission is granted for non-exclusive world English rights only. For other languages please reapply separately for each one required.

6. This includes permission for UMI to supply single copies, on demand, of the complete thesis. Should your thesis be published commercially, please reapply for permission.

Yours sincerely,

Manuela Beis

Rights Assistant, Elsevier

Chapter 1

Motivation & Research Goals

1.1 Motivation

The omnipresent bacterial biofilm is a naturally occurring sessile population of cells that forms at interfaces, for example, in oceans (1), soil (2), industrial equipment (3), and the human body (4). Biofilms are a normal, if not favorable, state of life for bacteria and are of benefit to the cells by reducing antibiotic susceptibility (4) and aiding in population dispersal (5). These cozy prokaryotic conditions make for biofilms' ubiquity and persistence, which causes hardships for humans.

1.1.1 Biofilm effects

No industry is immune to biofouling and its effects are broadly felt: for example, in oil recovery, water treatment, paper and consumer products manufacturing, and food processing. Biofilms increase resistance in membranes (6) and heat exchangers (7, 8), and friction in pipelines (Figure **1-1** A) (4, 9) and on ship hulls (10). Costs incurred due to biofilms in industrial settings are not only from increased energy consumption, but also from product loss and contamination (10), and system parts cleaning and replacement (8). For example, 10-20% of process interruption in paper plants is for biofilm-related maintenance (8).

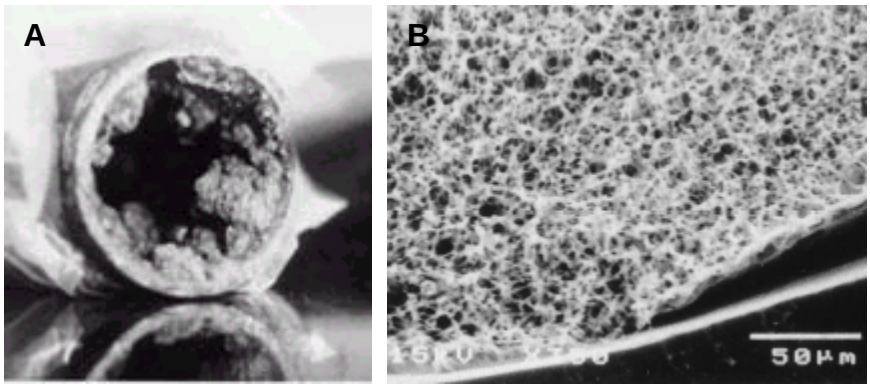

Figure 1-1: Growth in a carbon steel pipe (11) (A on the left) and a silicone catheter (12) (B on the right) due to bacterial biofilms.

Biofilms are also involved in human infection. Cystic fibrosis-related pneumonia is caused by *Pseudomonas aeruginosa* and *Burkholderia cepacia* forming biofilms on lung surfaces (4). The skin bacterium *Staphylococcus epidermidis* adheres to implants such as catheters (Figure **1-1** B) and prostheses and acts as a barrier to extended use of the biomaterial (4). Biofilms cause mechanical blockages, material deterioration, impeded tissue integration, and chronic infection (9). Once a biofilm forms on a surface it becomes difficult to remove because biofilm cells are less susceptible to antimicrobial treatments (4), resulting in device removal, amputation, or death (13). The probability of infection in urinary catheters increases 10% each day of implantation (14). Chamis et al. determined there is a 45% infection incidence in cardiac devices, including pacemakers and defibrillators (15).

Despite the detrimental effects of biofilms, they have also been advantageously used in food, sensor, and environmental applications. The dairy industry utilizes biofilms immobilized in gel beads, traditionally in Kefir production, and more recently in novel processes for yogurt and cheese production (16). In biosensor applications, biofilm cells

signal the presence of analytes by exhibiting a measurable biological change, such as metabolic or enzymatic activity (7, 17). A biosensor containing denitrifying bacteria to detect nitrate (18) has been used to study nitrifying biofilms (19)– important in wastewater treatment (20).

Biofilms are a vital tool in water treatment and act to remove organic carbon and other nutrients like nitrogen and phosphorous compounds (20) in both *ex situ* and *in situ* processes (21). Bioremediation is the degradation of pollutants through biofilms' cells' metabolic activities. Bioremediation aims to produce industrial wastewater streams that meet contaminant regulations, and groundwater and aquifers that provide potable water (22). As of 2003, 1.1 billion people in the world do not have adequate water supplies (23), including 75% of Ethiopia's population (24). The problem worsens as population growth increases pollution and water demands.

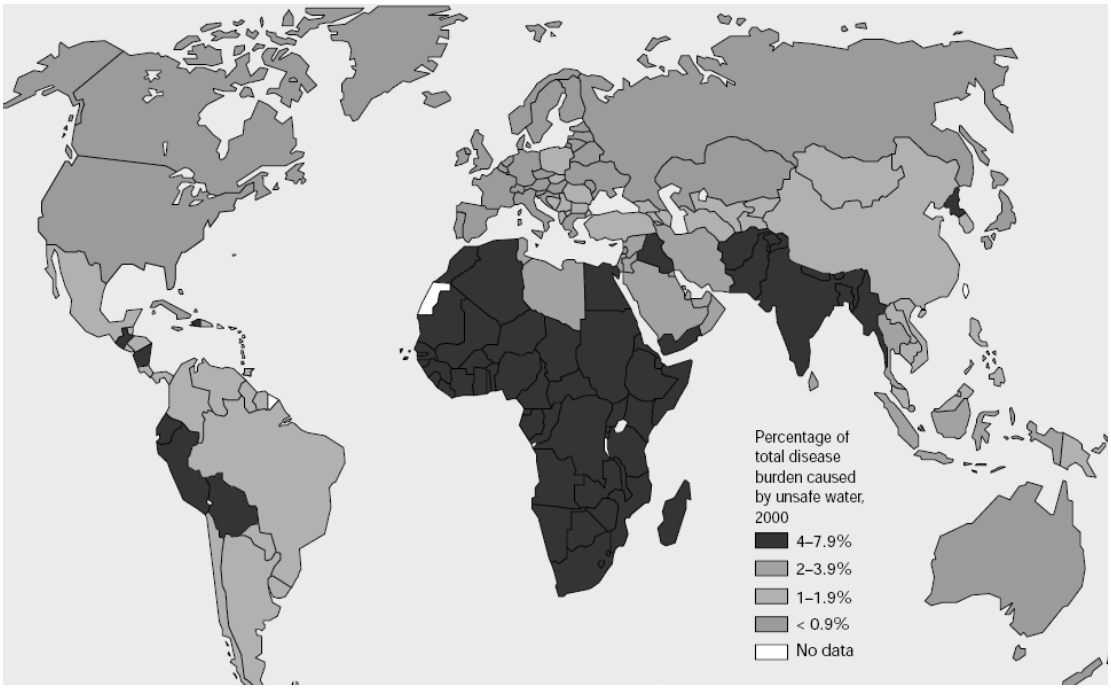

Figure 1-2: Percentage of total disease burden caused by unsafe water in 2000 (25).

Global population is over 6 billion and annual population growth rates are as high as 2.5% in the least developed countries (26). There are also regional water shortages, like in Nevada where population increased 66% in the past decade and annual precipitation is below 5 inches in areas (27). Dwindling water supplies raise public health concerns like hunger and sanitation (Figure **1-2**), and affect natural ecosystems.

Bioremediation can ease the water crisis. *Pseudomonas* species are capable of lowering the levels of pentachlorophenol in groundwater to meet regulatory drinking water standards (28), and *Escherichia coli* K-12 can remove carbon tetrachloride from polluted sites (29). In comparison to traditional remediation technologies such as pump-and-treat and thermal destruction, *in situ* bioremediation can cost less time and money and be more environmentally benign by avoiding chemical and physical processes (30). Many techniques have been used to enhance bioremediation, such as supplementing sites with nutrients to stimulate microbial activity or with organisms selected or engineered for specific degradation abilities (30). However, a major challenge preventing further improvements to bioremediation is bacterial transport. Optimally, there should be minimal bacterial adhesion to soil particles to maintain significant cell transport throughout the aquifer (31, 32). Once cells distribute through the polluted volume, however, adhesion is necessary for biofilm formation for contaminant degradation (7).

1.1.2 Biofilm control

With biofilms so prevalent and bearing such a vast impact on human life, it is desirable to be able to control them. Treatment of infectious biofilms via traditional

antibiotics has proven ineffectual in many cases because of their characteristic resistance (4). It is best to address the biofilm issue at the root– before the cells become sessile, fully colonize a surface, and are protected within the biofilm matrix.

Attempts have been made to control biofilms before they form through surface modification of the substratum. The use of traditional antifouling coatings such as cuprous oxide and tributyltin on ships has been regulated due to toxic chemicals leaching and affecting other marine life besides the targeted microorganisms (33). Replacement antifouling paint, like tetracycline, has been found to be ineffective (34). Conversely, Irgarol 1051 has been found to be overly effective and additionally harms alga reproduction in entire harbors (35). Silver coatings on implants help control infection, but over time genetic mutations in bacteria occur that impart resistance (36). Treatment of *P. aeruginosa* biofilms with monochloramine was less successful than a model predicted, due to the occurrence of an adaptive stress response in the cells (37).

Advances in materials use biomimicry (38) and substances that disrupt cell membranes (39) to cause death to bacteria that come into contact with the treated surface, without the risk of antibiotic resistance development. However, it is not always desirable to totally prevent biofilm formation, as in bioremediation. Also, the substratum surface cannot always be engineered, as in cystic fibrosis and *in situ* bioremediation. A better understanding of initial biofilm formation will lead to gains in both negative (eradication in industrial processes and human infection) and positive (exploitation in food processing, sensors, and bioremediation) biofilm scenarios.

1.1.3 Biofilm formation

The first step in biofilm formation is bacterial adhesion (4). Many interactions, such as electrostatic and van der Waals (40), hydrophobic (41), steric (42), and bridging (43), between the cell and substratum surfaces have been considered. However, under various experimental conditions, results do not match model predictions (44, 45) and show contrasting conclusions (46-49). This is due to different factors that affect bacterial adhesion, such as complexities of biological surfaces (43, 50-54) and variable environments (55). Adhesion mechanisms vary depending on the environment from which the cells in question were isolated, complicating the desire to discover a biofilm panacea.

Additionally, quorum sensing is implicated as necessary for proper biofilm formation for various species at different stages of biofilm development. This was first recognized in 1998 with *P. aeruginosa*, where quorum sensing signal mutants formed flat biofilms that were more susceptible to antimicrobial treatments but returned to normal after the addition of synthetic signal molecule (56). Subsequent studies also found other cases of quorum sensing involvement in biofilm development; *B. cepacia* (57), *Aeromonas hydrophila* (58), *Serratia liquefaciens* (59), *Pantoea stewartii* (60), and *Streptococcus mutans* (61-63) all cannot initiate biofilm formation or form mature biofilms when containing a disruptive quorum sensing genetic mutation.

It is clear that both bacterial adhesion and quorum sensing are important in biofilm formation. A better understanding of these processes will result in the emergence of novel techniques that are more effective at controlling biofilms.

1.2 Research goals

The main goal of this thesis is to address what occurs during the *early stages of biofilm formation* by investigating two processes that lead to biofilms– bacterial adhesion and quorum sensing. I break this down into four aims.

1. **Measure bacterial adhesion orientation and forces in the presence of various humic acid concentrations.**
2. **Model the diffusion of quorum sensing signals from bacteria arranged on a surface in two dimensions.**
3. **Determine if quorum sensing can occur locally in space and time.**
4. **Determine if biofilm formation can occur locally in space and time.**

Chapter 2 gives a literature review of biofilm formation, bacterial adhesion, and quorum sensing. Chapter 3 details the experimental methods and materials. Chapter 4 addresses the first aim to understand bacterial adhesion under a set of specifically defined environmental conditions. I investigate *E. coli* adhesion to silica in the presence of humic acid. This work is motivated by the biofilm application of *in situ* bioremediation. I examine how humic acid alters the strength of interactions between *E. coli* and silica and also the generality of end-on adhesion of particles to rod-shaped *E. coli* cells. The result is that humic acid causes only a slight increase in adhesion force and couplet formation, with no significant change in end-on adhesion of bacteria to silica particles.

Since bacterial adhesion is so specific to the cell and environmental conditions, the focus of this thesis work shifted to the biofilm formation process of quorum sensing. The main hypothesis governing the last three aims is that localized quorum sensing is

signal diffusion controlled. Typically population density is the only parameter considered to affect quorum sensing. Chapter 5 presents a diffusion model of quorum sensing signals from two-dimensional arrays of surface-attached bacteria, which shows that signal diffusion time, population density, *as well as population number* can affect quorum sensing. Chapter 6 uses luminescent quorum sensing *Vibrio fischeri* to show that quorum sensing occurs on a local scale and that it is affected by signal diffusion. Chapter 7 uses biofilm forming *P. aeruginosa* to show that biofilms might form locally as well and that signal diffusion might be involved in the biofilm formation.

The final chapter concludes the thesis and discusses the future direction of the work. The appendices give further details on experiments using fluorescent quorum sensing *E. coli*, experimental safety, and another bioremediation application– magnetic separation techniques for *in situ* environmental remediation of polycyclic aromatic hydrocarbons, from my comprehensive examination work.

1.3 References

1. Zobell, C.E., and E.C. Allen. 1935. The significance of marine bacteria in the fouling of submerged surfaces. *Journal of Bacteriology* 29:239-251.
2. Henrici, A.T. 1933. Studies of freshwater bacteria. *Journal of Bacteriology* 25:277-287.
3. Characklis, W.G. 1973. Attached microbial growths- II. Frictional resistance due to microbial slimes. *Water Research* 7:1249-1258.
4. Costerton, J.W., P.S. Stewart, and E.P. Greenberg. 1999. Bacterial biofilms: a common cause of persistent infections. *Science* 284:1318-1321.
5. Wilson, S., M.A. Hamilton, G.C. Hamilton, M.R. Schumann, and P. Stoodley. 2004. Statistical quantification of detachment rates and size distributions of cell clumps from wild-type (PAO1) and cell signaling mutant (JP1) Pseudomonas aeruginosa biofilms. *Applied and Environmental Microbiology* 70:5847-5852.
6. Flemming, H.-C. 1997. Reverse osmosis membrane biofouling. *Experimental Thermal and Fluid Science* 14:382-391.

7. Bryers, J.D. 1994. Biofilms and the technological implications of microbial cell adhesion. *Colloids and Surfaces B: Biointerfaces* 2:9-23.
8. Ludensky, M. 2003. Control and monitoring of biofilms in industrial applications. *International Biodeterioration and Biodegradation* 51:255-263.
9. Gristina, A.G. 1987. Biomaterial-centered infection: microbial adhesion versus tissue integration. *Science* 237:1588.
10. Characklis, W.G. 1981. Fouling biofilm development: a process analysis. *Biotechnology and Bioengineering* 23:1923-1960.
11. Mittelman, M.W. 2001. Microbially influenced corrosion of sprinkler piping. *PM Engineer* 7:46-49.
12. Stickler, D.J., N.S. Morris, R.J.C. McLean, and C. Fuqua. 1998. Biofilms on indwelling urethral catheters produce quorum sensing signal molecules in situ and in vitro. *Applied and Environmental Microbiology* 64:3486-3490.
13. Mittelman, M.W. 1996. Adhesion to biomaterials. In Bacterial Adhesion: Molecular and Ecological Diversity. M. Fletcher, editor Wiley-Liss, New York. 89-127.
14. McLean, R.J.C., J.C. Nickel, and M.E. Olsen. 1995. Biofilm associated urinary tract infections. In Microbial Biofilms. H.M. Lappin-Scott, and J.W. Costerton, editors. Cambridge University Press, New York. 261-273.
15. Chamis, A.L., G.E. Peterson, C.H. Cabell, G.R. Corey, R.A. Sorrentino, R.A. Greenfield, T. Ryan, L.B. Reller, and J. Vance G. Fowler. 2001. Staphylococcus aureus bacteremia in patients with permanent pacemakers or implantable cardioverter-defirillators. *Circulation* 104:1029-1033.
16. Champagne, C.P., C. Lacroix, and I. Sodini-Gallot. 1994. Immobilized cell technologies for the dairy industry. *Critical Reviews in Biotechnology* 14:109-134.
17. D'Souza, S.F. 2001. Microbial biosensors. *Biosensors & Bioelectronics* 16:337-353.
18. Larsen, L.H., N.P. Revsbech, and S.J. Binnerup. 1996. A microsensor for nitrate based on immobilized denitrifying bacteria. *Applied and Environmental Microbiology* 62:1248-1251.
19. Schramm, A., L.H. Larsen, N.P. Revsbech, N.B. Ramsing, R. Amann, and K.-H. Schleifer. 1996. Structure and function of a nitrifying biofilm as determined by in situ hybridization and the use of microelectrodes. *Applied and Environmental Microbiology* 62:4641-4647.
20. Gieseke, A., P. Arnz, R. Amann, and A. Schramm. 2002. Simultaneous P and N removal in a sequencing batch biofilm reactor: insights from reactor- and microscale investigations. *Water Research* 36:501-509.
21. Wyndham, R.C., and K.J. Kennedy. 1995. Microbial consortia in industrial wastewater treatment. In Microbial Biofilms. H.M. Lappin-Scott, and J.W. Costerton, editors. Cambridge University Press, New York. 183-195.
22. Langmark, J., M.V. Storey, N.J. Ashbolt, and T.A. Stenstrom. 2004. Artificial groundwater treatment: biofilm activity and organic carbon removal performance. *Water Research* 38:740-748.

23. WorldWaterAssesmentProgramme. 2003. Water for People, Water for Life - UN World Water Development Report. UNESCO with Berghahn Books, Paris.
24. Aldhous, P. 2003. The world's forgotten crisis. *Nature* 422:251.
25. Hoag, H. 2003. Atlas of a thirsty planet. *Nature* 422:252-253.
26. Chamie, J. 2003. World Population Prospects: The 2002 Revision. United Nations, New York.
27. Norton, G.A. 2005. Water 2025: Preventing Crises and Conflict in the West. US Department of the Interior, Washington, DC.
28. Schmidt, L.M., J.J. Delfino, J.F.P. III, and G.S.L. III. 1999. Biodegradation of low aqueous concentration pentachlorophenol (PCP) contaminated groundwater. *Chemosphere* 38:2897-2912.
29. Jin, G., and J. Andrew J. Englande. 1997. Effects of electron donor, dissolved oxygen, and oxidation-reduction potential biodegradation of carbon tetrachloride by *Escherichia coli* K-12. *Water Environment Research* 69:1100-1105.
30. Mohammed, N., R.I. Allayla, G.F. Nakhla, S. Farooq, and T. Husain. 1996. State-of-the-art review of bioremediation studies. *Journal of Environmental Science and Health* A31:1547-1574.
31. Marlow, H.J., K.L. Dunston, M.R. Weisner, M.B. Tomson, J.T. Wilson, and C.H. Ward. 1991. Microbial transport through porous media: The effects of hydraulic conductivity and injection velocity. *Journal of Hazardous Materials* 28:65-74.
32. Li, Q., and B.E. Logan. 1999. Enhancing bacterial transport for bioaugmentation of aquifers using low ionic strength solutions and surfactants. *Water Research* 33:1090-1100.
33. Thomas, K., K. Raymond, J. Chadwick, and M. Waldock. 1999. The effects of short-term changes in environmental parameters on the release of biocides from antifouling coatings: cuprous oxide and tributyltin. *Applied Organometallic Chemistry* 13:453-460.
34. Peterson, S.M., G.E. Batley, and M.S. Scammell. 1993. Tetracycline in antifouling paints. *Marine Pollution Bulletin* 26:96-100.
35. Scarlett, A., M.E. Donkin, T.W. Fileman, and P. Donkin. 1997. Occurrence of the marine antifouling agent Irgarol 1051 within the Plymouth Sound locality: implications for the green marcoalga Enteromorpha intestinalis. *Marine Pollution Bulletin* 34:645-651.
36. Summers, A.O., J. Wireman, M.J. Vimy, F.L. Lorscheider, B. Marshall, S.B. Levy, S. Bennett, and L. Billard. 1993. Mercury released from dental silver fillings provokes an increase in resistant bacteria in oral and intestinal floras of primates. *Antimicrobial Agents and Chemotherapy* 37:825-834.
37. Sanderson, S.S., and P.S. Stewart. 1997. Evidence of bacterial adaptation to monochloramine in *Pseudomonas aeruginosa* biofilms and evaluation of biocide action model. *Biotechnology and Bioengineering* 56:201-209.
38. Tew, G.N., D. Liu, B. Chen, R.J. Doerksen, J. Kaplan, P.J. Carroll, M.L. Klein, and W.F. DeGrado. 2002. *De novo* design of biomimetic antimicrobial polymers. *Proceedings of the National Academy of Sciences of the United States of America* 99:5110-5114.

39. Lin, J., J.C. Tiller, S.B. Lee, K. Lewis, and A.M. Klibanov. 2002. Insights into bactericidal action of surface-attached poly(vinyl-*N*-hexylpyridinium) chains. *Biotechnology Letters* 24:801-805.
40. Marshall, K.C., R. Stout, and R. Mitchell. 1971. Mechanism of the initial events in the sorption of marine bacteria to surfaces. *Journal of General Microbiology* 68:337-348.
41. Fletcher, M., and G.I. Loeb. 1979. Influence of substratum characteristics on the attachment of a marine pseudomonad to solid surfaces. *Applied and Environmental Microbiology* 37:67-72.
42. Ong, Y.-L., A. Razatos, G. Georgiou, and M.M. Sharma. 1999. Adhesion forces between *E. coli* bacteria and biomaterial surfaces. *Langmuir* 15:2719-2725.
43. Abu-Lail, N.I., and T.A. Camesano. 2003. Role of lipopolysaccharides in the adhesion, retention, and transport of *Escherichia coli* JM109. *Environmental Science and Technology* 37:2173-2183.
44. McEldowney, S., and M. Fletcher. 1986. Variability in the influence of physicochemical factors affecting bacterial adhesion to polystyrene substrata. *Applied and Environmental Microbiology* 52:460-465.
45. Hermansson, M. 1999. The DLVO theory in microbial adhesion. *Colloids and Surfaces B: Biointerfaces* 14:105-119.
46. Bos, R., H.C.v.d. Mei, J. Gold, and H.J. Busscher. 2000. Retention of bacteria on a substratum surface with micro-patterned hydrophobicity. *FEMS Microbiology Letters* 189:311-315.
47. Bruinsma, G.M., H.C.v.d. Mei, and H.J. Busscher. 2001. Bacterial adhesion to surface hydrophilic and hydrophobic contact lenses. *Biomaterials* 22:3217-3224.
48. Faille, C., C. Julien, F. Fontaine, M.-N. Bellon-Fontaine, C. Slomianny, and T. Benezech. 2002. Adhesion of Bacillus spores and Escherichia coli cells to inert surfaces: role of surface hydrophobicity. *Canadian Journal of Microbiology* 48:728-738.
49. Vadillo-Rodriguez, V., H.J. Busscher, H.C.v.d. Mei, J.d. Vries, and W. Norde. 2005. Role of lactobacillus cell surface hydrophobicity as probed by AFM in adhesion to surfaces at low and high ionic strength. *Colloids and Surfaces B: Biointerfaces* 41:33-41.
50. Razatos, A., Y.-L. Ong, M.M. Sharma, and G. Georgiou. 1998. Molecular determinants of bacterial adhesion monitored by atomic force microscopy. *Proceedings of the National Academy of Sciences of the United States of America* 95:11059-11064.
51. Jucker, B.A., H. Harms, and A.J.B. Zehnder. 1998. Polymer interactions between five gram-negative bacteria and glass investigated using LPS micelles and vesicles as model systems. *Colloids and Surfaces B: Biointerfaces* 11:33-45.
52. Vadillo-Rodriguez, V., H.J. Busscher, W. Norde, and H.C.v.d. Mei. 2002. Softness of the bacterial cell wall of *Streptococcus mitis* as probed by microelectrophoresis. *Electrophoresis* 23:2007-2011.
53. Poortinga, A.T., R. Bos, W. Norde, and H.J. Busscher. 2002. Electric double layer interactions in bacerial adhesion to surfaces. *Surface Science Reports* 47:1-32.

54. Walker, S.L., J.A. Redman, and M. Elimelech. 2004. Role of cell surface lipopolysaccharides in *Escherichia coli* K12 adhesion and transport. *Langmuir* 20:7736-7746.
55. Bakker, D.P., B.R. Postmus, H.J. Busscher, and H.C.v.d. Mei. 2004. Bacterial strains isolated from different niches can exhibit different patterns of adhesion to substata. *Applied and Environmental Microbiology* 70:3758-3760.
56. Davies, D.G., M.R. Parsek, J.P. Pearson, B.H. Iglewski, J.W. Costerton, and E.P. Greenberg. 1998. The involvement of cell-to-cell signals in the development of bacterial biofilm. *Science* 280:295-298.
57. Huber, B., K. Riedel, M. Hentzer, A. Heydorn, A. Gotschlich, M. Givskov, S. Molin, and L. Eberl. 2001. The *cep* quorum-sensing system of *Burkholderia cepacia* H111 controls biofilm formation and swarming motility. *Microbiology* 147:2517-2528.
58. Lynch, M.J., S. Swift, D.F. Kirke, C.W. Keevil, C.E.R. Dodd, and P. Williams. 2002. The regulation of biofilm development by quorum sensing in *Aeromonas hydrophila*. *Environmental Microbiology* 41:18-28.
59. Labbate, M., S.Y. Queck, K.S. Koh, S.A. Rice, M. Givskov, and S. Kjelleberg. 2004. Quroum sensing-controlled biofilm development in *Serratia liquefaciens* MG1. *Journal of Bacteriology* 186:692-698.
60. Koutsoudis, M.D., D. Tsaltas, T.D. Minogue, and S.B.v. Bodman. 2006. Quorum-sensing regulation governs bacterial adhesion, biofilm development, and host colonization in Pantoea stewartii subspecies stewartii. *Proceedings of the National Academy of Sciences of the United States of America* 103:5983-5988.
61. Li, Y.-H., N. Tang, M.B. Aspiras, P.C.Y. Lau, J.H. Lee, R.P. Ellen, and D.G. Cvitkovitch. 2002. A quorum-sensing signaling system essential for genetic competence in *Streptococcus mutans* is involved in biofilm formation. *Journal of Bacteriology* 184:2699-2708.
62. Merritt, J., F. Qi, S.D. Goodman, M.H. Anderson, and W. Shi. 2003. Mutation of *luxS* affects biofilm formation in *Streptococcus mutans*. *Infection and Immunity* 71:1972-1979.
63. Wen, Z.T., and R.A. Burne. 2004. LuxS-mediated signaling in *Streptococcus mutans* is involved in regulation of acid and oxidtative stress tolerance and biofilm formation. *Journal of Bacteriology* 186:2682-2891.

Chapter 2

Literature Review

2.1 Biofilms

2.1.1 Biofilms in history

Bacteria are ubiquitous organisms that are found in both free-floating planktonic and sessile biofilm states. Biofilms are surface-associated bacterial populations encased in a protective auto-produced matrix (1) and are colloquially referred to as "slime". One of the first observations of bacteria (in 1683) resulted from a sampling of slime formed on the teeth of Antony van Leeuwenhoek (Figure **2-1**). He wrote how he, "almost always saw with great wonder that there were very many 'animalcules'," when studying his dental plaque biofilms with his microscopes (2).

Figure 2-1: Antony van Leeuwenhoek holding an example of one of his microscopes in 1686 (3).

In 1933 it was noted that, "for the most part bacteria are not free floating organisms, but grown upon submerged surfaces; they are of the *benthos* rather than the *plancton*," as Henrici concluded from comparisons of enumerations of bacteria from lake water and bottom mud samples (4). However, it was not until 1978 that biofilms were appreciated as a significant form of bacterial life. Geesey et al. developed fluorescent microscopy methods to accurately count biofilm bacteria and realized their "numerical importance" in comparison to the planktonic cells from the same mountain stream (5). The enumeration method was applied to other environments and biofilms' prevalence was seen across all natural, industrial, and medical settings (6). In an inspiring presentation by the biofilm expert Bill Costerton at the 232nd American Chemical Society Meeting, it was affirmed that greater than 99.9% of bacteria in aquatic ecosystems are in biofilms (7). After understanding the pervasiveness of biofilms, researchers moved on to detail biofilm structure, function, and genetic expression.

Biofilms were first described in 1933 (before the designation "biofilm" existed) by Henrici in his paper, "Studies of freshwater bacteria."

> The deposit of bacteria [onto slides] becomes apparent in a few days and increases progressively, eventually becoming so thick that individual cells may be distinguished with difficulty. That the cells are actually growing upon the glass is indicated by their occurrence in microcolonies of steadily increasing size. They are fairly firmly adherent to the glass, not removed by washing under a tap… the groups of cells are evidently surrounded by a sheath of gum which also serves to fasten the colony to the glass. (4)

The same qualities were detailed in subsequent biofilm studies and as microscopic techniques grew more advanced, the true complexity of biofilm structures became apparent.

2.1.2 Biofilm structure

One of the first introductions of biofilms to the public was in a 1978 issue of *Scientific American*, in which Costerton et al. detailed "How bacteria stick" via a glycocalyx (8). The glycocalyx is a mesh of polysaccharide fibers extending from a cell surface, which becomes entangled with other cells to form a network in a biofilm, for example as in dental plaque (8). It is now known that this network is actually made up of more than just polysaccharides, but rather general extracellular polymeric substances (EPS), which also contain proteins, lipids, and DNA (9). The EPS is the "sheath of gum" (4) Henrici referred to in his 1933 study.

Living cells make up a small percentage of a biofilm. Water channels and EPS constitute 73-98% of the total biofilm volume (10). Large (2,000 kDa) molecules can pass through the channels (Figure **2-2**) (11). The arrangement of cells, EPS, and channels is heterogeneous and distinct depending on the species present in the biofilm. For example, *Pseudomonas* biofilms have highest cell densities (27% cellular material) at the biofilm-solid interface whereas *Vibrio parahaemolyticus* biofilms show the opposite distribution with highest cell densities (16%) at the biofilm-liquid interface (10).

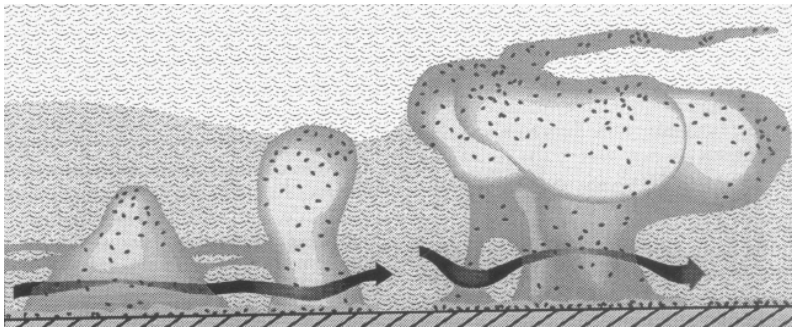

Figure 2-2: Costerton et al. depict the three-dimensional and heterogeneous nature of mature biofilms: cells, EPS, and channels (11).

Biofilm heterogeneity is evident through other properties besides cell density and is demonstrated through various techniques. A distribution of cell density leads to varying biofilm thicknesses, which have ranged from 0–90 μm in a 72-hour *P. fluorescens* biofilm (12) and 13–60 μm in a 140-hour *P. aeruginosa* biofilm (13), for example. Thickness variability, also referred to as roughness, imparts frictional resistance in pipes (14) and unexpectedly low convective transport of particles across biofilms (15). An NMR study showed three biofilm fractions with significantly different diffusion coefficients (16). Using light microscopy, Walker and Keevil found that, "this mosaic nature of the biofilm would aggravate localised corrosion," on their metal substrata (17).

Biofilms' heterogeneous structure plays a role in nutrient and antimicrobial agent transport and thus biofilm survival. Channels allow for convective and diffusive transport whereas areas containing EPS are diffusion limited (6, 18, 19). Hindered nutrient transport is evident in investigations of metabolic activity throughout a biofilm. Adenylate energy charge increases to a maximum at the biofilm-liquid interface from the substratum (20). Similarly, protein synthesis is concentrated at biofilm locales closest to the biofilm-gas interface and the depth of activity correlates with oxygen availability (21, 22). A measurement of EPS yields throughout a biofilm showed that the yield per viable cell was lower deeper in the biofilm (23). Zhang and Bishop hypothesized that this is because nutrient availability is lower at these depths so cells are less able to produce EPS and/or cells are consuming EPS.

2.1.3 Antibiotic resistance

In 1985 Nickel et al. found that *P. aeruginosa* cells in a biofilm were more resistant to antibiotics than the planktonic cells (24). This has since been frequently described (1, 25-28) and one explanation for the reduced susceptibility is that the biofilm structure does not allow for penetration of antibiotic agents to the cells due to transport limitations (1, 12, 26). Nichols et al. determined that tobramycin binding to alginate, a *P. aeruginosa* EPS constituent, slows the antibiotic's diffusion and thus increases the penetration time into biofilms (26). Korber et al. reported a gradient effect of fleroxacin on *P. fluorescens* biofilm cells (12). However, both groups noted that hindered transport alone could not be the major mechanism of resistance.

By modeling the diffusion and possible sorption and reaction of antibiotic in biofilms, Stewart concluded that diffusion limitations alone were not great enough to impart resistance (29). A combination enzymatic (catalytic) reaction and diffusion mechanism is, mathematically, a more plausible scenario (29), in which an enzyme destroys the antibiotic agent. If this is the case, then biofilm cells should still be able to grow. The distinction needs to be made that biofilms are resistant to being killed by antimicrobial agents and are not necessarily able to grow. In fact, Spoering et al. demonstrated that *P. aeruginosa* biofilm and log phase planktonic cells have the same *growth* in antibiotic conditions (30).

Brown et al. suggested that biofilms' characteristic antibiotic resistance was related to the decreased activity of deeply located cells (25). Nutrient limitations and decreases in cell growth can cause changes in the cell envelope and thus susceptibility

(25). Antibiotics are 99.9% effective against log phase cells, but have greatly reduced efficacy against slowly growing cells (31). Korber et al. recognized the effect of cell growth on reistance in their fleroxacin treated biofilms, which displayed a gradient of elongated cells (12). Elongation is characteristic of fleroxacin-treated cells. The authors observed longer cells at the biofilm-liquid interface, which also elongated faster than the cells at the substratum (12). The reduced activity of cells within biofilms facilitates resistance against antibiotic treatments. Other known methods that confer antibiotic resistance in biofilms are multidrug resistance pumps (28, 32) and glucose polymers that interact with antibiotic agents (33).

2.1.4 Biofilms as a community of bacteria

The heterogeneous structure among the cells, EPS, and channels of biofilms gives transport qualities that ultimately lead to the characteristic persistent survival. "Selection favors cells that are protected" (8). In fact, silicified biofilm matrices containing silicified filaments are some of the earliest fossil records of life from 3 billion years ago (34, 35). Recently biofilms have been regarded as communities (35-40), cities (36, 41), and multicellular organisms (11, 35, 42) given their structural organization and metabolic specialization (11, 35), as well as their developmental sequences (35) and coordinated behaviors (37, 42, 43).

Biofilms go through distinct (44) developmental stages and the parallel has been made to multicellular organism development (35). The steps include attachment, microcolony formation and EPS production, structure maturation, and dispersion (1, 35,

36, 41, 45-47) (Figure **2-3**). There is a genetic basis for each of these steps. *P. aeruginosa* mutants defective in flagellar-based motility are unable to effectively attach to substrata and therefore do not form biofilms (48). In the same *P. aeruginosa* study, pili-based motility (twitching, or surface motility) mutants do attach, but do not form microcolonies, and therefore are biofilm deficient (48). Once attached, *P. aeruginosa* cells show up-expression of *algC*, a gene responsible for the synthesis of alginate, a major component of *P. aeruginosa* EPS (49). Friedman and Kolter identified two gene clusters (*pel* and *psl*) involved in *P. aeruginosa* carbohydrate EPS component synthesis (50). Mutants with deletions in both the *pel* and *psl* gene clusters do not form mature biofilms. Mutation in an *Actinobacillus actinomycetemcomitans* protein synthesis gene that encodes a hydrolase that degrades polysaccharides leads to biofilms that are unable perform cell detachment (51). Similarly, in *P. aeruginosa*, there is an alginate lyase expressed to degrade EPS and bring about cell detachment in biofilms (52).

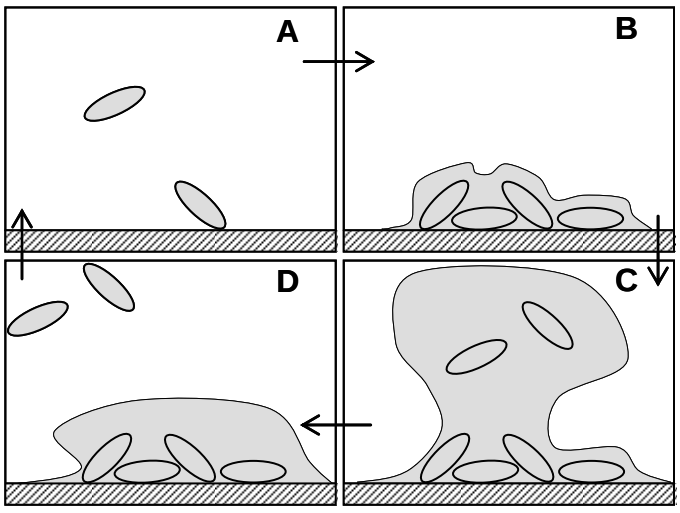

Figure 2-3: Schematic of the stages of biofilm development: attachment (A), microcolony formation and EPS production (B), structure maturation (C), and dispersal (D).

The coordinated behaviors of biofilms are brought about through response to cues sensed from the surroundings. The cues can be external inducers, or specifically in the case of quorum sensing, autoinducers. Surface contact causes disturbances to the cell envelope, which induces decreased flagellin synthesis as well as increased EPS component synthesis in *E. coli* (53) and, as discussed above, in *P. aeruginosa* (49). Nutrient availability affects biofilm depth and cell detachment (54-56). Whitely determined in 2001 that *P. aeruginosa* biofilms exposed to antibiotic agents express genes involved in stress response and efflux systems (57). Other environmental stresses, such as pH fluctuations, cause changes in multispecies biofilm diversity (58).

Quorum sensing allows bacteria to detect the surrounding cell density via autoinducer signals that each cell produces. A critical concentration of the signals in the medium triggers a response to high cell density conditions. This has been shown to occur during all stages of biofilm development in various species. Examples of responses elicited through quorum sensing signals are as follows: EPS production in *V. cholerae* (41) and *P. aeruginosa* (35); maturation into heterogeneous architecture in *P. aeruginosa* (59), *Bacillus subtilis* (39), and *Streptococcus gordonii* (60); virulence in *P. aeruginosa* (61, 62), *B. cenocepacia* (63), and *S. aureus* (64); antibiotic synthesis in *Streptomyces* and *B. subtilis* (64); antibiotic resistance in *P. aeruginosa* (59); formation of dormant cells in *P. aeruginosa* (42) and recovery of dormant cells in *Nitrosomonas europae* (65); detachment (35, 66); and programmed death (43).

The heterogeneous structure of the cells, EPS, and channels of biofilms and the coordination of the key developmental features allows for heightened survival. "Biofilms are clearly more than the sum of their parts" (47). Biofilms are a protected community of

bacteria. Given their deleterious effects of infection and fouling and their advantageous applications in sensors and remediation, it is desirable to be able to control biofilm formation as discussed in Chapter 1. Key factors in biofilm formation and maturation are bacterial adhesion and quorum sensing, which are the focus of this thesis.

2.2 Bacterial adhesion

Numerous interactions must be considered when studying bacterial adhesion. Zobell first suggested that bacterial adhesion happens in two phases, reversible and irreversible (67). This was theoretically confirmed by Marshall et al. using the Derjaguin-Landau-Verwey-Overbeek (DLVO) theory of colloid stability (68).

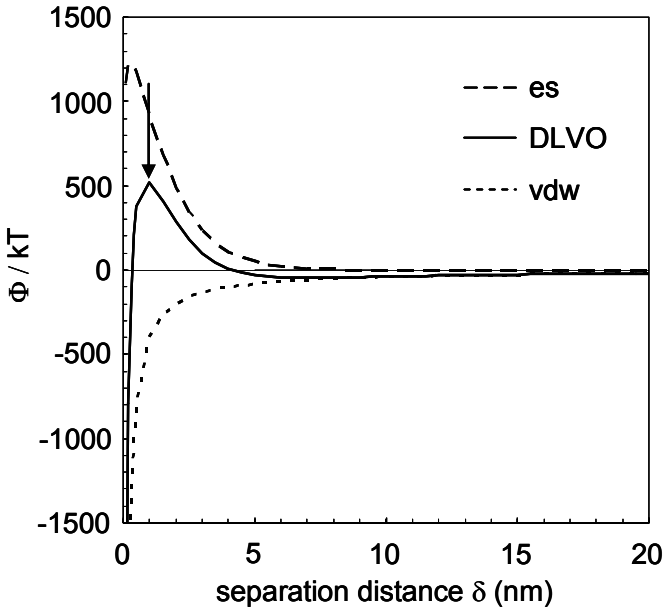

Figure 2-4: An example DLVO (es + vdw) plot for the interaction energy between a model soil particle (r = 250 μm, ζ = -50 mV) and cell (r = 1 μm, ζ = -25 mV) in an ionic strength solution of 60 mM. The arrow demarks the repulsion barrier between the secondary and primary minimums. DLVO (solid curve), electrostatics (long dashes), and van der Waals (short dashes).

The DLVO model accounts for electrostatic and van der Waals forces, giving the interaction energy as a function of separation distance. Reversible adhesion occurs in the secondary minimum, an area of weak attraction, in the interaction energy versus separation distance plot (Figure **2-4**). Irreversible adhesion requires the cell overcome the repulsion barrier between the secondary and primary minimums.

The DLVO model, however, is often not sufficient to explain bacterial adhesion events (69, 70), due in part to complexities of biological surfaces (71-76). The surface complexities add hydrophobic (77), steric (78), and bridging (72, 75) interactions. Irreversible adhesion occurs via short-range chemical and molecular interactions like hydrogen, ionic, and covalent bonding (79) as well as interactions involving extracellular structures including lipopolysachharides (LPS), pili, and fimbriae (80).

2.2.1 Bacterial cell surface

Since varied surfaces influence bacterial adhesion, it is important to understand the surfaces involved. Bacterial species are categorized as either Gram-negative or Gram-positive based on cell wall differences (Figure **2-5)** (81). Gram-positive cells have cell walls consisting of many layers of peptidoglycan that retain the Gram stain's crystal violet-iodine complex. There are also teichoic acids and proteins associated with the Gram-positive cell wall. All the cells used in this thesis are Gram-negative cells. Gram-negative cell walls contain a thin peptidoglycan layer that does not allow for retention of the crystal violet-iodine dye in Gram stains. Beyond the Gram-negative cell wall is a lipid bilayer outer membrane made up of phospholipids, lipoproteins, lipopolysaccharides

(LPS), and proteins. The LPS is located on the outer side of the outer membrane via lipid A (81). The polysaccharides of the LPS extend away from the cell 30–50 nm (70).

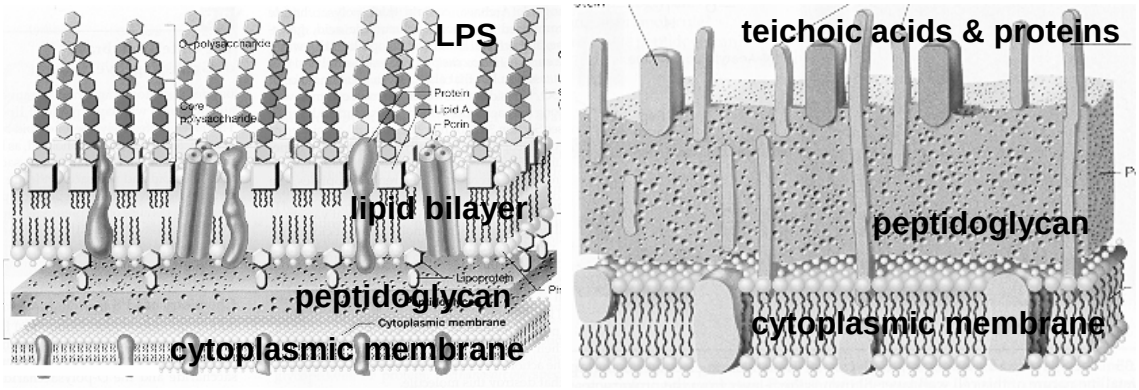

Figure 2-5: The structures of Gram-negative (left) and Gram-positive (right) cell surfaces (81).

LPS composition can influence adhesion by affecting cell surface charge, hydrophobicity, steric interactions, bridging, and hydrogen bonding (72, 78, 82). EPS is found associated with the cell surface as well as in free matrix form (83) as discussed above. Cell-bound EPS can increase surface softness and decrease negative surface charge density, and thus affect adhesion (73, 84).

Flagella, pili, and fimbriae are surface protein structures that extend 2 μm (pili and fimbriae) to 10 μm (flagella) away from the cell (85) and can function in adhesion. For example, *P. aeruginosa* flagella mutants are unable to attach to PVC substrata (48). Surface proteins are also involved in specific bacterial adhesion via ligand-receptor interactions between bacteria cell and another biologically active surface. A common example is *E. coli* type 1 fimbriae tips, which contain the adhesin FimH that binds to mannose-containing receptors present on the surface of epithelial cells (86). This thesis however focuses only on the passive, non-specific adhesion of a cell to a surface.

2.2.2 Batch growth and cell division

The various lipids, polysaccharides, and proteins covering the cell surface make it heterogeneous. However, the bacterial cell surface is not only spatially heterogeneous, but also temporally, and varies during both batch growth and division. A bacterial population batch growth cycle consists of four phases (87): the lag (adjustment) phase, the log (exponential growth) phase, the stationary (nutrient limited-steady cell concentration) phase, and the death phase. Bacterial adhesion varies depending on growth phase. *Lactococcus lactis* stationary phase cells, but not exponential phase cells, achieve high adhesion densities to polystyrene due to the release of ionized substances and EPS (88). *E. coli* K-12 stationary phase cells also show more adhesion than log phase cells, possibly due to a more heterogeneous distribution of charged functional groups (89, 90). Cell wall hydrophobicity may also vary with growth phase and affect adhesion (91).

Bacteria reproduce via binary fission. Individual cells grow and then divide by forming a septum where there is an inward growth of the cytoplasmic membrane and cell wall until two distinct walls form. The two daughter cells, each with a complete chromosome, then separate (87). At the division site in *E. coli* there is a localized area of peptidoglycan synthesis and the new pole of a freshly divided *E. coli* bacterium remains more active in cell wall synthesis than the old pole (92). The preferential end-on adhesion observed in *E. coli* may arise from cell surface differences that occur during the division process (93-95).

2.2.3 Substratum and surrounding environment

A further complication in describing bacterial adhesion is that the adhesion mechanisms vary depending on the particular niche of interest (96). Not only is it important to consider the cell surface, but also the substrate surface and the environment. The various interactions between the cell and substratum surfaces have been considered under various conditions and results show contrasting conclusions. The following chronological list of results from surface hydrophobicity investigations demonstrates some discrepancies that have arisen. In 2000 it was shown that substratum hydrophobicity does not affect bacterial adhesion, but rather adhesion strength, and that cells adhere less strongly to hydrophobic surfaces (97). Reports came out during the next two years finding that substratum hydrophobicity does play a role (98, 99) and that cells adhere more strongly to more hydrophobic surfaces (99). Then, in 2005 it was concluded that adhesion does vary with substratum hydrophobicity but depends on other factors such as cell hydrophobicity and electrostatic interactions (100).

Due to the various surfaces and conditions involved in separate instances of bacterial adhesion, bacterial adhesion can only be considered on an individual specific case basis. There is no generalized theory of bacterial adhesion that applies to all situations (96). In this thesis, the focus is on the adhesion of *E. coli* in the presence of humic acid, which makes up a large component (70-80%) of soil organic matter (101).

After bacterial adhesion occurs, biofilms can develop through EPS production and microcolony formation (1, 46). The biofilm "community" is able to coordinate behaviors by responding to environmental signals. One such cue is the presence of other cells,

which is detected through quorum sensing.

2.3 Quorum Sensing

A simple analogy for quorum sensing is a bar brawl, where the instigator, who would not normally initiate a fight, decides to do so with enough friends present. This describes the specific quorum sensing response of virulence. A more general analogy is the namesake– 'quorum'. A quorum is the minimum number of people necessary to conduct a vote. If enough cells are detected through quorum sensing, then the transcription of specific target genes is activated.

Over thirty years ago, Nealson reported that *Vibrio fischeri* produces an extracellular autoinducer, which accumulates as a function of cell population growth and activates luminescence at a threshold concentration (102) (Figure **2-6**).

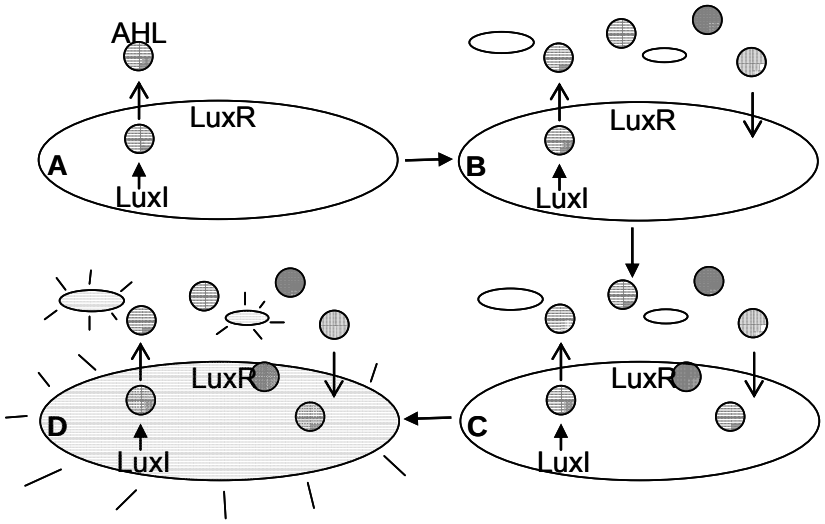

Figure 2-6: The process of quorum sensing in *Vibrio fischeri*. The cells produce AHL signal molecules with protein LuxI (A). The AHL concentration increases with time or population growth (B). At a threshold AHL concentration, receptor protein LuxR binds AHL (C), which activates the transcription of luminescence genes (D).

When quorum sensing was first observed, it was originally thought to be a special occurrence unique to just a few species. These included for example luminescence in *V. fischeri* (103), fruiting body formation in *Myxococcus xanthus* (104), and competence in *Streptococcus pneumoniae* (105). Quorum sensing, however, occurs in numerous species and in various forms. Typically, Gram-negative bacteria use acylated homoserine lactone (AHL) signals (106) whereas Gram-positive bacteria use a different type of autoinducer, oligopeptides (107). There is yet another type of signal molecule, a furanosyl borate diester (108), now recognized, for example in *Vibrio harveyi* (109) and *Escherichia coli* (110). These furanosyl borate diesters make up the autoinducer 2 (AI-2) family of quorum sensing signals whereas AHL is referred to as AI-1. An organism can use multiple quorum sensing signals, networked in parallel as with *Vibrio harveyi* or in series as in *Pseudomonas aeruginosa* (62). Not only is quorum sensing an intraspecies activity, but it also occurs on an interspecies level. Bacteria use AI-2 to detect other species' populations (111, 112), which allows for one species to be able to interfere with another species' quorum sensing. For example, *E. coli* can inhibit *V. harveyi* luminescence, even at quorum-sized cell densities, by consuming AI-2 (112).

In 2002 Redfield hypothesized that autoinduction was diffusion controlled rather than population controlled and that it was not a cooperative action of a bacterial population, but rather a way for individual cells to gather information about the transport properties (e.g., diffusion and mixing) of the surrounding medium (113). Redfield's hypothesis is plausible because the response to quorum sensing in many species is frequently a secretion, for example of virulence factors (62, 64), antibiotics (64), or extracellular polymeric substances (35, 41), which are of benefit to an individual cell

only if the secreted biomolecules stay local (113). The "diffusion sensing" hypothesis however does not apply for all cases, such as with *V. fischeri* luminescence, which is not a secretory response to quorum sensing. It is therefore reasonable that quorum sensing is indeed due to both population and diffusion, and that different species developed quorum sensing based on one aspect (population or diffusion) of the possibly dualistic phenomenon.

Recently Hense et al. introduced the term "efficiency sensing" to unify the theories of quorum sensing and diffusion sensing and hypothesized that autoinducers measure the *combination* of population density, signal molecule diffusion, and spatial distribution (i.e., localized cell density) (114). This combination of information allows cells to determine whether or not it is worth producing effector molecules, such as antibiotics or bioluminescent proteins, which are more energetically costly to synthesize than AHL (114).

The influence of diffusion on quorum sensing has not been thoroughly examined. The first pieces of experimental evidence came out of Basu et al.'s 2005 publication, which uses quorum sensing signal diffusion to form programmed patterns of cells (115). *V. fischeri* autoinducer signals from sender cells elicit different fluorescent responses in receiver cells, which are genetically engineered to respond to different bands of signal concentrations with either red or green fluorescence, depending on the band-detect. Thus, plated mixtures of different band-detect cells surrounding a center disk of sender cells results in a bulls-eye pattern formation (115). This work, however, was not directly interested in the effect of diffusion on quorum sensing and only bulk samples of cells of very high population densities were used.

Quorum sensing has most often been described *only* in terms of population *density* (106, 116, 117). There is no evidence in the literature of a "true quorum"– a specific *number* of cells necessary to elicit a response. Nor is there any work investigating signal diffusion in quorum sensing on a local scale (only bulk).

2.4 References

1. Costerton, J.W., P.S. Stewart, and E.P. Greenberg. 1999. Bacterial biofilms: a common cause of persistent infections. *Science* 284:1318-1321.
2. Gest, H. 2004. The discovery of microorganisms by Robert Hooke and Antoni van Leeuwenhoek, Fellows of The Royal Society. *Notes and Records of the Royal Society of London* 58:187-201.
3. Verkolje, J. 1686. Antoni van Leeuwenhoek. In National Library of Medicine, Bethesda.
4. Henrici, A.T. 1933. Studies of freshwater bacteria. *Journal of Bacteriology* 25:277-287.
5. Geesey, G.G., R. Mutch, J.W. Costerton, and R.B. Green. 1978. Sessile bacteria: An important component of the microbial population in small mountain streams. *Limnology and Oceanography* 23:1214-1223.
6. Costerton, J.W., Z. Lewandowski, D.E. Caldwell, D.R. Korber, and H.M. Lappin-Scott. 1995. Microbial biofilms. *Annual Review of Microbiology* 49:711-745.
7. Costerton, J.W. 2006. Role of microbial biofilms in the fouling of surfaces. In American Chemical Society 232nd National Meeting and Exposition. San Francisco.
8. Costerton, J.W., G.G. Geesey, and K.-J. Cheng. 1978. How bacteria stick. *Scientific American* 238:86-95.
9. Sutherland, I.W. 2001. The biofilm matrix - an immobilized but dynamic microbial environment. *TRENDS in Microbiology* 9:222-227.
10. Lawrence, J.R., D.R. Korber, B.D. Hoyle, J.W. Costerton, and D.E. Caldwell. 1991. Optical sectioning of microbial biofilms. *Journal of Bacteriology* 173:6558-6567.
11. Costerton, J.W., Z. Lewandowski, D. DeBeer, D.E. Caldwell, D.R. Korber, and G. James. 1994. Biofilms, the customized microniche. *Journal of Bacteriology* 176:2137-2142.
12. Korber, D.R., G.A. James, and J.W. Costerton. 1994. Evaluation of flexorxacin activity against established Pseudomonas fluorescens biofilms. *Applied and Environmental Microbiology* 60:1663-1669.

13. Stewart, P.S., B.M. Peyton, and W.J. Drury. 1993. Quantitative observations of heterogeneities in *Pseudomonas aeruginosa* biofilms. *Applied and Environmental Microbiology* 59:327-329.
14. Characklis, W.G. 1973. Attached microbial growths- II. Frictional resistance due to microbial slimes. *Water Research* 7:1249-1258.
15. Drury, W.J., P.S. Stewart, and W.G. Characklis. 1993. Transport of 1-μm latex particless in *Pseudomonas aeruginosa* biofilms. *Biotechnology and Bioengineering* 42:111-117.
16. Vogt, M., H.-C. Flemming, and W.S. Veeman. 2000. Diffusion in *Pseudomonas aeruginosa* biofilms: a pulsed field gradient NMR study. *Journal of Bacteriology* 77:137-146.
17. Walker, J.T., and C.W. Keevil. 1994. Study of microbial biofilms using light microscope techniques. *International Biodeterioration and Biodegradation* 34:223-236.
18. Stewart, P.S. 2003. Diffusion in Biofilms. *Journal of Bacteriology* 185:1485-1491.
19. DeBeer, D., P. Stoodley, and Z. Lewandowski. 1994. Liquid flow in heterogeneous biofilms. *Biotechnology and Bioengineering* 44:636-641.
20. Klinnement, S.L., and J.W.T. Wimpenny. 1992. Measurements of the distribution of adenylate concentrations and adenylate energy charge across *Pseudomonas aeruginosa* biofilms. *Applied and Environmental Microbiology* 58:1629-1635.
21. Xu, K.D., P.S. Stewart, F. Xia, C.-T. Huang, and G.A. McFeters. 1998. Spatial physiological heterogeneity in *Pseudomonas aeruginosa* biofilm is determined by oxygen availabilty. *Applied and Environmental Microbiology* 64:4035-4039.
22. Werner, E., F. Roe, A. Bugnicourt, M.J. Franklin, A. Heydorn, S. Molin, and B. Pitts. 2004. Stratified growth in Pseduomonas aeruginosa biofilms. *Applied and Environmental Microbiology* 70:6188-6196.
23. Zhang, X., and P.L. Bishop. 2001. Spatial distribution of extracellular polymeric substances in biofilms. *Journal of Environmental Engineering* 127:850-856.
24. Nickel, J.C., I. Ruseska, J.B. Wright, and J.W. Costerton. 1985. Tobramycin resistance of Pseudomonas aeruginosa cells growing as a biofilm on urinary catheter material. *Antimicrobial Agents and Chemotherapy* 27:619-624.
25. Brown, M.R.W., D.G. Allison, and P. Gilbert. 1988. Resistance of bacteiral biofilms to antibiotics: a growth-rate related effect? *Journal of Antimicrobial Chemotherapy* 22:777-783.
26. Nichols, W.W., S.M. Dorrington, M.P.E. Slack, and H.L. Walmsley. 1988. Inhibition of tobramycin diffusion by binding to alginate. *Antimicrobial Agents and Chemotherapy* 32:518-523.
27. Allison, D.G., and P. Gilbert. 1995. Modification by surface association of antimicrobial susceptibility of bacterial populations. *Journal of Industrial Microbiology* 15:311-317.
28. Brooun, A., S. Liu, and K. Lewis. 2000. A dose-response study of antibiotic resistance in Pseudomonas aeruginosa biofilms. *Antimicrobial Agents and Chemotherapy* 44:640-646.

29. Stewart, P.S. 1996. Theoretical aspects of antibiotic diffusion into microbial biofilms. *Antimicrobial Agents and Chemotherapy* 40:2517-2522.
30. Spoerling, A.L., and K. Lewis. 2001. Biofilms and planktonic cells of Pseudomonas aeruginosa have similar resistance to killing by antimicrobials. *Journal of Bacteriology* 183:6746-6751.
31. Eng, R.H.K., F.T. Padberg, S.M. Smith, E.N. Tan, and C.E. Cherubin. 1991. Bactericidal effects of antibiotics on slowly growing and nongrowing bacteria. *Antimicrobial Agents and Chemotherapy* 35:1824-1828.
32. Lewis, K. 2001. Riddle of biofilm resistance. *Antimicrobial Agents and Chemotherapy* 45:999-1007.
33. Mah, T.-F., B. Pitts, B. Pellock, G.C. Walker, P.S. Stewart, and G.A. O'Toole. 2003. A genetic basis for *Pseudomonas aeruginosa* biofilm antibiotic resistance. *Nature* 426:306-310.
34. Reysenbach, A.-L., and S.L. Cady. 2001. Microbiology of ancient and modern hydrothermal systems. *TRENDS in Microbiology* 9:79-86.
35. Stoodley, P., K. Sauer, D.G. Davies, and J.W. Costerton. 2002. Biofilms as complex differentiated communities. *Annual Review of Microbiology* 56:187-209.
36. Watnick, P., and R. Kolter. 2000. Biofilm, city of microbes. *Journal of Bacteriology* 182:2675-2679.
37. Rice, K.C., and K.W. Bayles. 2003. Death's toolbox: examining the molecular components of bacterial programmed cell death. *Molecular Microbiology* 50:729-739.
38. O'Toole, G.A. 2004. Jekyll or hide? *Nature* 432:680-681.
39. Branda, S.S., J.E. Gonzalez-Pastor, E. Dervyn, S.D. Ehlich, R. Losick, and R. Kolter. 2004. Genes involved in the formation of structured multicellular communities by *Bacillus subtilis*. *Journal of Bacteriology* 186:3970-3979.
40. Kolter, R., and E.P. Greenberg. 2006. The superficial life of microbes. *Nature* 441:300-302.
41. Heithoff, D.M., and M.J. Mahan. 2004. *Vibrio cholerae* biofilms: Stuck between a rock and a hard place. *Journal of Bacteriology* 186:4835-4837.
42. Shapiro, J.A. 1998. Thinking about bacterial populations as multicellular organisms. *Annual Review of Microbiology* 52:81-104.
43. Jefferson, K.K. 2004. What drives bacteria to produce a biofilm? *FEMS Microbiology Letters* 236:163-173.
44. Sauer, K., A.K. Camper, G.D. Ehrlich, J.W. Costerton, and D.G. Davies. 2002. *Pseudomonas aeruginosa* displays multiple phenotypes during development as a biofilm. *Journal of Bacteriology* 184:1140-1154.
45. Davey, M.E., and G.A. O'Toole. 2000. Microbial biofilms: from ecology to molecular genetics. *Microbiology and Molecular Biology Reviews* 64:847-867.
46. Reisner, A., J.A.J. Haagensen, M.A. Schembri, E.L. Zechner, and S. Molin. 2003. Development and maturation of *Escherichia coli* K-12 biofilms.
47. Parsek, M.R., and C. Fuqua. 2004. Biofilms 2003: Emerging themes and challenges in studies of surface-associated microbial life. *Journal of Bacteriology* 186:4427-4440.

48. O'Toole, G.A., and R. Kolter. 1998. Flagellar and twitching motility are necessary for Pseudomonas aeruginosa biofilm development. *Molecular Microbiology* 30:295-304.
49. Davies, D.G., and G.G. Geesey. 1995. Regulation of the alginate biosynthesis gene *algC* in *Pseudomonas aeruginosa* during biofilm development in continuous culture. *Applied and Environmental Microbiology* 61:860-867.
50. Friedman, L., and R. Kolter. 2004. Two genetic loci produce distinct carbohydrate-rich structural components of the *Pseudomonas aeruginosa* biofilm matrix. *Journal of Bacteriology* 186:4457-4465.
51. Kaplan, J.B., C. Ragunath, N. Ramasubbu, and D.H. Fine. 2003. Detachment of *Actinobacillus actinomycetemcomitans* biofilm cells by an endogenous β-hexosaminidase activity. *Journal of Bacteriology* 185:4693-4698.
52. Boyd, A., and A.M. Chakrabarty. 1994. Role of alginate lyase in cell detachment of Pseudomonas aeruginosa. *Applied and Environmental Microbiology* 60:2355-2359.
53. Prigent-Combaret, C., O. Vidal, C. Dorel, and P. Lejeune. 1999. Abiotic surface sensing and biofilm-dependent regulation of gene expression in Escherichia coli. *Journal of Bacteriology* 181:5993-6002.
54. Stanley, N.R., and B.A. Lazazzera. 2004. Environmental signals and regulatory pathways that influence biofilm formation. *Molecular Microbiology* 52:917-924.
55. Fux, C.A., S. Wilson, and P. Stoodley. 2004. Detachment characteristics and oxacillin resistance of Staphyloccocus aureus biofilm emboli in an in vitro catheter infection model. *Journal of Bacteriology* 186:4486-4491.
56. Hunt, S.M., E.M. Werner, B. Huang, M.A. Hamilton, and P.S. Stewart. 2004. Hypothesis for the rolse of nutrient starvation in biofilm detachment. *Applied and Environmental Microbiology* 70:7418-7425.
57. Whiteley, M., M.G. Bangera, R.E. Bumgarner, M.R. Parsek, G.M. Teitzel, S. Lory, and E.P. Greenberg. 2001. Gene expression in Pseduomonas aeruginoas biofilms. *Nature* 413:860-864.
58. Paddick, J.S., S.R. Brailsford, E.A.M. Kidd, S.C. Gilbert, and D.T. Clark. 2003. Effect of the environment on genotypic diversity of *Actinomyces naeslundii* and *Streptococcus oralis* in the oral biofilm. *Applied and Environmental Microbiology* 69:6475-6480.
59. Davies, D.G., M.R. Parsek, J.P. Pearson, B.H. Iglewski, J.W. Costerton, and E.P. Greenberg. 1998. The involvement of cell-to-cell signals in the development of bacterial biofilm. *Science* 280:295-298.
60. Loo, C.Y., D.A. Corliss, and N. Ganeshkumar. 2000. *Streptococcus godonii* biofilm formation: identification of genes that code for biofilm phenotypes. *Journal of Bacteriology* 182:1374-1382.
61. Winson, M.K., M. Camara, A. Latifi, M. Foglino, S.R. Chhabra, M. Daykin, M. Bally, V. Chapon, G.P.C. Salmond, B.W. Bycroft, A. Lazdunski, G.S.A.B. Stewart, and P. Williams. 1995. Multiple *N*-acyl-L-homoserine lactone signal molecules regulate production of virulence determinants and secondary metabolites in *Pseudomonas aeruginosa*. *Proceedings of the National Academy of Sciences of the United States of America* 92:9427-9431.

62. Smith, R.S., and B.H. Iglewski. 2003. *P. aeruginosa* quorum sensing systems and virulence. *Current Opinion in Microbiology* 6:56-60.
63. Sokol, P.A., U. Sajjan, M.B. Visser, S. Gingues, J. Forstner, and C. Kooi. 2003. The CepIR quorum-sensing system contributes to the virulence of *Burkholderia cenocepacia* respiratory infections. *Microbiology* 149:3649-3658.
64. Kleerebezem, M., L.E.N. Quadri, O.P. Kuipers, and W.M.d. Vos. 1997. Quorum sensing by peptide pheromones and two-component signal-transduction in Gram-positive bacteria. *Molecular Microbiology* 24:895-904.
65. Batchelor, S.E., M. Cooper, S.R. Chhabra, L.A. Glover, G.S.A.B. Stewart, P. Williams, and J.I. Prosser. 1997. Cell density-regulated recovery of starved biofilm populations of ammonia-oxidizing bacteria. *Applied and Environmental Microbiology* 63:2281-2286.
66. Puskas, A., E.P. Greenberg, S. Kaplan, and A.L. Schaefer. 1997. A quorum-sensing system in the free-living photosynthetic bacterium *Rhodobacter sphaeroides*. *Journal of Bacteriology* 179:7530-7537.
67. Zobell, C.E. 1943. The effect of solid surfaces upon bacterial activity. *Journal of Bacteriology* 46:39-59.
68. Marshall, K.C., R. Stout, and R. Mitchell. 1971. Mechanism of the initial events in the sorption of marine bacteria to surfaces. *Journal of General Microbiology* 68:337-348.
69. McEldowney, S., and M. Fletcher. 1986. Variability in the influence of physicochemical factors affecting bacterial adhesion to polystyrene substrata. *Applied and Environmental Microbiology* 52:460-465.
70. Hermansson, M. 1999. The DLVO theory in microbial adhesion. *Colloids and Surfaces B: Biointerfaces* 14:105-119.
71. Razatos, A., Y.-L. Ong, M.M. Sharma, and G. Georgiou. 1998. Molecular determinants of bacterial adhesion monitored by atomic force microscopy. *Proceedings of the National Academy of Sciences of the United States of America* 95:11059-11064.
72. Jucker, B.A., H. Harms, and A.J.B. Zehnder. 1998. Polymer interactions between five gram-negative bacteria and glass investigated using LPS micelles and vesicles as model systems. *Colloids and Surfaces B: Biointerfaces* 11:33-45.
73. Vadillo-Rodriguez, V., H.J. Busscher, W. Norde, and H.C.v.d. Mei. 2002. Softness of the bacterial cell wall of *Streptococcus mitis* as probed by microelectrophoresis. *Electrophoresis* 23:2007-2011.
74. Poortinga, A.T., R. Bos, W. Norde, and H.J. Busscher. 2002. Electric double layer interactions in bacerial adhesion to surfaces. *Surface Science Reports* 47:1-32.
75. Abu-Lail, N.I., and T.A. Camesano. 2003. Role of lipopolysaccharides in the adhesion, retention, and transport of *Escherichia coli* JM109. *Environmental Science and Technology* 37:2173-2183.
76. Walker, S.L., J.A. Redman, and M. Elimelech. 2004. Role of cell surface lipopolysaccharides in *Escherichia coli* K12 adhesion and transport. *Langmuir* 20:7736-7746.

77. Fletcher, M., and G.I. Loeb. 1979. Influence of substratum characteristics on the attachment of a marine pseudomonad to solid surfaces. *Applied and Environmental Microbiology* 37:67-72.
78. Ong, Y.-L., A. Razatos, G. Georgiou, and M.M. Sharma. 1999. Adhesion forces between *E. coli* bacteria and biomaterial surfaces. *Langmuir* 15:2719-2725.
79. Gristina, A.G. 1987. Biomaterial-centered infection: microbial adhesion versus tissue integration. *Science* 237:1588.
80. An, Y.H., and R.J. Friedman. 1998. Concise review of mechanisms of bacterial adhesion to biomaterial surfaces. *Journal of Biomedical Materials Research* 43:338-348.
81. Madigan, M.T., J.M. Martinko, and J. Parker. 2000. Chapter 3 Cell Biology. In Brock Biology of Microorganisms, Ninth Edition. Prentice-Hall, Upper Saddle River.
82. Jucker, B.A., S.J. Hug, and A.J.B. Zehnder. 1997. Adsorption of bacterial surface polysaccharides on mineral oxides is mediated by hydrogen bonds. *Colloids and Surfaces B: Biointerfaces* 9:331-343.
83. Omoike, A., and J. Chorover. 2004. Spectroscopic study of extracellular polymeric substances from *Bacillus subtilis*: Aqueous chemistry and adsorption effects. *Biomacromolecules* 5:1219-1230.
84. Tsuneda, S., J. Jung, H. Hayashi, H. Aikawa, A. Hirata, and H. Sasaki. 2003. Influence of extracellular polymers on electrokinetic properties of heterotrophic bacterial cells examined by soft particle electrophoresis theory. *Colloids and Surfaces B: Biointerfaces* 29:181-188.
85. Fernandez, L.A., and J. Berenguer. 2000. Secretion and assembly of regular surface structures in Gram-negative bacteria. *FEMS Microbiology Reviews* 24:21-44.
86. Sourenko, E.V., V. Chesnokova, D.E. Dykhuizen, I. Ofek, X.-R. Wu, K.A. Krogfelt, C. Struve, M.A. Schembri, and D.L. Hasty. 1998. Pathogenic adaptation of *Escherichia coli* by natural variation of the FimH adhesin. *Proceedings of the National Academy of Sciences of the United States of America* 95:8922-8926.
87. Madigan, M.T., J.M. Martinko, and J. Parker. 2000. Chapter 5 Microbial Growth. In Brock Biology of Microorganisms, Ninth Edition. Prentice-Hall, Upper Saddle River.
88. Boonaert, C.J.P., Y.F. Dufrene, S.R. Derclaye, and P.G. Rouxhet. 2001. Adhesion of Lactococcus lactis to model substrata: direct study of the interface. *Colloids and Surfaces B: Biointerfaces* 22:171-182.
89. Walker, S.L., J.E. Hill, J.A. Redman, and M. Elimelech. 2005. Influence of growth phase on adhesion kinetics of *Escherichia coli* D21g. *Applied and Environmental Microbiology* 71:3093-3099.
90. Walker, S.L., J.A. Redman, and M. Elimelech. 2005. Influence of growth phase on bacterial deposition: Interaction mechanisms in packed-bed column and radial stagnation point flow systems. *Environmental Science and Technology* 39:6405-6411.
91. Chavant, P., B. Martinie, T. Meylheuc, M.-N. Bellon-Fontaine, and M. Hebraud. 2002. *Listeria monocytogenes* LO28: Surface physicochemical properties and

ability to form biofilms at different temperatures and growth phases. *Applied and Environmental Microbiology* 68:728-737.

92. dePedro, M.A., J.C. Quintela, J.-V. Holtje, and H. Schwarz. 1997. Murein segregation in *Escherichia coli*. *Journal of Bacteriology* 179:2823-2834.
93. Jones, J.F., J.D. Feick, D. Imoudu, N. Chukwumah, M. Vigeant, and D. Velegol. 2003. Oriented adhesion of *Escherichia coli* to polystyrene particles. *Applied and Environmental Microbiology* 69:6515-6519.
94. Jones, J.F., and D. Velegol. 2006. Laser trap studies of end-on *E. coli* adhesion to glass. *Colloids and Surfaces B: Biointerfaces* 50:66-71.
95. Jones, J.F., D. Waters, M. Flamm, and D. Velegol. 2006. Orientation of irreversible adhesion of spherical particles on prolate spheroidal collectors. *Journal of Colloid and Interface Science* 299:696-702.
96. Bakker, D.P., B.R. Postmus, H.J. Busscher, and H.C.v.d. Mei. 2004. Bacterial strains isolated from different niches can exhibit different patterns of adhesion to substata. *Applied and Environmental Microbiology* 70:3758-3760.
97. Bos, R., H.C.v.d. Mei, J. Gold, and H.J. Busscher. 2000. Retention of bacteria on a substratum surface with micro-patterned hydrophobicity. *FEMS Microbiology Letters* 189:311-315.
98. Bruinsma, G.M., H.C.v.d. Mei, and H.J. Busscher. 2001. Bacterial adhesion to surface hydrophilic and hydrophobic contact lenses. *Biomaterials* 22:3217-3224.
99. Faille, C., C. Julien, F. Fontaine, M.-N. Bellon-Fontaine, C. Slomianny, and T. Benezech. 2002. Adhesion of Bacillus spores and Escherichia coli cells to inert surfaces: role of surface hydrophobicity. *Canadian Journal of Microbiology* 48:728-738.
100. Vadillo-Rodriguez, V., H.J. Busscher, H.C.v.d. Mei, J.d. Vries, and W. Norde. 2005. Role of lactobacillus cell surface hydrophobicity as probed by AFM in adhesion to surfaces at low and high ionic strength. *Colloids and Surfaces B: Biointerfaces* 41:33-41.
101. Hayes, M.H.B. 1998. Chapter 1. In Humic Substances: Structures, Properties and Uses. G. Davies, E.A. Ghabbour, and K.A. Khairy, editors. Royal Society of Chemistry, Cambridge.
102. Nealson, K.H. 1977. Autoinduction of bacterial luciferase: occurrence, mechanism and significance. *Archives of Microbiology* 112:73-79.
103. Nealson, K.H., T. Platt, and J.W. Hastings. 1970. Cellular control of the synthesis and activity of the bacterial luminescent system. *Journal of Bacteriology* 104:313-322.
104. Ramsey, W.S., and M. Dworkin. 1968. Microcyst germination in *Myxococcus xanthus*. *Journal of Bacteriology* 95:2249-2257.
105. Tomasz, A. 1965. Control of the competent state in *Pneumococcus* by a hormone-like cell product: an example for a new type of regulatory mechanism in bacteria. *Nature* 208:155-159.
106. Fuqua, C., and E.P. Greenberg. 2002. Listening in on bacteria: acyl-homoserine lactone signaling. *Nature Reviews Molecular Cell Biology* 3:685-695.
107. Lazazzera, B.A., and A.D. Grossman. 1998. The ins and outs of peptide signaling. *TRENDS in Microbiology* 6:288-294.

108. Chen, X., S. Schauder, N. Potier, A.V. Dorsselaer, I. Pelczer, B.L. Bassler, and F.M. Hughson. 2002. Structural identification of a bacterial quorum-sensing signal containing boron. *Nature* 415:545-549.
109. Bassler, B.L., M. Wright, R.E. Showalter, and M.R. Silverman. 1993. Multiple signaling systems controlling expression of luminescence in *Vibrio harveyi*: sequence and function of genes encoding a second sensory pathway. *Molecular Microbiology* 9:773-786.
110. Xavier, K.B., and B.L. Bassler. 2005. Regulation of uptake and processing of the quorum sensing autoinducer AI-2 in *Escherichia coli*. *Journal of Bacteriology* 187:238-248.
111. Bassler, B.L., E.P. Greenberg, and A.M. Stevens. 1997. Cross-species induction of luminescence in the quorum sensing bacterium *Vibrio harveyi*. *Journal of Bacteriology* 179:4043-4045.
112. Xavier, K.B., and B.L. Bassler. 2005. Interference with AI-2-mediated bacterial cell-cell communication. *Nature* 437:750-753.
113. Redfield, R.J. 2002. Is quorum sensing a side effect of diffusion sensing? *TRENDS in Microbiology* 10:365-370.
114. Hense, B.A., C. Kuttler, J. Muller, M. Rothballer, A. Hartmann, and J.-U. Kreft. 2007. Does efficiency sensing unify diffusion and quorum sensing? *Nature Reviews Microbiology* 5:230-239.
115. Basu, S., Y. Gerchman, C.H. Collins, F.H. Arnold, and R. Weiss. 2005. A synthetic multicellular system for programmed pattern formation. *Nature* 434:1130-1134.
116. Miller, M.B., and B.L. Bassler. 2001. Quorum sensing in bacteria. *Annual Review of Microbiology* 55:165-199.
117. Waters, C.M., and B.L. Bassler. 2005. Quorum sensing: cell-to-cell communication in bacteria. *Annual Review of Cell and Developmental Biology* 21:319-346.

Chapter 3

Experimental Methods

3.1 Bacteria preparation

3.1.1 *Escherichia coli* K-12 D21

E. coli K-12 strain D21 was obtained from the *E. coli* Genetic Stock Center, (Yale University, Department of Biology, New Haven, CT). *E. coli* K-12 is a well-characterized (1), common soil bacterium used in bioremediation (2). The strain D21 has the core polysaccharide portion of the LPS layer. Bacteria were grown in Luria Bertani (LB) broth (Amresco, Solon, OH) at 37^{o}C on a radial shaker table (Queue Systems, Parkersburg, WV) at 150 rpm. At the mid-exponential phase of growth, bacteria were harvested for experimentation. The time for mid-exponential growth was found from growth curves determined in our laboratory. *E. coli* K-12 strain D21 had a doubling time of 35 minutes and a mid-exponential phase that occurred 2.5 hours after inoculation. Cell preparation for experimentation involved a series of three washes in phosphate buffered saline (PBS) solution (pH 7.3, 60 mM ionic strength- potassium dihydrogen phosphate and dipotassium monohydrogen phosphate) with centrifugation (Sorvall, Asheville, NC) at 3500 $\times$ g for 10 minutes. The pH and conductivity (Fisher Scientific Accumet Research AR50, Waltham, MA) of the PBS was measured for every sample to check consistency. The bacteria concentration was kept constant between samples by checking

absorbance with a Helios UV-visible spectrophotometer (Thermo Electron Corp., Waltham, MA) and adjusting cell concentration if necessary.

3.1.2 *Vibrio fischeri*

V. fischeri (ATCC Number 7744, Manassas, VA) was revived from a freeze-dried sample in Marine Broth (Difco 2216, Becton, Dickinson and Co., Franklin Lakes, NJ) and stocks were stored on Microbank solid porous bead carriers (Pro-Lab Diagnostics, Richmond Hill, ON) in a liquid nitrogen cryogenic refrigerator (Taylor-Wharton, Theodore, AL). Stock cells were revived in autoclaved sterile photobacterium broth (PB). The medium ingredients were based on Photobacterium Broth (Fluka 38719, Buchs, Switzerland) but modified to reduce precipitation, and thus medium turbidity, which influences luminescence measurements. The PB medium contained, in g/L deionized (DI) water (Millipore, Billerica, MA): potassium dihydrogen phosphate (3.0 g/L), ammonium chloride (0.3), sodium chloride (30), iron (II) sulfate heptahydrate (0.01), magnesium sulfate heptahydrate (0.3), sodium β-glycerophosphate pentahydrate (23.5), tryptone (5), yeast extract (2.5), calcium chloride dihydrate (0.15), and sodium bicarbonate (1.0).

Once the revived culture reached the stationary phase of growth the cells were transferred to an absorbance of 0.01 at a wavelength of 600 nm measured in a UV-vis spectrophotometer, corresponding to a bulk cell concentration of $1.88 \pm 0.5 \times 10^6$ cells/mL. Harvest for experimentation from this sub-culture occurred near the start of the stationary phase when the luminescence per cell reached a maximum.

All cell growth was in sterile culture tubes and flasks filled to a volume 1/5 of the total container volume to allow for proper oxygenation. Incubation conditions were 30°C and 200 rpm on a radial shaker.

3.1.3 *Pseudomonas aeruginosa*

P. aeruginosa PAO1, a well-characterized and common environmental and pathogenic bacterium (3), was obtained from the Penn State Department of Civil and Environmental Engineering (Logan Lab, originally obtained from Parsek Lab, Northwestern University Department of Civil and Environmental Engineering, Evanstan, IL). The cultures were revived from a frozen stock in LB broth at 37°C on a radial shaker at 150 rpm until the stationary phase of growth. At that time, cells were diluted via a transfer into fresh LB broth and grown to the mid-exponential phase (130 minutes with a 30-minute doubling time). Mid-exponential phase cell concentration was verified with a UV-vis spectrophotometer.

P. aeruginosa cells for use in patterned array experiments via laser trapping (see section 3.3.1) were prepared by diluting in fresh LB broth to the desired experimental cell concentration and then loading into the sample holder.

3.1.4 General bacteria preparation comments

A summary of the bacteria and growth conditions is given in Table **3-1**. All glass growth flasks were sterilized by autoclaving, washing with Alconox cleaner, and

autoclaving again. The *E. coli* and *V. fischeri* strains used in this thesis work are biosafety level 1, whereas *P. aeruginosa* PAO1 is biosafety level 2, which means it is an opportunistic pathogen and will affect immuno-compromised individuals. Safety glasses and gloves were donned for all work with bacteria and transfers were conducted under a laminar flow hood (Labconco class II biosafety cabinet delta series, Kansas City, MO). Bacteria waste was stored in biohazard receptacles and autoclaved before disposal. Biosafety level 2 waste was always stored under the laminar flow hood. Surfaces were cleaned with 70% ethyl alcohol before and after experiments and any major spills were cleaned with 10% bleach solutions. Aseptic technique was utilized for all bacteria procedures.

Table 3-1: A summary of the bacteria and growth conditions.

organism	biosafety level	growth medium	growth T (oC)	agitation (rpm)	~growth time (min)
E. coli K-12 D21	1	LB	37	150	150
V. fischeri	1	PB	30	200	600
E. coli QSg	1	M9 minimal	30	200	480
P. aeruginosa	2	LB	37	150	130

3.2 Humic acid adsorption & analyses

3.2.1 Humic acid adsorption to silica

Humic acid solutions were made from humic acid sodium salt technical grade H16752 (Sigma-Aldrich Co., St. Louis, MO) dissolved in DI water and were set to pH 7 with hydrochloric acid. The literature reports the molecular weight to be 4100 g/mol (4).

No further purification of the humic acid was conducted before the adsorption procedure, considering the inorganic components as part of the structure. Some previous studies using commercial humic acid have purified it to remove ash (4, 5), salts (6), and metals (4), whereas others did not (7-9).

Silica particles of 0.9-μm diameter (Bangs Laboratories, Inc., Fishers, IN) were coated with humic acid by placing the particles in a humic acid solution on a roller for continuous settling overnight at ambient temperature. Particles were neither cleaned nor altered before the adsorption process. After the adsorption procedure, particles were washed three times using PBS with centrifugation at 3500 × g for 10 minutes. Particle concentration was kept constant between samples. A borosilicate electrophoresis cell (10) was coated with humic acid by soaking the cell in humic acid solution overnight. Glassware was cleaned with Alconox cleaner and the electrophoresis cell was sonicated (VWR 550T, West Chester, PA) and then soaked in nitric acid overnight before use.

3.2.2 Zeta potential measurements

To verify that humic acid adsorbed to the particles, zeta (ζ) potentials were measured for particles from each humic acid coating solution using ZetaPALS (Brookhaven Instruments Corp., Holtsville, NY) in the Smoluchowski equation mode at 25^{o}C. Surfaces exposed to polyelectrolyte solutions like humic acid acquire electrical charge, which can be exploited for quantification of the adsorbed layer (11). Electrophoretic mobility measurements of coated substances were used to characterize changes in surface charge properties (8, 12), ascertaining the effectiveness of the coating

process. Other techniques exist for measuring humic acid adsorption, including elemental analysis of particle organic carbon content (11, 13, 14) and UV-vis spectrophotometry for suspending media absorbance before and after adsorption (6, 7, 15). However, the ζ potential measurements were simple to conduct directly on the particles, and enabled the detection of less than 3 μg of adsorbed humic acid in 10 mL.

3.2.3 Adherence to hydrocarbons (ATH) tests

Hydrophobicity of the bare and humic acid-coated silica particles was determined in an adherence to hydrocarbon (ATH) test. ATH test results vary with aqueous phase ionic strength, mixing time, particle concentration, and the oil phase total volume (16). The same conditions were used in the ATH experiments as in the humic acid adsorption. The particles were placed in acid-washed 12 × 75 mm borosilicate glass tubes (Kimble, Vineland, NJ) with 1.3 mL DI water. 0.3 mL hexadecane (Mallinckrodt Baker, Phillipsburg, NJ) was added and the solution was vortexed (VWR, West Chester, PA) for 2 minutes. After 15 minutes to allow for phase separation, the aqueous phase was pipetted out and the absorbance was measured with a UV-vis spectrophotometer at wavelength λ = 600 nm, calibrated for particle concentration. The percent difference in absorbance between the ATH test sample and the original particle suspension represents the percent of particles adhering to the hydrocarbon phase and thus the particle hydrophobicity. The results were also easily visible by eye and microscope images of the ATH samples revealed that most particles partitioned inside the oil droplets.

3.3 Cell localizations on glass surfaces

3.3.1 Laser trap

The optical trap was set up by aligning a 2.5 W neodymium-doped yttrium aluminium garnet (Nd:YAG) 1064 nm infrared laser (Compass 1064-2500MN, Coherent Inc., Santa Clara, CA) into the epi-port of an inverted transmitted light microscope (Nikon Eclipse TE 2000-U, Melville, NY). The beam was sent into the back aperture of a 100× oil objective (NA 1.3) and off a dichroic mirror. A collimating 20× beam expander (Newport HB-20X, Irvine, CA) was used so the laser completely filled the objective aperture. A "trapped" bacterium remains in place because any movements out of the highest light intensity region cause refraction, which produces a force that restores displacement of the cell from the focal point (17) (Figure **3-1**).

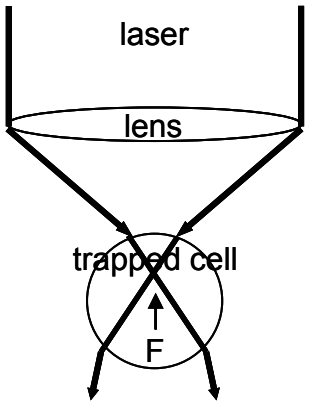

Figure 3-1: Schematic of laser trap with a trapped bacterium.

Log phase *P. aeruginosa*, loaded in either an electrophoresis or flow cell, was spatially manipulated in the sample holder with the laser trap, taken from the bulk suspension and brought into contact with the glass surface. This was repeated with

individual cells until the desired array with $n \times n$ bacteria spaced L μm apart was complete (Figure **3-2**).

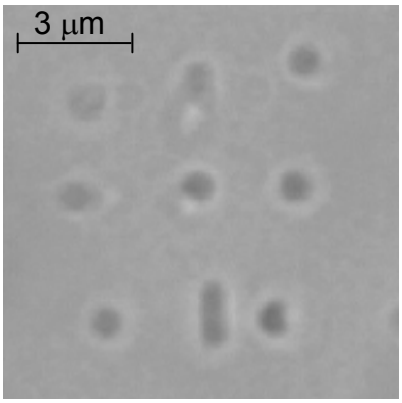

Figure 3-2: A representative 3 × 3 engineered biofilm bacteria array made with *E. coli* K-12 D21 with the laser trap technique (L = 3μm).

3.3.2 Nanofabrication

Nanofabrication of glass slides can produce arrays of large n and exact L, which cannot be obtained by laser trapping. A polydimethylsiloxane (PDMS) (Dow Corning Sylgard 184, Midland, MI) stamp was formed from a silicon master that is patterned with L-spaced $n \times n$ arrays by photolithography through a photomask (Figure **3-3**). The photomask was made in a Heidelberg DWL66 laser writer. The production of the photomask and master was executed in the Penn State Nanofabrication Facility (Materials Research Institute, University Park, PA).

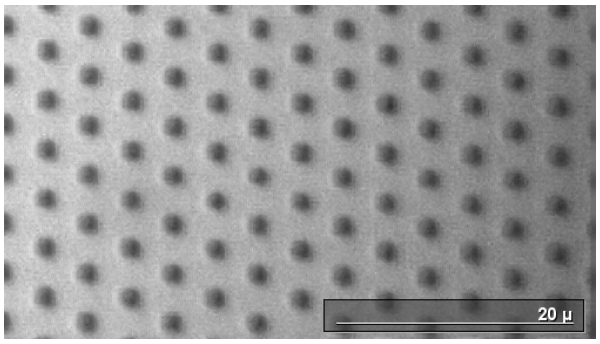

Figure 3-3: One of the photomasks produced using the Nanofabrication Facility's laser writer. This particular mask contains hexagonally-packed features. The scale bar is 20 μm.

The PDMS stamp was coated with either a positive or negative bacterial adhesion agent. Positive adhesion agents used to enhance adhesion were poly-D-lysine (PDL) (Sigma-Aldrich Co., St. Louis, MO) and poly (ethylene imine) (PEI) (Sigma-Aldrich Co., St. Louis, MO) and the negative adhesion agent used to prevent adhesion was polyethylene glycol (PEG) silane (2-[methoxy(polyethylenoxy)propyl]trimethoxy silane, Gelest, Inc., Morrisville, PA). The agent was transferred to a glass coverslip via stamping and the result was a surface with patterned patches of positive or negative adhesion agent. *P. aeruginosa* PAO1 suspensions were introduced to the surface for preferential cell adhesion in pattern formation to make engineered biofilms with various spacing L and cell number n.

3.3.3 Random adhesion

3.3.3.1 *V. fischeri* in well plate

Bulk cell concentration of harvested cells was fixed by dilution in PB and verification in the spectrophotometer. Bulk suspensions were transferred to a depth of 500 μm in a microwell (1.3-cm diameter) on a 24-well glass plate (MatTek, Ashland, MA). The glass plate surface was cleaned before cell introduction by sonication with an Alconox soap solution, then sonication with 70% ethyl alcohol, and finally soaking in 6 M hydrochloric acid for at least 1 hour. Each step was followed by copious rinsing with DI water. Sterilization of the surface was ensured before the glass cleaning procedure was executed by exposing to ultra-violet light for at least 20 minutes.

Surface cell density was varied by using different initial bulk concentrations and allowing those cells to settle and adhere to the glass for different times. Remaining bulk cells were removed by repeated gentle rinses using slow pipetting. Bulk suspension removed was replaced with fresh PB (Figure **3-4**). This procedure was performed directly on the microscope stage, which was equipped with a stage plate custom machined in-house (Don Lucas, Penn State Chemical Engineering Department machine shop) to hold the well plate. Vibrations were reduced with the microscope set on an optical table (Newport RS1000, Irvine, CA).

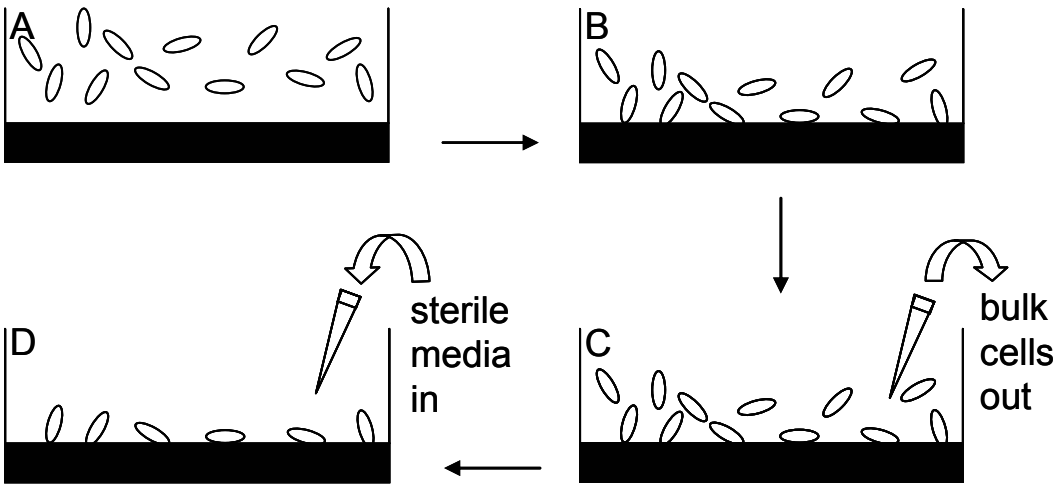

Figure 3-4: The procedure to create local surface cell densities. First, a bulk suspension of cells is introduced into the microwell (A). After allowing for settling and adhesion time (B), the bulk cells remaining in suspension are removed (C) and the solution is replaced with fresh PB (D). Steps C and D are repeated 3-5 times or until most of the bulk cells are removed from the sample. The result is a local concentration of cells on the surface of the microwell. The local cell density is controlled by adjusting the original bulk suspension cell concentration and the settling time.

3.3.3.2 *P. aeruginosa* in flow chamber

Engineered biofilms were also formed via random adhesion, which modeling of concentration profiles of excreted biomolecules in Chapter 5 shows is an acceptable approximation to patterned arrays of surface cells for reasonable experimental time scales. Controlled random adhesion was possible by varying the bulk cell concentration in the suspension and allowing the cells to settle to the coverslip for specified times. After settling time, a new dilute suspension of cells was briefly flowed through the flow chamber.

3.4 Adhesion force measurements

3.4.1 Differential electrophoresis

Adhesion forces of *E. coli* K-12 D21 on humic acid-coated glass were determined through the technique of differential electrophoresis (18, 19). Prepared bacterial suspensions were transferred into bare (uncoated) and humic acid-coated electrophoresis cells, placed on the microscope stage for observation, and connected to a current source (Keithley 2410, Cleveland, OH). The bacteria swayed by electrophoresis in the applied electric field (Figure **3-5** A and B) or broke off the wall if the field was strong enough (Figure **3-5** C). For each experimental run the applied electric field was programmed to increase in set increments while alternating between positive and negative. This allowed for ease in changing the direction of flow and for sensitive control of the applied force due to electrophoresis.

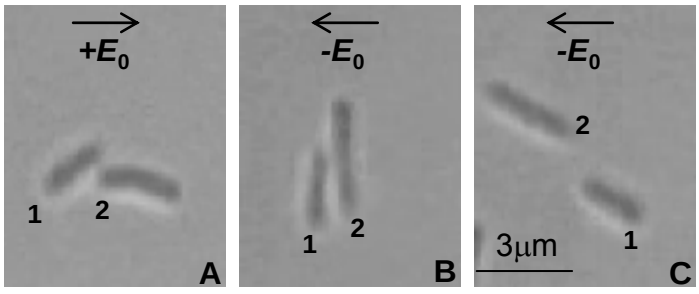

Figure 3-5: Electrophoresis images captured during adhesion force measurements. Cells swayed right (A) or left (B) in the applied electric field, depending on the direction of the electric field. When the electric field was large enough to overcome the adhesion force, bacterium 2 was sheared off the glass capillary surface (C). Bacterium 1 remains with one end still adhered.

When a bacterium sheared off the wall the electric field was recorded for adhesion force calculation. As long as the bacterium is not moving, the adhesion force (*adh*) balances the forces acting on the bacterium due to electrophoresis (*ep*) of the bacterium and electroosmosis (*eo*) within the capillary cell.

$$F_{adh} + F_{ep} + F_{eo} = 0 \tag{3.1}$$

The forces are written as scalars because they are applied along only the *x* direction. Electrophoresis is the movement of charged colloidal particles, like bacteria, in an applied electric field. The electrophoretic velocity (U_{ep}) of the bacterium that would result in the absence of the cell being anchored can be approximated by the Smoluchowski equation (19).

$$U_{ep} = \frac{\varepsilon \zeta_b E_0}{\eta} \tag{3.2}$$

ε is the dielectric permittivity of the solution, ζ_b is the ζ potential of the bacteria (determined using the ZetaPALS in the Smoluchowski equation mode at 25^{o}C), E_0 is the applied electric field, and η is the viscosity of the solution. Although this equation neglects additional fluid resistance due to the neighboring wall, the estimate is expected to be good (18).

The force (F_{ep}) required to hold the bacterium from translating at *U* due to electrophoresis can be estimated from applying Stokes law for a sphere, with an equivalent particle size (*a*).

$$F_{ep} = -6\pi\eta a U = -6\pi a \varepsilon \zeta_b E_0 \tag{3.3}$$

The sphere result was used despite the fact that the forces on a translating ellipsoid are well-known in the literature (20). Added resistance due to the wall is already neglected and the improvement in accuracy from approximating a bacterium as a spheroid would be lost.

An additional force acting on the bacterium is from the electroosmotic velocity field, which results due to electroosmosis at the walls and fluid continuity within the capillary cell. If $2h$ is the thickness of the capillary cell (i.e., its narrow dimension), and y is the distance from the center of the capillary, then

$$v(y) \approx \frac{\varepsilon \zeta_w E_0}{\eta}\left(1 - \frac{3y^2}{h^2}\right), \tag{3.4}$$

where ζ_w is the ζ potential of the wall (21). The shear stress (τ) at the wall due to electroosmosis can then be calculated as

$$\tau = \eta \left.\frac{\partial v}{\partial y}\right|_{y \to \pm h} = -\frac{6\varepsilon \zeta_w E_0}{h}. \tag{3.5}$$

If the exposed area on a single bacterium is estimated as a^2 and the force due to electroosmosis is calculated as $a^2\tau$, it is estimated that the electroosmotic force is order O(a/h) smaller than the electrophoretic force, and this factor was typically 2 orders of magnitude in the experiments. Thus, the force due to the electroosmotic velocity field within the capillary cell is neglected.

Adhesion forces of laser trap-formed biofilms were initially determined with the use of the electrophoresis cell. The original Feick electrophoresis cell (10) (Figure **3-6** A) was modified to allow for the easy surface modification of the capillary sample holder, creation of a gradient of cell concentration in the capillary, and easy clean-up of

the capillary via disposal after experimentation (Figure **3-6** B). However, it was determined that electrophoresis did not produce forces great enough (F > 7 pN) to effectively detach the *P. aeruginosa* PAO1 cells from the surface, so a flow chamber was used after initial experiments.

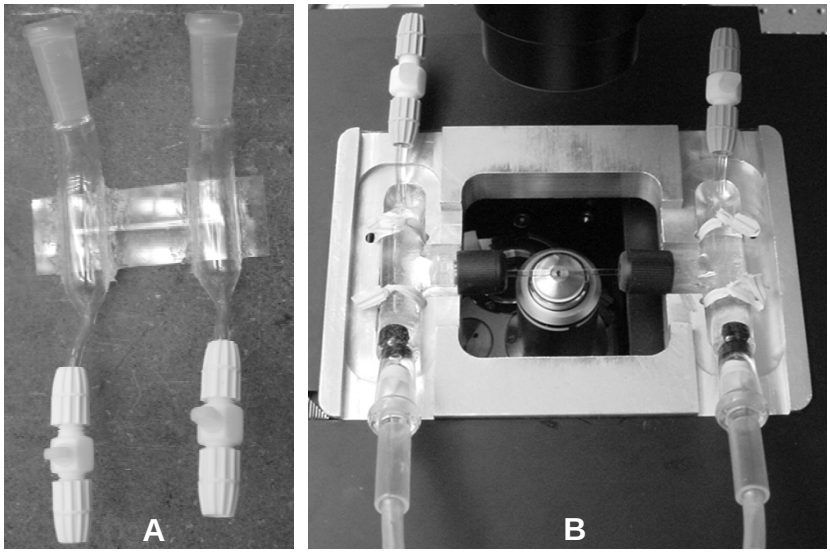

Figure 3-6: The original Feick electrophoresis cell (A) and the newly designed electrophoresis cell (B) on the microscope stage (stage plate fabricated by Don Lucas).

3.4.2 Parallel plate flow chamber

The parallel plate flow chamber used was the Focht Chamber (FC) System 2 (Bioptechs, Butler, PA), depicted in Figure **3-7**. It was assembled with cleaned borosilicate glass cover slips 40 mm in diameter (part 7 in Figure **3-7**) and a custom-made gasket (part 6, but cut with different dimensions) to give the flow chamber the following rectangular geometry: 0.25 mm high × 3 mm wide × 22 mm long. Although the chamber can be used with a temperature controller (part 1), it was not in these

experiments because ambient conditions still allowed for *P. aeruginosa* PAO1 growth. Not heating the assembly minimized the formation of air bubbles in the system.

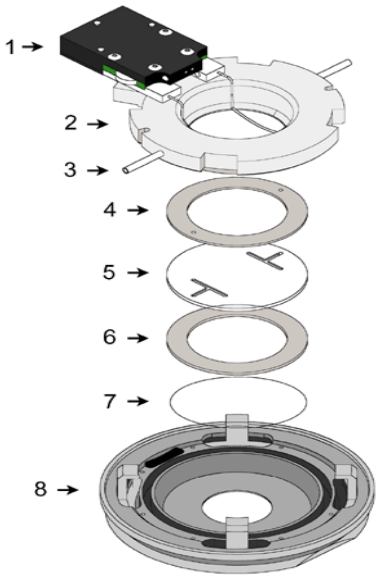

Figure 3-7: Bioptech's Focht Chamber System 2 assembly.

The chamber assembly was mounted on Nikon Eclipse TE 2000-U inverted transmitted light microscope and connected to a Harvard PHD 22/2000 syringe pump (Harvard Apparatus, Holliston, MA) with 1/16"-inner diameter Tygon tubing (St. Gobain, Akron, OH). The surface cells were then exposed to a series of increasing flow rates and the detachment was noted.

Forces were calculated based on the following equations. From the Navier-Stokes equation in Cartesian coordinates, the velocity profile ($v(z)$) across the capillary height (h) is,

$$v(z) = \frac{\Delta P}{2\eta L}\left(z^2 - zh\right), \tag{3.6}$$

where ΔP is the pressure differential across the capillary, η is the fluid viscosity, and L is the capillary length. The shear stress τ at the surface is,

$$\tau = -\eta \left. \frac{\partial v}{\partial z} \right|_{z=0} = \frac{\Delta P h}{2L}. \tag{3.7}$$

Also, integrating the velocity profile (Equation **3.6**) over the cross-sectional area of the capillary ($w \times h$) results in the flow rate, Q.

$$Q = \frac{\Delta P w h^3}{12 \eta L} \tag{3.8}$$

Substituting Q into the shear stress expression (Equation **3.7**) results in

$$\tau = \frac{6 Q \eta}{w h^2}. \tag{3.9}$$

Finally, adhesion force F is determined through τ. The definition of shear stress is,

$$\tau = \frac{F}{A}, \tag{3.10}$$

where A is the exposed area of a bacterium.

3.5 Microscopy

3.5.1 Bacterial adhesion and orientation on humic acid silica particles

Bacteria and particle suspensions were combined in a 50-mL Falcon tube (Becton, Dickinson and Co., Franklin Lakes, NJ) after the wash procedure and were mixed by vortexing the 50-mL Falcon tube containing the sample. The tube was then placed on a roller for 1 hour to allow for adhesion. The sample was pipetted into a capillary tube

(VitroCom, Mountain Lakes, NJ) with inner dimensions 0.2 mm thick × 2.0 mm wide × 5 cm long that was mounted on a standard microscope slide. The suspension was viewed with an inverted transmitted light microscope (Nikon TE 300 Eclipse, Melville, NY) with a 100× oil objective in differential interference contrast (DIC) mode. Images were captured with a CCD camera (Cohu, San Diego, CA) and Scion frame grabber (Scion Corp., Frederick, MD). The resulting couplets were counted, and the bacterium-particle adhesion location (middle or end) was noted (Figure **3-8**).

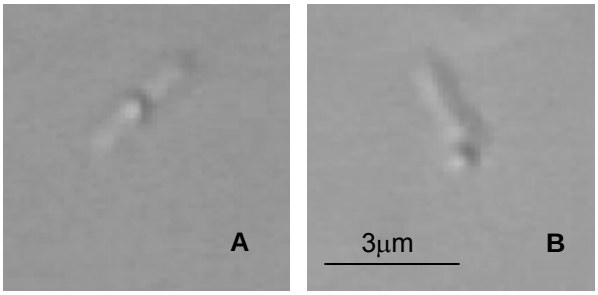

Figure 3-8: Couplet images captured during adhesion percentage and orientation measurements. Orientation was observed as either middle (A), or end-on (B).

To ensure that couplets were counted only once, observation was started at one end of the capillary and moved along its length in one direction. Couplets at each position along the tube length were counted starting from the capillary surface, and moving into the solution as far as possible before moving to the next position. To verify that bacteria cell concentration was conserved between samples, the total number of cells, both single cells and adhered cells, was counted during microscopy. Particle concentration was checked by counting the number of particles in one frame that settled onto the surface of the capillary after each sample's microscopy run.

3.5.2 Engineered biofilm development and local surface cell density

The local surface cell samples were viewed with the Nikon Eclipse TE 2000-U transmitted light inverted microscope with a 40× objective. When using the well plate open systems, sample depths were maintained at a depth of 500 μm by monitoring the glass-sample and sample-air interfaces' *z* axis positions and adding fresh medium if necessary. Images were captured with a CCD camera and Scion frame grabber. Cell density was quantified by adjusting the images' threshold values and using the area density measurement function in ImageJ image processing program or by using a visual direct count of the cells in the images.

3.5.3 Quorum sensing luminescence measurements

V. fischeri luminescence was quantified with a photomultiplier tube (PMT) (Hamamatsu photosensor module H6780, Hamamatsu City, Japan) placed in the front port of the microscope. The PMT gain setting was set to the maximum recommended 0.9 V to maximize the signal and a 10× objective was used to allow more light from the sample to enter the PMT. Luminescence was monitored with the Keithley 2410 source meter configured to source no voltage and measure the current from the PMT. The linear response of the PMT was verified in a calibration with multiple light bulbs. Ambient light was minimized with turned-off lights, window and door coverings, and a microscope housing that blocked all light going to the PMT except *V. fischeri*

luminescence. Luminescence was reported in W/cell; for the emission wavelength 500 nm, there are 2.5×10^{12} photons/s in 1 W.

3.6 References

1. Blattner, F.R., G.P. III, G.A. Block, N.T. Perna, V. Burland, M. Riley, J. Collado-Vides, J.D. Glasner, C.K. Rode, G.F. Mayhew, J. Gregor, N.W. Davis, H.A. Kirkpatrick, M.A. Goeden, D.J. Rose, B. Mau, and Y. Shao. 1997. The complete genome sequence of Escherichia coli K-12. *Science* 277:1453-1469.
2. Jin, G., and J. Andrew J. Englande. 1997. Effects of electron donor, dissolved oxygen, and oxidation-reduction potential biodegradation of carbon tetrachloride by *Escherichia coli* K-12. *Water Environment Research* 69:1100-1105.
3. Stover, C.K., X.Q. Pham, A.L. Erwin, S.D. Mizoguchi, P. Warrener, M.J. Hickey, F.S.L. Brinkman, W.O. Hufnagle, D.J. Kowalik, M. Lagrou, R.L. Garber, L. Goltry, E. Tolentino, S. Westbrock-Wadman, Y. Yuan, L.L. Brody, S.N. Coulter, K.R. Folger, A. Kas, K. Larbig, R.L.K. Smith, D. Spencer, G.K.-S. Wong, Z. Wu, I.T. Paulsen, J. Reizer, M.H. Saier, R.E.W. Hancock, S. Lory, and M.V. Olsen. 2000. Complete genome sequence of Pseudomonas aeruginosa PA01, an opportunistic pathogen. *Nature* 406:959-964.
4. Chin, Y.-P., G. Aiken, and E. O'Loughlin. 1994. Molecular weight, polydispersity, and spectroscopic properties of aquatic humic substances. *Environmental Science and Technology* 28:1853-1858.
5. Ochs, M., B. Cosovic, and W. Stumm. 1994. Coordinative and hydrophobic interaction of humic substances with hydrophilic Al_2O_3 and hydrophobic mercury surfaces. *Geochimica et Cosmochimica Acta* 58:639-650.
6. Koopal, L.K., Y. Yang, A.J. Minnaard, P.L.M. Theunissen, and W.H.V. Riemsdijk. 1998. Chemical immobilisation of humic acid on silica. *Colloids and Surfaces A: Physicochemical and Engineering Aspects* 141:385-395.
7. Fein, J.B., J.-F. Boily, K. Guclu, and E. Kaulbach. 1999. Experimental study of humic acid adsorption onto bacteria and Al-oxid mineral surfaces. *Chemical Geology* 162:33-45.
8. Yuan, W., and A.L. Zydney. 2000. Humic acid fouling during ultrafiltration. *Environmental Science and Technology* 34:5043-5050.
9. Klavins, M., and L. Eglite. 2002. Immobilisation of humic substances. *Colloids and Surfaces A: Physicochemical and Engineering Aspects* 203:47-54.
10. Feick, J.D., and D. Velegol. 2002. Measurements of charge nonuniformity on polystyrene latex particles. *Langmuir* 18:3454-3458.
11. Fleer, G.J., M.A.C. Stuart, M.H.M. Scheutjens, T. Cosgrove, and B. Vincent. 1998. Chapters 2 & 3. In Polymer at Interfaces. Chapman & Hall, New York.

12. Davis, C.J., E. Eschenazi, and K.D. Papdopoulos. 2002. Combined effects of Ca^{2+} and humic acid on colloid transport through porous media. *Colloid and Polymer Science* 280:52-58.
13. Davis, J.A. 1982. Adsorption of natural dissolved organic matter at the oxide/water interface. *Geochimica et Cosmochimica Acta* 46:2381-2393.
14. Lahlou, M., H. Harms, D. Springael, and J.-J. Ortega-Calvo. 2000. Infuence of soil components on the transport of polycyclic aromatic hydrocarbon-degrading bacteria through saturated porous media. *Environmental Science and Technology* 34:3649-3656.
15. Bob, M.M., and H.W. Walker. 2001. Effect of natural organic coatings on the polymer-induced coagulation of colloidal particles. *Colloids and Surfaces A: Physicochemical and Engineering Aspects* 177:215-222.
16. Rosenburg, M. 1984. Bacterial adherence to hydrocarbons: a useful technique for studying cell surface hydrophobicity. *FEMS Microbiology Letters* 22:289-295.
17. Ashkin, A. 1997. Optical trapping and manipulation of neutral particles using lasers. *Proceedings of the National Academy of Sciences of the United States of America* 94:4853-4860.
18. Velegol, D., J.L. Anderson, and S. Garoff. 1996. Determining the forces between polystyrene latex spheres using differential electrophoresis. *Langmuir* 12:4103-4110.
19. Holtzer, G.L., and D. Velegol. 2003. Force measurements between colloidal particles of identical zeta potentials using differential electrophoresis. *Langmuir* 19:4090-4095.
20. vandeVen, T.G.M. 1989. Colloidal Hydrodynamics. Academic Press, New York.
21. Hunter, R.J. 1981. Zeta Potential in Colloid Science: Principles and Applications. Academic Press, New York.

Chapter 4

E. coli Adhesion to Silica in the Presence of Humic Acid [1*]

The influence of humic acid on the adhesion of *Escherichia coli* to silica particles or glass surfaces was investigated. After adsorbing various amounts of humic acid to the particles or surfaces, bacteria were added to the sample and allowed to adhere. For the silica particles the number of bacteria-particle couplets formed were counted from video microscopy images. For the glass surfaces, a shear field was applied and the stress required to detach the bacteria was quantified. These experiments showed a slight increase in the number of couplets formed in the presence of humic acid, and also showed a slight increase in the shear stress required for detachment of the bacteria. Although an increase in adhesion number and strength was measured, the magnitude of the increase was small, indicating that humic acid plays a small role in bacterial adhesion to silica or glass surfaces.

4.1 Introduction

Bacterial adhesion is important in a variety of fields, causing inefficiencies in membrane separations (2), heat exchangers (3, 4), pipelines (5, 6), and marine applications (7). Another critical application is in bioremediation, which uses bacteria *in*

---

[*] The material in this chapter has been previously published and is reprinted from Parent and Velegol 2004 (1) with permission from Elsevier.

situ to degrade specific contaminants in industrial wastewater streams to meet regulations as well as in groundwater and aquifers for potable water (8-10). For example, *Pseudomonas* species are capable of lowering the levels of pentachlorophenol (PCP) in groundwater to meet regulatory drinking water standards (11), and *Escherichia coli* K-12 is able to remove carbon tetrachloride from polluted sites (12). Successful bioremediation processes require minimal bacterial adhesion to soil particles to maintain significant cell transport throughout the aquifer (9, 13). However, once cells distribute through the polluted volume, adhesion is necessary for biofilm formation for contaminant degradation (3). Since 70-80% of soil organic matter can consist of humic substances (14), the work in this chapter studies the impact of humic acid on bacterial adhesion to soil-like surfaces.

Humic acid is a subset of humic substances, which originate from decayed plants and animals (14). It is insoluble in water at pH below 2 (14). The complex, heterogeneous humic acid macromolecules have various conformations and sizes depending on solution pH and ionic strength, so their structure is difficult to characterize (15). Humic acid in particular contains hydrophobic aromatic rings linked by carbon chains with different functional groups, including carboxyls, phenols, alcohols, carbonyls, ethers, and esters (16), as well as amines and amides (17). The prevalence of carboxyl groups confers a negative charge (18). Humic acid forms complexes with clays, minerals, and metal ions through surface interactions, and it complexes with hydrophobic organic compounds through partitioning (19). Thus, humic acid has an important ecological function because it transports contaminants through this complexation (20,

21). Also, humic substances act as water retainers and buffers (17), and in microbial respiration humic substances serve as electron acceptors and electron donors (22).

Past studies show that when adsorbed to particles, humic acid increases particle stability and transport. This effect has been attributed to an increase in repulsive electrostatic interactions from the negatively charged humic acid for polystyrene latex (PSL) (18), iron oxide (23), and bacteria (24, 25) systems. Also, adsorbed humic acid is thought to increase steric interactions, leading to increased stability of PSL (18, 26) and iron oxide (23) particles. Adsorbed humic acid decreases binding sites for polymer bridging for increased PSL stability (18). The few studies that have focused on the effect of humic acid on bacterial adhesion show contradictory results. Johnson and Logan (24) and Lahlou et al. (25) showed that humic acid enhances bacterial transport, whereas Butterfield et al. showed that humic acid increases biofilm formation by serving as a carbon source for the organisms (27).

Numerous interactions must be considered when studying bacterial adhesion in the presence of humic acid. Bacterial adhesion events depend on the bacterial cell, the substrate surface, and the environment (28). Bacterial adhesion is often divided into two phases, reversible and irreversible, and has been described by the DLVO theory of colloid stability (29). This model accounts for electrostatic and van der Waals forces, giving the interaction energy as a function of separation distance. However, the DLVO model is often not sufficient to explain bacterial adhesion events (30-32), due in part to complexities of biological surfaces (33-37) and the presence of organic matter like humic acid (38). The surface complexities add hydrophobic (39), steric (30), and bridging (37) interactions. Irreversible adhesion occurs via short-range chemical and molecular

interactions like hydrogen, ionic, and covalent bonding (5), as well interactions involving extracellular structures including lipopolysachharides (LPS), pili, and fimbriae (40). Biofilms develop after extracellular polymeric substance (EPS) production and microcolony formation (6, 41). A further complication to describing bacterial adhesion is that the adhesion mechanisms vary depending on the particular niche of interest (42).

The first of two goals in this chapter was to examine how humic acid alters the strength of interactions between *E. coli* and silica or glass. To quantify the interactions, the number of humic acid-coated silica-bacterium couplets was counted, and then the force on the individual bacteria required to detach them from humic acid-treated glass surfaces was measured. The second goal was to examine end-on adhesion of particles to *E. coli*. Jones et al. found that non-flagellated *E. coli* K-12 preferentially adhere end-on to sulfated polystyrene latex particles and glass capillary surfaces (43). The cause of this phenomenon has not been fully elucidated, but protein localization and polarization at the adhering end of the rod-shaped cells may be an important factor. Since the number of silica-bacterium couplets was counted, it was straightforward to also count the number of particles that adhere to the *end* of the bacteria. Therefore, this count examined the generality of oriented adhesion. The finding for both of these goals is that humic acid causes only a slight increase in adhesion force and number of couplets, and no significant change in end-on adhesion of bacteria to silica particles.

4.2 Experiments

The results presented in this chapter are derived from four main sets of measurements.

1. Humic acid adsorption to silica particles based on zeta potential and ATH tests
2. Oriented *E. coli* adhesion to humic acid-silica particles via microscopy
3. *E. coli* adhesion rate to humic acid-silica particles via microscopy
4. *E. coli* adhesion forces with differential electrophoresis

The details of the experimental methods, materials, and theory are found in Chapter 3. Briefly, silica particles were coated with humic acid solutions of varying concentrations. To verify that humic acid adsorbed to the particles, zeta (ζ) potentials were measured for particles from each humic acid coating solution using ZetaPALS and the hydrophobicity of bare and humic acid-coated silica particles was determined in an adherence to hydrocarbon (ATH) test.

Mid-exponential *E. coli* K-12 strain D21 cells were suspended in phosphate buffered saline (PBS) solution and combined with the silica particles that were coated with varying concentrations of humic acid solution. The resulting couplets were counted and the orientation (middle or end) was noted (Figure **4-1**).

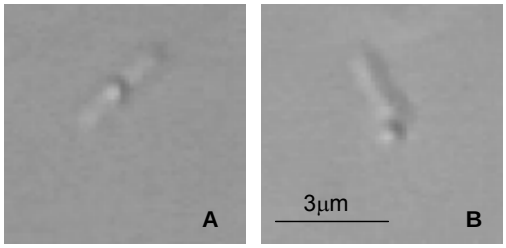

Figure 4-1: Couplet images captured during adhesion percentage and orientation measurements. Orientation was observed as either middle (A), or end-on (B).

Adhesion forces were determined through the technique of differential electrophoresis (44, 45). Prepared bacterial suspensions were transferred into uncoated (bare) and humic acid-coated electrophoresis cells, placed on the microscope stage for observation, and connected to a Keithley 2410 current source. The bacteria swayed by electrophoresis in the applied electric field (Figure **4-2** A, B) or broke off the wall if the field was strong enough (Figure **4-2** C).

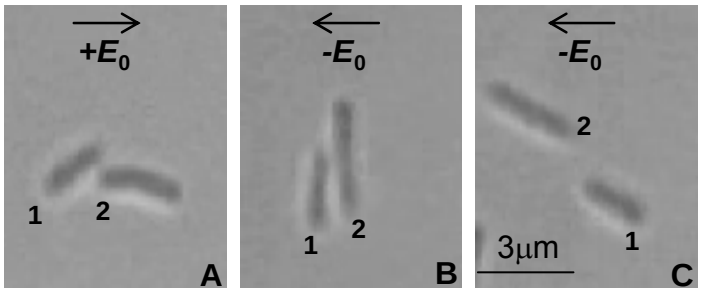

Figure 4-2: Electrophoresis images captured during adhesion force measurements. Cells swayed right (A) or left (B) in the applied electric field, depending on the direction of the electric field. When the electric field was large enough to overcome the adhesion force, bacterium 2 was sheared off the glass capillary surface (C). Bacterium 1 remains with one end still adhered.

4.3 Results & discussion

4.3.1 Humic acid adsorption

Humic acid adsorption to silica particles is evident from the ζ potential measurements (Figure **4-3**). Surfaces exposed to polyelectrolyte solutions like humic acid acquire electrical charge, which can be exploited for quantification of the adsorbed layer (46). Electrophoretic mobility measurements of coated substances were used to

characterize changes in surface charge properties (26, 47), ascertaining the effectiveness of the coating process. Other techniques exist for measuring humic acid adsorption, including elemental analysis of particle organic carbon content (25, 46, 48) and UV-vis spectrophotometry for suspending media absorbance before and after adsorption (18, 20, 49). However, the ζ potential measurements were simple to conduct directly on the particles, and enabled us to detect less than 3 μg of adsorbed humic acid in 10 mL.

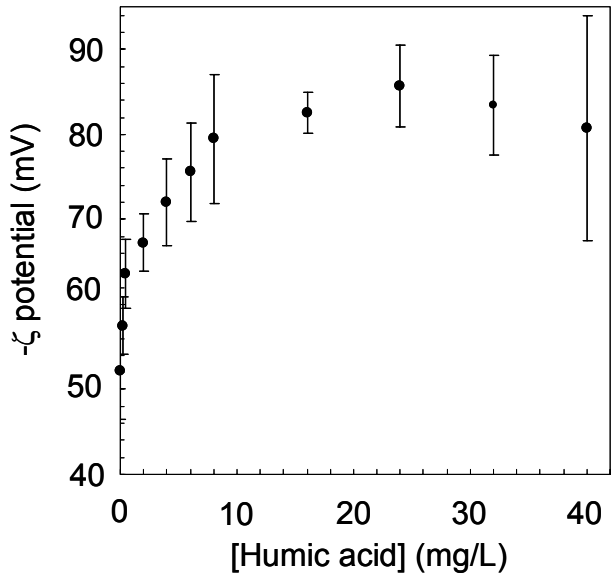

Figure 4-3: The ζ potential measurements for silica particles with humic acid adsorbed from varying bulk concentration. Each point is the average of three measurements from Zeta PALS with five runs of fifteen collecting cycles for each measurement. The error bars represent the 95% confidence interval. The higher the concentration of bulk humic acid, the more negative the ζ potential, indicating more adsorption. The ζ potential plot, representing an "adsorption isotherm", is steep at low humic acid concentrations between 0.0 and 0.4 mg/L and reaches saturation after about 8.0 mg/L.

The $|\zeta|$ increased as the bulk concentration of humic acid coating solution increased from 0.0 mg/L ($\zeta = -52 \pm 6$ mV) to 24.0 mg/L ($\zeta = -86 \pm 5$ mV). The increased $|\zeta|$ occurs with the added negative surface charge from humic acid carboxyl groups.

Humic acid saturation of the silica surface occurs at bulk concentrations of about 8.0 mg/L (Figure **4-3**). The decrease in $|\zeta|$ at bulk concentrations greater than 24.0 mg/L may arise from charge shielding by a hairy humic acid polymer layer that extends from the silica surface. To ensure that the humic acid did not desorb from the silica particles during the course of the adhesion experiments, ζ potentials were measured for both the bare particles and the 8.0-mg/L humic acid coated particles at an initial time and 1 hour later. There was no change in ζ potential, indicating there was no humic acid desorption during the 1-hour period.

It has been shown in the literature that humic acid does not adsorb onto cleaned silica surfaces because of electrostatic repulsion (23, 48); however, Figure **4-3** shows that humic acid did adsorb to untreated and uncleaned silica particles. This is perhaps due to organic or other contamination natural to these systems, which might create hydrophobic or positively-charged patches on the silica surface. Data from the literature has shown that for uncleaned silica particles, the surface charge does not become significantly greater than zero until the pH is greater than 8 (49). Therefore, electrostatic repulsion between silica and humic acid in our system was perhaps not a great influence.

The organic contamination can also cause the silica particles to be hydrophobic rather than hydrophilic. The adherence to hydrocarbons (ATH) test shows the untreated particles were indeed hydrophobic. There were 72±9% of the silica particles that partitioned to the hydrocarbon phase. In addition, the commercial humic acid used is more hydrophobic than humic acid from natural sources because of its lower carbohydrate and carboxyl content (50). Once coated with the humic acid, the particles

were less hydrophobic, with 27±10% partitioned to the hydrocarbon phase. Amphiphilic humic acid forms micelles with hydrophobic groups in the interior (19, 51, 52). Adsorption occurs after a structural rearrangement takes place and the hydrophobic groups are on the exterior of the humic acid molecules (52) or after the particle partitions into the humic acid hydrophobic interior (19). The hydrophobic nature of the silica particles and humic acid coupled with low electrostatic repulsion brought about humic acid adsorption to silica via hydrophobic interactions.

4.3.2 Bacterial adhesion orientation

Preferential end-on adhesion is observed (Figure **4-4**), but humic acid did not affect the adhesion orientation (Figure **4-5**). The percent of bacteria that was adhered end-on to particles varied between 60±11% and 74±5% with no trend associated with increasing bulk humic acid coating solution concentration. In total, 55±5% of all 1120 couplets (140 couplets from each humic acid condition) showed silica particles adhered to a single end, and 70±3% had particles adhered to a single end or both ends of the rod-shaped cell. This preferential end-on bacterial adhesion is lower than Jones et al.'s results for adhesion to 1.5-μm polystyrene latex (PSL) particles in the absence of humic acid (43). In that research 93% of couplets had particles adhered to single ends, and there were no instances of PSL particles adhering to both ends (43). This indicates that preferential end-on adhesion is not a general phenomenon and is dependent on the substrate surface and geometry.

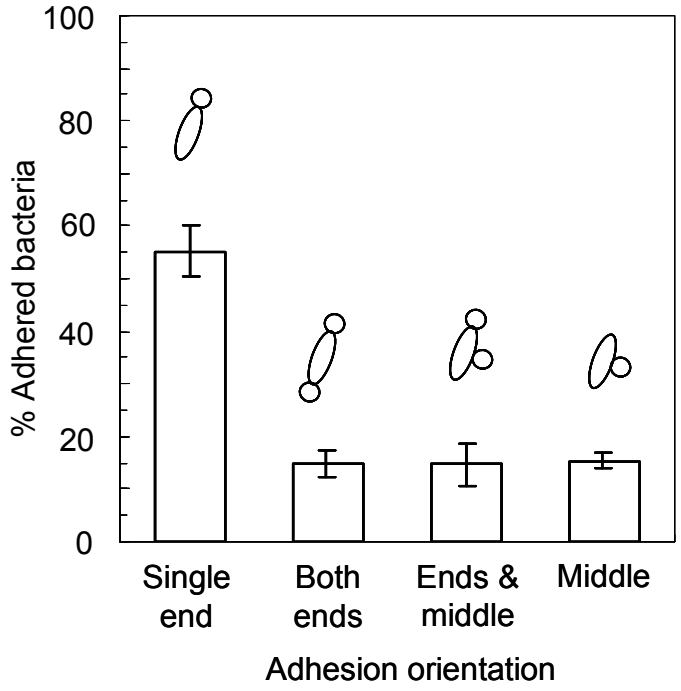

Figure 4-4: Preferential end-on bacterial adhesion of the bacteria to silica particles. Most particles stick to the end of the bacteria. These data include all concentrations of humic acid (0.0-8.0 mg/L) because there is little variation in orientation with humic acid.

The presence of humic acid does not affect orientation, and so it is the silica surface, not the humic acid, causing this decrease in end-on adhesion compared with PSL. The theory that protein localization at one end of the bacterium produces a "sticky" end may be valid, but if so then in this case bacterial polarity is being overshadowed by another adhesion mechanism. Further research into the generality of end-oriented bacterial adhesion is needed.

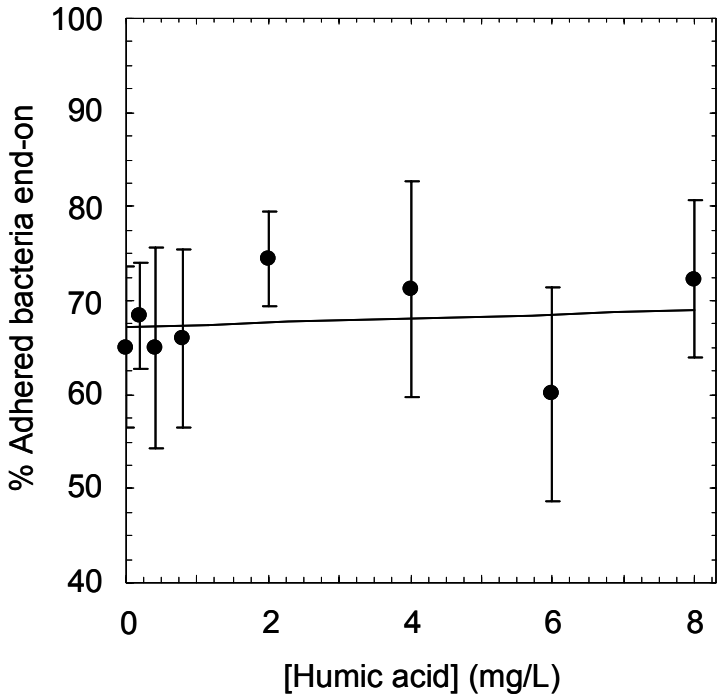

Figure 4-5: Oriented bacterial adhesion results for couplets formed with silica particles coated with humic acid from solutions of varying bulk concentrations. Values include both "single end" and "both end" couplets. Error bars represent the 95% confidence interval. Humic acid does not affect the orientation of adhesion.

4.3.3 Bacterial adhesion occurrence & force

Humic acid enhances bacterial adhesion, although the effect is slight (Figure **4-6**). Linear regression of the data shows that there is a small increase in the percent of bacteria adhered to silica coated in the high bulk concentration humic acid solution (8.0 mg/L). This is represented by Equation **4.1**,

$$A = a[HA] + b, \qquad (4.1)$$

where A is the average percentage of total bacteria as couplets and [HA] is the bulk humic acid coating solution concentration in mg/L. The slope a = 1.1±0.5 and the intercept b = 4.8±4.2. Thus, with 95% confidence, a > 0. Quantitatively, the percent of bacteria adhered to bare silica particles was 4.3±0.8%, whereas 7.3±1.6% of the bacteria adhered to particles coated in 8.0-mg/L humic acid (Figure **4-6**).

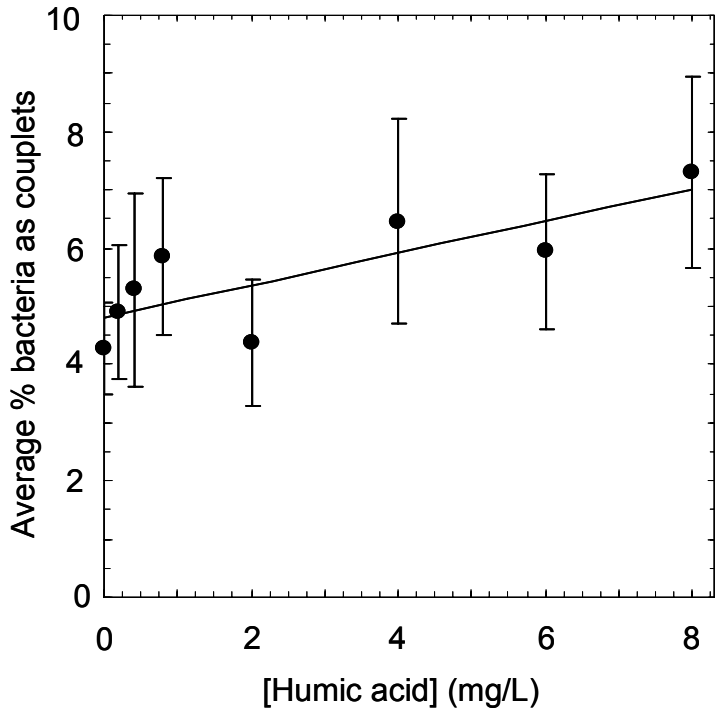

Figure 4-6: Humic acid increases bacterial adhesion to silica. The plot shows the average of eleven runs for each humic acid coating solution concentration with 95% confidence level error bars. The linear fit shows there is a slight increase in adhesion to humic acid-coated particles. High bulk humic acid (8.0 mg/L) increases bacterial adhesion.

Adhesion force measurements show that humic acid slightly increases the strength of bacterial adhesion. Fewer bacteria were sheared off the wall in the presence of humic acid, indicating the force of adhesion is stronger (Figure **4-7**).

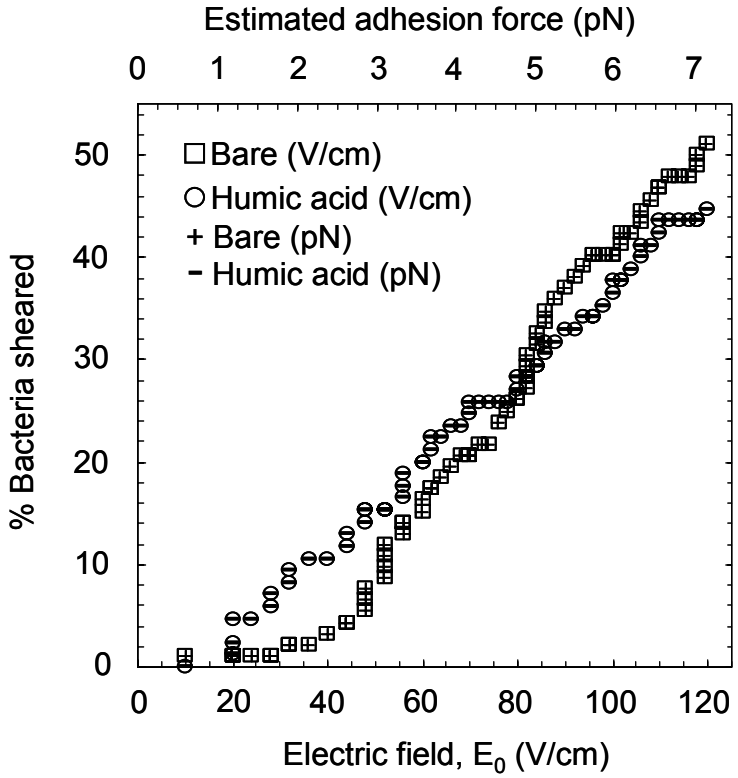

Figure 4-7: Percent of bacteria sheared off the wall at different electric field strengths. Adhesion force was estimated based on the force due to electrophoresis (Equation 3.3). For the humic acid case, the electrophoresis cell was soaked in a humic acid solution of high bulk concentration (8.0 mg/L).

Past research shows reduced colloidal adhesion in the presence of humic acid, opposite to the findings in this work. This reduced adhesion occurs through increased electrostatic repulsion (18, 23-25), steric interactions (26), or decreased binding sites (18). In comparison with studies researching the effect of humic acid on bacteria (24, 25), the experiments presented in this chapter did not have the confounding effect of hydrodynamic flow through a column, and the results show slightly increasing adhesion with humic acid, rather than decreasing. This might indicate that the bacteria-surface contact time is important. Column studies may not allow for sufficient adhesion time,

and steric interactions may dominate at that short time. In the experiments presented in this chapter, the bacteria and particles are able to interact for longer times so that the steric repulsion significant in short times is overcome by other attractive mechanisms. In fact, instances of non-adhered bacteria and particles closely interacting and then eventually adhering were observed. During the close interaction, the bacterium and particle each underwent Brownian motion, and the particle moved about the cell surface for a time on the order of minutes before adhering.

Electrostatic repulsion may not have a large influence on couplet formation, even though the bacteria have a negative surface and the silica surface increases in negativity with humic acid adsorption. However, humic acid is highly functionalized, with not only the carboxyl and phenol groups that confer its net negative charge, but also positively-charged amine groups for example (17). Therefore, humic acid structure contains areas of positive charge, and this charge nonuniformity (53, 54) can lead to electrostatic attraction to the negative bacteria surface.

There might also be biological reasons for the observed enhanced adhesion. In the experiments the bacteria were removed from the growth media and placed in stress conditions in PBS where there was a lack of nutrients. With organic humic acid molecules present on the silica surface, the bacteria would be more inclined to adhere for survival purposes, using the humic acid as a carbon source (27).

4.4 Conclusion

The influence of humic acid on the adhesion of *E. coli* to silica particles or glass surfaces was examined. Humic acid did adsorb to the particles, as measured by ζ potential measurements, or to the glass surface. The number of silica-bacterium couplets, counted using video microscopy, increased with adsorbed humic acid. Similarly, adhesion strength, measured using a differential electrophoresis technique, increased. Both effects were slight. Also, whereas end-on adhesion orientation to the 0.9-μm silica particles is the preferred orientation, the data revealed no relationship between humic acid coating and adhesion orientation. It is concluded that humic acid plays a small role in bacterial adhesion to silica or glass surfaces.

4.5 References

1. Parent, M.E., and D. Velegol. 2004. *E. coli* adhesion to silica in the presence of humic acid. *Colloids and Surfaces B: Biointerfaces* 39:45-51.
2. Flemming, H.-C. 1997. Reverse osmosis membrane biofouling. *Experimental Thermal and Fluid Science* 14:382-391.
3. Bryers, J.D. 1994. Biofilms and the technological implications of microbial cell adhesion. *Colloids and Surfaces B: Biointerfaces* 2:9-23.
4. Ludensky, M. 2003. Control and monitoring of biofilms in industrial applications. *International Biodeterioration and Biodegradation* 51:255-263.
5. Gristina, A.G. 1987. Biomaterial-centered infection: microbial adhesion versus tissue integration. *Science* 237:1588.
6. Costerton, J.W., P.S. Stewart, and E.P. Greenberg. 1999. Bacterial biofilms: a common cause of persistent infections. *Science* 284:1318-1321.
7. Characklis, W.G. 1981. Fouling biofilm development: a process analysis. *Biotechnology and Bioengineering* 23:1923-1960.
8. Wyndham, R.C., and K.J. Kennedy. 1995. Microbial consortia in industrial wastewater treatment. In Microbial Biofilms. H.M. Lappin-Scott, and J.W. Costerton, editors. Cambridge University Press, New York. 183-195.

9. Li, Q., and B.E. Logan. 1999. Enhancing bacterial transport for bioaugmentation of aquifers using low ionic strength solutions and surfactants. *Water Research* 33:1090-1100.
10. Langmark, J., M.V. Storey, N.J. Ashbolt, and T.A. Stenstrom. 2004. Artificial groundwater treatment: biofilm activity and organic carbon removal performance. *Water Research* 38:740-748.
11. Schmidt, L.M., J.J. Delfino, J.F.P. III, and G.S.L. III. 1999. Biodegradation of low aqueous concentration pentachlorophenol (PCP) contaminated groundwater. *Chemosphere* 38:2897-2912.
12. Jin, G., and J. Andrew J. Englande. 1997. Effects of electron donor, dissolved oxygen, and oxidation-reduction potential biodegradation of carbon tetrachloride by *Escherichia coli* K-12. *Water Environment Research* 69:1100-1105.
13. Marlow, H.J., K.L. Dunston, M.R. Weisner, M.B. Tomson, J.T. Wilson, and C.H. Ward. 1991. Microbial transport through porous media: The effects of hydraulic conductivity and injection velocity. *Journal of Hazardous Materials* 28:65-74.
14. Hayes, M.H.B. 1998. Chapter 1. In Humic Substances: Structures, Properties and Uses. G. Davies, E.A. Ghabbour, and K.A. Khairy, editors. Royal Society of Chemistry, Cambridge.
15. Balnois, E., K.J. Wilkinson, J.R. Lead, and J. Buffle. 1999. Atomic force microscopy of humic substances: Effects of pH and ionic strength. *Environmental Science and Technology* 33:3911-3917.
16. Beckett, R. 1990. Chapter 1. In Surface and Colloid Chemistry in Natural Waters and Water Treatment. R. Beckett, editor Plenum Press, New York.
17. Davies, G., and E.A. Ghabbour. 1998. Preface. In Humic Substances: Structures, Properties and Uses. G. Davies, E.A. Ghabbour, and K.A. Khairy, editors. Royal Society of Chemistry, Cambridge.
18. Bob, M.M., and H.W. Walker. 2001. Effect of natural organic coatings on the polymer-induced coagulation of colloidal particles. *Colloids and Surfaces A: Physicochemical and Engineering Aspects* 177:215-222.
19. Wershaw, R.L. 1986. A new model for humic matierals and their interactions with hydrophobic organic chemicals in soil-water or sediment-water systems. *Journal of Contaminant Hydrology* 1:29-45.
20. Fein, J.B., J.-F. Boily, K. Guclu, and E. Kaulbach. 1999. Experimental study of humic acid adsorption onto bacteria and Al-oxid mineral surfaces. *Chemical Geology* 162:33-45.
21. Klavins, M., and L. Eglite. 2002. Immobilisation of humic substances. *Colloids and Surfaces A: Physicochemical and Engineering Aspects* 203:47-54.
22. Lovley, D.R., J.L. Fraga, J.D. Coates, and E.L. Blunt-Harris. 1999. Humics as an electron donor for anaerobic respiration. *Environmental Microbiology* 1:89-98.
23. Mosley, L.M., K.A. Hunter, and W.A. Ducker. 2003. Forces between colloid particles in natural waters. *Environmental Science and Technology* 37:3303-3308.
24. Johnson, W.P., and B.E. Logan. 1996. Enhanced transport of bacteira in porous media by sediment-phase and aqueous-phase natural organic matter. *Water Research* 30:923-931.

25. Lahlou, M., H. Harms, D. Springael, and J.-J. Ortega-Calvo. 2000. Infuence of soil components on the transport of polycyclic aromatic hydrocarbon-degrading bacteria through saturated porous media. *Environmental Science and Technology* 34:3649-3656.
26. Davis, C.J., E. Eschenazi, and K.D. Papdopoulos. 2002. Combined effects of Ca^{2+} and humic acid on colloid transport through porous media. *Colloid and Polymer Science* 280:52-58.
27. Butterfield, P.W., A.K. Camper, J.A. Biederman, and A.M. Bargmeyer. 2002. Minimizing biofilm in the presence of iron oxides and humic substances. *Water Research* 36:3898-3910.
28. Fletcher, M. 1985. Bacterial attachment in aquatic environmnets: A diversity of surfaces and adhesion strategies (Chapter 1). In Bacterial adhesion: mechanisms and physiological significance. D.C. Savage, and M. Fletcher, editors. Plenum, New York.
29. Marshall, K.C., R. Stout, and R. Mitchell. 1971. Mechanism of the initial events in the sorption of marine bacteria to surfaces. *Journal of General Microbiology* 68:337-348.
30. Ong, Y.-L., A. Razatos, G. Georgiou, and M.M. Sharma. 1999. Adhesion forces between *E. coli* bacteria and biomaterial surfaces. *Langmuir* 15:2719-2725.
31. Hermansson, M. 1999. The DLVO theory in microbial adhesion. *Colloids and Surfaces B: Biointerfaces* 14:105-119.
32. Camesano, T.A., and B.E. Logan. 2000. Probing bacterial electrosteric interactions using atomic force microscopy. *Environmental Science and Technology* 34:3354-3362.
33. Razatos, A., Y.-L. Ong, M.M. Sharma, and G. Georgiou. 1998. Molecular determinants of bacterial adhesion monitored by atomic force microscopy. *Proceedings of the National Academy of Sciences of the United States of America* 95:11059-11064.
34. Jucker, B.A., H. Harms, and A.J.B. Zehnder. 1998. Polymer interactions between five gram-negative bacteria and glass investigated using LPS micelles and vesicles as model systems. *Colloids and Surfaces B: Biointerfaces* 11:33-45.
35. Vadillo-Rodriguez, V., H.J. Busscher, W. Norde, and H.C.v.d. Mei. 2002. Softness of the bacterial cell wall of *Streptococcus mitis* as probed by microelectrophoresis. *Electrophoresis* 23:2007-2011.
36. Poortinga, A.T., R. Bos, W. Norde, and H.J. Busscher. 2002. Electric double layer interactions in bacerial adhesion to surfaces. *Surface Science Reports* 47:1-32.
37. Abu-Lail, N.I., and T.A. Camesano. 2003. Role of lipopolysaccharides in the adhesion, retention, and transport of *Escherichia coli* JM109. *Environmental Science and Technology* 37:2173-2183.
38. Dexter, S.C. 1979. Influence of substratum critical surface tension on bacterial adhesion- *in situ* studies. *Journal of Colloid and Interface Science* 70:346-354.
39. Fletcher, M., and G.I. Loeb. 1979. Influence of substratum characteristics on the attachment of a marine pseudomonad to solid surfaces. *Applied and Environmental Microbiology* 37:67-72.

40. An, Y.H., and R.J. Friedman. 1998. Concise review of mechanisms of bacterial adhesion to biomaterial surfaces. *Journal of Biomedical Materials Research* 43:338-348.
41. Reisner, A., J.A.J. Haagensen, M.A. Schembri, E.L. Zechner, and S. Molin. 2003. Development and maturation of *Escherichia coli* K-12 biofilms.
42. Bakker, D.P., B.R. Postmus, H.J. Busscher, and H.C.v.d. Mei. 2004. Bacterial strains isolated from different niches can exhibit different patterns of adhesion to substata. *Applied and Environmental Microbiology* 70:3758-3760.
43. Jones, J.F., J.D. Feick, D. Imoudu, N. Chukwumah, M. Vigeant, and D. Velegol. 2003. Oriented adhesion of *Escherichia coli* to polystyrene particles. *Applied and Environmental Microbiology* 69:6515-6519.
44. Holtzer, G.L., and D. Velegol. 2003. Force measurements between colloidal particles of identical zeta potentials using differential electrophoresis. *Langmuir* 19:4090-4095.
45. Velegol, D., J.L. Anderson, and S. Garoff. 1996. Determining the forces between polystyrene latex spheres using differential electrophoresis. *Langmuir* 12:4103-4110.
46. Fleer, G.J., M.A.C. Stuart, M.H.M. Scheutjens, T. Cosgrove, and B. Vincent. 1998. Chapters 2 & 3. In Polymer at Interfaces. Chapman & Hall, New York.
47. Yuan, W., and A.L. Zydney. 2000. Humic acid fouling during ultrafiltration. *Environmental Science and Technology* 34:5043-5050.
48. Davis, J.A. 1982. Adsorption of natural dissolved organic matter at the oxide/water interface. *Geochimica et Cosmochimica Acta* 46:2381-2393.
49. Koopal, L.K., Y. Yang, A.J. Minnaard, P.L.M. Theunissen, and W.H.V. Riemsdijk. 1998. Chemical immobilisation of humic acid on silica. *Colloids and Surfaces A: Physicochemical and Engineering Aspects* 141:385-395.
50. Chiou, C.T., D.E. Kile, T.I. Brinton, R.L. Malcolm, and J.A. Leenheer. 1987. A comparison of water solubility enhancements of organic solutes by aquatic humic materials and commercial humic acids. *Environmental Science and Technology* 21:1231-1234.
51. Ochs, M., B. Cosovic, and W. Stumm. 1994. Coordinative and hydrophobic interaction of humic substances with hydrophilic Al_2O_3 and hydrophobic mercury surfaces. *Geochimica et Cosmochimica Acta* 58:639-650.
52. Avena, M.J., and L.K. Koopal. 1999. Kinetics of humic acid adsorption at solid-water interfaces. *Environmental Science and Technology* 33:2739-2744.
53. Feick, J.D., and D. Velegol. 2000. Electrophoresis of spheroidal particles having a random distribution of zeta potential. *Langmuir* 16:10315-10321.
54. Feick, J.D., N. Chukwumah, A.E. Noel, and D. Velegol. 2004. Altering surface charge nonuniformity on individual colloidal particles. *Langmuir* 20:3090-3095.

Chapter 5

Quorum Sensing Signal Diffusion Modeling*

Quorum sensing is almost always regarded as a population density effect in three-dimensional bulk samples of bacteria. Here, *two*-dimensional samples of bacteria cells on a surface are modeled to examine the effect of *local* population densities on quorum sensing. The three-dimensional quorum sensing system is in steady state; however, two-dimensional bacterial populations allow for time effects to be evaluated. Thus, this chapter considers quorum sensing in terms of signal diffusion by examining both distance and time effects. The modeling compares two local bacteria formations (patterned and random) and shows that for typical experimental time and length scales both result in similar signal concentration profiles. It is concluded that quorum sensing is indeed a function of both population density and signal diffusion time, but the concept of a "true quorum" (a population *number* necessary for quorum sensing) is discussed.

5.1 Introduction

Over thirty years ago, Nealson reported that *Vibrio fischeri* produces an extracellular autoinducer, which accumulates as a function of cell population growth and activates luminescence at a threshold concentration (1). This phenomenon is now

---

* **Charles Snyder** must be acknowledged for his work developing and running this modeling (Snyder Comprehensive Exam, 2006). The material in this chapter is being prepared for publication in Biophysical Journal.

recognized in many bacterial species and is known to occur typically via an autoinducer producer and receptor protein pair. Briefly, a LuxI-type protein produces autoinducer molecules, acylated homoserine lactones (AHL), which diffuse across the cell membrane into the surrounding medium. At a critical autoinducer concentration, interactions with receptor proteins like LuxR are possible and binding occurs (2). In turn, the LuxR-AHL complex is able to bind to a target promoter to activate transcription, for example, of the *V. fischeri* luminescence gene for light production.

Winans named these events the now familiar term "quorum sensing" (first seen in the literature in 1994) as a colorful way to describe the concept of autoinduction as being cell-number controlled (3, 4). In 2002 Redfield hypothesized that autoinduction was diffusion controlled rather than population controlled (5). If this hypothesis is verified, then quorum sensing might become a misnomer and a name change to diffusion sensing (or some other moniker equally as clever as quorum) might more aptly describe autoinduction. Recently Hense et al. introduced the term "efficiency sensing" to unify the theories of quorum sensing and diffusion sensing and hypothesized that autoinducers measure the *combination* of population density, signal molecule diffusion, and spatial distribution (i.e., localized cell density) (6).

Experimental evidence suggesting the importance of diffusion in quorum sensing is presented in a Weiss group publication, which uses *V. fischeri* autoinducer signals in sender cells to elicit different fluorescent responses in receiver cells in a synthetic multicellular system for programmed pattern formation (7). The receiver cells are genetically engineered to respond to different bands of signal concentrations with either red or green fluorescence, depending on the band-detect. Thus, plated mixtures of

different band-detect cells surrounding a center disk of sender cells result in a bulls-eye pattern formation visible under fluorescence microscopy. This proof of concept work indirectly showed that diffusion is involved in quorum sensing; however, these experiments were conducted using bulk samples of cells of very high population density.

To investigate population versus diffusion sensing, the diffusion of quorum sensing signals from cells on a surface is modeled. The hypothesis is that due to the physical phenomenon of AHL diffusion from surface cells, quorum sensing depends on both the *local* cell density *and* the total time the AHL signals are allowed to diffuse from the cells. Traditionally, quorum sensing is studied in three dimensions in bulk suspensions where cells are evenly distributed throughout the medium. In contrast, a local cell density occurs in a sample if cells are concentrated at the surface with none in planktonic form. On yet a smaller scale, local cell density can vary on the surface, with some areas being more highly concentrated with cells than others.

The diffusion modeling shows that:

1. Surface cell concentrations formed via random adhesion and via patterned adhesion give similar AHL concentration profiles.
2. Both population density and signal diffusion contribute to quorum sensing.
3. There is a specific *number* of bacteria that makes up a “true quorum” for a given cell density and signal diffusion time.

5.2 Diffusion modeling

The diffusion of AHL from surface cells is modeled starting with the general transport equation in spherical coordinates considering only radial diffusion,

$$\frac{\partial c}{\partial t} = D\left(\frac{\partial^2 c}{\partial r^2} + \frac{2}{r}\frac{\partial c}{\partial r}\right), \tag{5.1}$$

where c is the AHL concentration and D is the AHL diffusion coefficient. This assumes that there is no bulk flow in the system, the diffusion coefficient is constant and uniform, and that AHL molecules do not adsorb, react, or degrade in the system. The Green's function solution (point source solution) to Equation **5.1** is well-known, and is given in Equation **5.2** (8). It is found by taking Laplace transforms (8-10) of Equation **5.1** and applying the initial condition that there is no AHL in the system at $t = 0$ and the boundary conditions that AHL concentration is zero at positions $r \rightarrow \infty$ and that there is conservation of mass.

$$c(t,r) = \frac{M}{8(\pi D t)^{\frac{3}{2}}}\exp\left(\frac{-r^2}{4Dt}\right) \tag{5.2}$$

Equation **5.2** is the concentration profile for an instantaneous point source that produces M mass of AHL. However, an adhered cell is more like a continuous point source. Integrating from time zero to a time t gives the solution for a continuous point source,

$$c(t,r) = \frac{q}{4\pi D r}\operatorname{erfc}\left(\frac{r}{2\sqrt{Dt}}\right), \tag{5.3}$$

where q is the constant production rate of AHL. Equation **5.3** is the solution for radial diffusion with spherical symmetry; however, this modeling involves diffusion radially

only above the plane where the bacteria reside (i.e., hemispherical diffusion), because the lower surface is glass. Nevertheless, Equation **5.3** can be used due to symmetry arguments, because in the spherically-symmetric solution no flux occurs across the plane where the bacteria reside. One simply makes the point source production rate (q) of AHL twice as strong, and does not further consider the result for below the plane. This is mathematically valid because the diffusion below the plane of the bacteria does not affect the diffusion above it.

To take multiple point sources into account, such as an array of AHL-producing bacteria on a surface, one uses the linearity of the diffusion equation and simply sums all point sources from Equation **5.3** to obtain

$$c(t,\mathbf{r}) = \sum_{i=1}^{n} \frac{q_i}{4\pi D\sqrt{(\mathbf{r}-\mathbf{r}_i)\cdot(\mathbf{r}-\mathbf{r}_i)}} \operatorname{erfc}\left(\frac{\sqrt{(\mathbf{r}-\mathbf{r}_i)\cdot(\mathbf{r}-\mathbf{r}_i)}}{2\sqrt{Dt}}\right), \qquad (5.4)$$

where $\mathbf{r} = (x, y, z)$ represents a position of interest and $\mathbf{r_i}$ represents the position of a point source (i.e., a bacterium). The bacteria can be patterned on a surface in a number of ways, but here two types of packing are considered: a) square-packed arrays of bacteria and b) random packing of bacteria. For the patterned adhesion model the same number of points with the same even spacing distance (L) between the point sources in x and y is used to give square arrays of bacteria. For the random adhesion model the x and y positions are randomly chosen within set coordinate bounds.

All results are given in nondimensional form. The nondimensional definitions are: AHL concentration $C^* = CDL/q$, distance $W = x/L$, number of bacteria n = array area/L^2, and time $\tau = tD/L^2$, where L is the spacing between cells (identical in x and y). Based on previously reported values, $D = 100\ \mu m^2/s$ (11, 12) and $q = 10^{-24}$ g/s (13) for all

cells. All concentration profiles are shown at a height of z = 1 μm above the substrate surface.

5.3 Results

Localized populations of cells can be formed on a surface by two methods: random adhesion or specific patterning (Chapter 3.3). Random adhesion is a simple and economical technique, but specific patterning allows for tight control of the local cell density. The diffusion model was developed to compare the resulting AHL concentration profiles from the two methods to see if such exact control of local cell density is necessary, as well as to analyze the diffusion versus population concepts of quorum sensing.

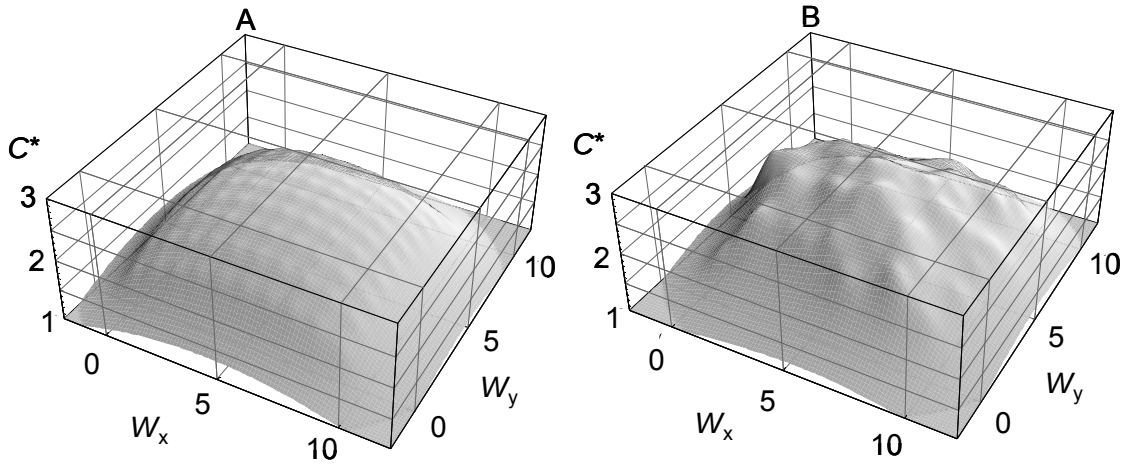

Figure 5-1: The dimensionless signal concentration profiles for a square patterned array of cells (A) and the random case (B) for n = 100 and $\tau = 10^7$ at a height z = 1 μm above the substrate surface. n = array area/L^2, $\tau = tD/L^2$, $C^* = CDL/q$, $W_x = x/L$, and $W_y = y/L$, where L is the spacing between cells, L = 2 μm.

Three-dimensional plots (Figure **5-1**) of the concentration profiles for the patterned and random adhesion cases show similar trends in signal concentration maximum value and location. To more thoroughly compare the patterned and random cases, signal concentration profiles for different numbers of surface cells n producing signaling molecules for different times τ were created at a central cross-section in W_y (Figure **5-2**). For the cell numbers and adhesion times shown in Figure **5-2**, the concentration profiles match qualitatively. Also, the difference between the two cases is not statistically significant with 95% confidence, for reasonable experimental times, based on Student's *t*-tests.

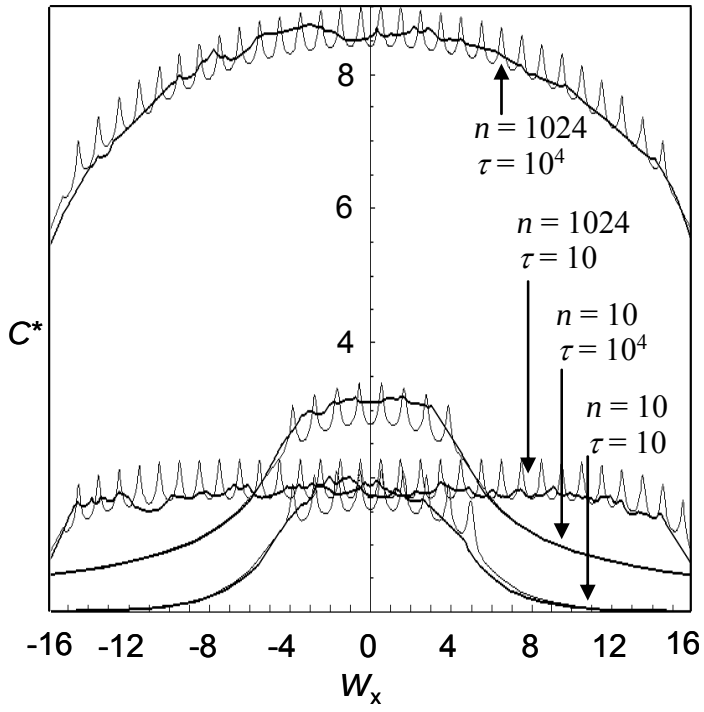

Figure 5-2: The dimensionless signal concentration profiles of four cases with different n (n = array area/L^2) and τ ($\tau = tD/L^2$), where L is the spacing between cells, L = 10 μm. $C^* = CDL/q$ and $W_x = x/L$. Concentration is examined at a height z = 1 μm and at the center in the y direction. The thin line represents patterned cell arrays and the thick line represents the random case.

Larger τ causes a decrease in the difference between the patterned and random cases and for the experimental times and cell spacings involved (t > 5 minutes, L < 20 μm), it is acceptable to use random adhesion to control the local surface cell densities.

In the limit of large n, a continuum solution is known (14) (Equation **5.5**) and can be used to describe an array of cells producing AHL on a surface as an infinite plane source.

$$C = q\left(\frac{t}{D}\right)^{1/2}\frac{1}{4}\left(\frac{a^2}{Dt}\right)^{1/2}\int_0^{2\left(\frac{Dt}{a^2}\right)^{1/2}}\operatorname{erf}\left[\frac{1}{u}\operatorname{erf}\left(\frac{1-y/a}{u}\right)+\operatorname{erf}\left(\frac{1+y/a}{u}\right)\right]du \qquad (5.5)$$

The symbol a in Equation **5.5** represents the size of the side of the square source (Equation **5.6**).

$$2a = \sqrt{n}L \qquad (5.6)$$

Then, with Equation **5.5**, dimensionless concentration (C*) can be calculated for various τ and n to consider the case of infinite area (large n), which actually best represents the experiments described in Chapter 6 that use lawns of bacteria extending to the walls of the sample wells. The results are presented in Figure **5-3** on the far right ($n = \infty$) as black squares.

Figure **5-3** is an important result of the modeling. The dimensionless signal concentration ($C^* = CDL/q$) is plotted on the y axis versus cell number n (n = array area/L^2) on the x axis. Each of the curves extending from n = 1 to 10^8 is created from Equation **5.4** (the sum of arrayed bacteria point sources, for different τ). Signal concentration is examined at the center of the square arrays at a height z = 1 μm. Also presented in Figure **5-3** is the case of a plane source of infinite area (large n) with the

calculations of Equation **5.5** for different τ shown as the black squares on the far right at $n = \infty$. The discrete point source summation solution at large n (10^8) compares well with the infinite plane source solution.

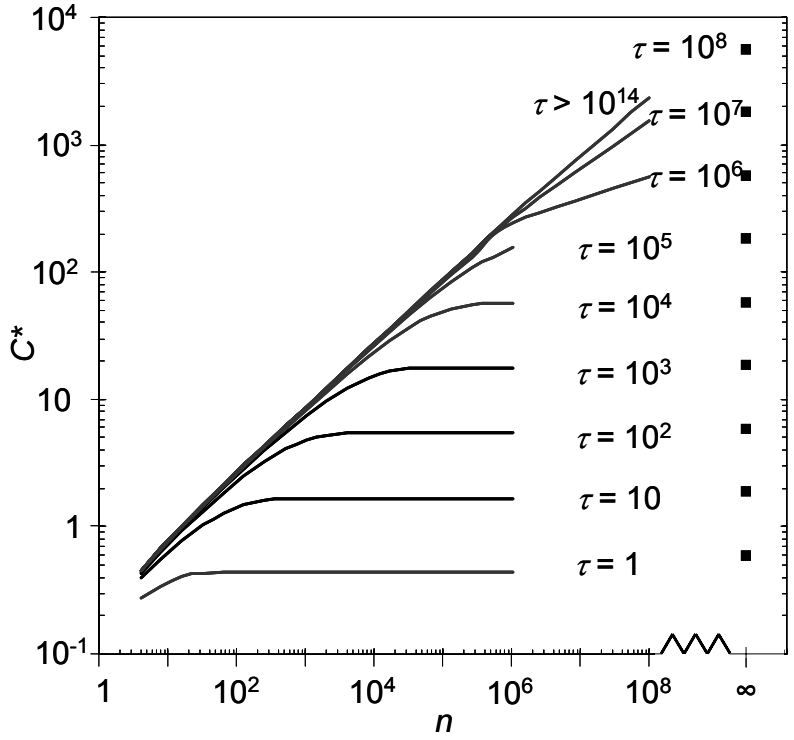

Figure 5-3: The dimensionless signal concentration ($C^* = CDL/q$) as a function of n (n = array area/L^2) and τ ($\tau = tD/L^2$), where L is the spacing between cells. Typically L^2/D is roughly 1 second. Signal concentration is examined at the center of the square arrays at a height z = 1 μm. The black curves are for arrays of bacteria as discrete point sources. The black squares are for a plane source of infinite area.

If the concentration of autoinducer required to elicit the quorum sensing response is known, then Figure **5-3** can be used to determine the size and time scales of the system necessary to observe quorum sensing. As an example, consider the aquatic observation of quorum sensing in the *V. fischeri-Euprymna scolopes* symbiosis. *V. fischeri* is present in the "light organs" of the Hawaiian squid at cell densities of 10^{11} cells/mL (15). This

corresponds to a spacing L = 1 μm. If the AHL production rate is assumed to be a constant $q = 10^{-21}$ g/s for each cell with D = 100 μm^2 and the AHL concentration sufficient for quorum sensing (luminescence) is 1 ng/mL (16), then $C^* = 10^2$. For $\tau = 10^5$, n needs to be at least 2×10^5 for luminescence, based on Figure **5-3**. If the number of cells n present in the light organ is less than 2×10^5 at $\tau = 10^5$, then there will be no quorum sensing even though there is a cell density of 10^{11} cells/mL. If instead $n = 1\times10^5$, then quorum sensing would occur only after $\tau = 10^6$. If $n = 1\times10^4$, then quorum sensing would not occur at these conditions. From this example it becomes clear that there is a "true quorum"– a number of cells necessary for quorum sensing. Quorum sensing is not merely an effect of cell density, but also cell number, and diffusion time.

5.4 Discussion

Quorum sensing has most often been described *only* in terms of population density (17-19). The concept of diffusion in quorum sensing was introduced in 2002 by Redfield who hypothesized that quorum sensing was not a cooperative action of a bacteria population, but rather a way for individual cells to gather information about the transport properties (diffusion and mixing) of the surrounding medium (5). Redfield's hypothesis is plausible because the response to quorum sensing in many species is frequently a secretion, for example of virulence factors (20-23), antibiotics (20), or EPS (24, 25) (see the literature review in Chapter 2 for details), which are of benefit to an individual cell only if the secreted biomolecules stay local (5).

Diffusion's influence on quorum sensing, however, has not been thoroughly examined. Basu et al.'s 2005 publication uses the fact that quorum sensing signals diffuse to build programmed patterns of cells, but this work was not directly interested in the effect of diffusion on quorum sensing *per se*. Also, only bulk samples of cells of very high population density were used (7). Incidentally, the concept of quorum sensing signal diffusion is not new. In 1985, Kaplan and Greenberg showed that AHL associates with cells via diffusive transport (26). However, this was a mechanistic study of how AHL transports across cell membranes and did not delve into the impact of signal diffusion between individual neighboring cells.

Redfield's "diffusion sensing" hypothesis however does not apply for all cases, such as with *V. fischeri* luminescence, which is not a secretory response to quorum sensing. It is therefore reasonable that quorum sensing is indeed due to both population density and diffusion, and that different species developed quorum sensing based on one aspect (population density or signal diffusion) of the dualistic phenomenon. This is exactly the concept Hense et al. recently discussed in, "Does efficiency sensing unify diffusion and quorum sensing?", which hypothesized that autoinducers measure the *combination* of population density, signal molecule diffusion, and spatial distribution (i.e., localized cell density) (6). This combination of information allows cells to determine whether or not it is worth producing effector molecules, such as antibiotics or bioluminescent proteins, which are more energetically costly to synthesize than AHL (6).

5.5 Conclusions

Signal diffusion time, population density, and population number all affect quorum sensing. The influence of diffusion on quorum sensing implies that a "quorum" of cells may not produce a response unless signal diffusion time is allowed to pass. This becomes important on local scales, such as in two-dimensional samples like biofilms, which are known to develop due to quorum sensing (27). The diffusion modeling presented in this chapter shows that under any given set of conditions of diffusion time *and* cell spacing (density), there exists a "true quorum"– a number of cells necessary to elicit a response. For a known critical concentration of AHL that is needed to trigger quorum sensing in a local cell population density, the model allows experimenters to determine the cell number and diffusion time required to observe quorum sensing. The modeling also shows that random adhesion of local cell densities produces similar signal concentration profiles as patterned bacterial arrays and helps devise the corresponding quorum sensing experiments presented in the next chapter (Chapter 6).

5.6 References

1. Nealson, K.H. 1977. Autoinduction of bacterial luciferase: occurrence, mechanism and significance. *Archives of Microbiology* 112:73-79.
2. Pappas, K.M., C.L. Weingart, and S.C. Winans. 2004. Chemical communication in proteobacteria: biochemical and structure of signal synthases and receptors required for intercellular signaling. *Molecular Microbiology* 53:755-769.
3. Dunny, G.M., and S.C. Winans. 1999. Bacterial life: neither lonely nor boring. In Cell-Cell Signaling in Bacteria. G.M. Dunny, and S.C. Winans, editors. ASM Press, Washington, D.C. 1-5.
4. Fuqua, W.C., S.C. Winans, and E.P. Greenberg. 1994. Quorum Sensing in Bacteria: the LuxR-LuxI Family of Cell Density-Responsive Transcriptional Regulators. *Journal of Bacteriology* 176:269-275.

5. Redfield, R.J. 2002. Is quorum sensing a side effect of diffusion sensing? *TRENDS in Microbiology* 10:365-370.
6. Hense, B.A., C. Kuttler, J. Muller, M. Rothballer, A. Hartmann, and J.-U. Kreft. 2007. Does efficiency sensing unify diffusion and quorum sensing? *Nature Reviews Microbiology* 5:230-239.
7. Basu, S., Y. Gerchman, C.H. Collins, F.H. Arnold, and R. Weiss. 2005. A synthetic multicellular system for programmed pattern formation. *Nature* 434:1130-1134.
8. Crank, J. 1975. Chapter 3 Infinite and semi-infinite media. In The Mathematics of Diffusion, 2nd Edition. Oxford University Press, New York.
9. Duffy, D.G. 2001. Green's Functions with Applications. Chapman & Hall / CRC, New York.
10. Stakgold, I. 1998. Green's Functions and Boundary Value Problems. John Wiley & Sons,
11. Stewart, P.S. 2003. Diffusion in Biofilms. *Journal of Bacteriology* 185:1485-1491.
12. Muller, J., C. Kuttler, and B.A. Hense. 2005. Cell-Cell Communication by Quorum Sensing and Dimension-Reduction.
13. Schaefer, A.L., D.L. Val, B.L. Hanzelka, J.E.J. Cronan, and E.P. Greenberg. 1996. Generation of Cell-To-Cell Signals in Quorum Sensing: Acyl Homoserine Lactone Synthase Activity of a Purified Vibrio fischeri LUXI Protein. *Proceedings of the National Academy of Sciences of the United States of America* 93:9505-9509.
14. Jaeger, J.C. 1951. Approximations in transient surface heating. *Australian Journal of Scientific Research* 5:1-9.
15. Visick, K.L., and M.J. McFall-Ngai. 2000. An exclusive contract: Specificity in the *Vibrio fischeri-Euprymna scolopes* partnership. *Journal of Bacteriology* 182:1779-1787.
16. Eberhard, A., A.L. Burlingame, C. Eberhard, G.L. Kenyon, K.H. Nealson, and N.J. Oppenheimer. 1981. Structural identification of autoinducer of *Photobacterium fischeri* luciferase. *Biochemistry* 20:2444-2449.
17. Miller, M.B., and B.L. Bassler. 2001. Quorum sensing in bacteria. *Annual Review of Microbiology* 55:165-199.
18. Fuqua, C., and E.P. Greenberg. 2002. Listening in on bacteria: acyl-homoserine lactone signaling. *Nature Reviews Molecular Cell Biology* 3:685-695.
19. Waters, C.M., and B.L. Bassler. 2005. Quorum sensing: cell-to-cell communication in bacteria. *Annual Review of Cell and Developmental Biology* 21:319-346.
20. Kleerebezem, M., L.E.N. Quadri, O.P. Kuipers, and W.M.d. Vos. 1997. Quorum sensing by peptide pheromones and two-component signal-transduction in Gram-positive bacteria. *Molecular Microbiology* 24:895-904.
21. Winson, M.K., M. Camara, A. Latifi, M. Foglino, S.R. Chhabra, M. Daykin, M. Bally, V. Chapon, G.P.C. Salmond, B.W. Bycroft, A. Lazdunski, G.S.A.B. Stewart, and P. Williams. 1995. Multiple *N*-acyl-L-homoserine lactone signal molecules regulate production of virulence determinants and secondary

metabolites in *Pseudomonas aeruginosa*. *Proceedings of the National Academy of Sciences of the United States of America* 92:9427-9431.

22. Smith, R.S., and B.H. Iglewski. 2003. *P. aeruginosa* quorum sensing systems and virulence. *Current Opinion in Microbiology* 6:56-60.
23. Sokol, P.A., U. Sajjan, M.B. Visser, S. Gingues, J. Forstner, and C. Kooi. 2003. The CepIR quorum-sensing system contributes to the virulence of *Burkholderia cenocepacia* respiratory infections. *Microbiology* 149:3649-3658.
24. Heithoff, D.M., and M.J. Mahan. 2004. *Vibrio cholerae* biofilms: Stuck between a rock and a hard place. *Journal of Bacteriology* 186:4835-4837.
25. Stoodley, P., K. Sauer, D.G. Davies, and J.W. Costerton. 2002. Biofilms as complex differentiated communities. *Annual Review of Microbiology* 56:187-209.
26. Kaplan, H.B., and E.P. Greenberg. 1985. Diffusion of auotinducer is involved in regulation of the *Vibrio fischeri* luminescence system. *Journal of Bacteriology* 163:1210-1214.
27. Davies, D.G., M.R. Parsek, J.P. Pearson, B.H. Iglewski, J.W. Costerton, and E.P. Greenberg. 1998. The involvement of cell-to-cell signals in the development of bacterial biofilm. *Science* 280:295-298.

Chapter 6

Localized Quorum Sensing in *Vibrio fischeri*[*]

Quorum sensing is almost always regarded as a population effect in three-dimensional bulk samples of bacteria. Here *two*-dimensional samples of *Vibrio fischeri* cells adhered onto glass surfaces are created to examine the effect of *local* population densities on quorum sensing. This is done by measuring the luminescent response. The 2-D bacterial populations allow for the measurement of both time and distance effects on quorum sensing, which were previously very challenging to access in typical 3-D bulk samples. Thus, quorum sensing is considered in terms of signal diffusion. The results show quorum sensing can occur locally in 2-D surface samples and is a function of both population density and signal diffusion time.

6.1 Introduction

The modeling of surface-associated bacteria producing signaling molecules in Chapter 5 suggests that both population density and signal diffusion contribute to quorum sensing and that there exists under set conditions (population density and signal diffusion time) a "true quorum"– a number a cells necessary for quorum sensing. In this chapter, the analogous experiments are performed. *V. fischeri* is used to investigate population and diffusion effects in quorum sensing.

---

[*] The material in this chapter is being prepared for publication in Biophysical Journal.

Quorum sensing occurs in *V. fischeri* via an autoinducer producer and receptor protein pair. Briefly, the LuxI protein produces autoinducer molecules, acylated homoserine lactones (AHL), which diffuse across the cell membrane into the surrounding medium. At a critical autoinducer concentration, interaction with the receptor protein LuxR is possible and binding occurs (1). The LuxR-AHL complex is then able to bind to the promoter of the *V. fischeri* luminescence gene to activate transcription, resulting in light production.

The hypothesis is that due to the physical phenomenon of AHL diffusion from surface cells, quorum sensing depends on both the *local* cell density *and* the total time the AHL signals are allowed to diffuse from the cells. Traditionally, quorum sensing is studied in three dimensions in bulk suspensions in which cells are evenly distributed throughout the medium. In contrast, a local cell density occurs in a sample if cells are concentrated at the surface, perhaps with none in the planktonic form. At a smaller scale yet, heterogeneity in local cell density creates some areas that are more highly concentrated with cells than others.

To test diffusion effects on quorum sensing, the surface cell density is varied and the change in luminescence in *V. fischeri* is measured with time. Luminescence experiments show that quorum sensing happens on a local scale and that signal diffusion has an effect. Larger cell concentrations and longer times result in more luminescence. The three main experiments presented are as follows:

1. Bulk quorum sensing measurements of 3-D *V. fischeri* samples to use as comparisons with local 2-D samples.
2. Measurements of localized quorum sensing as a function of surface cell density.

3. Measurements of localized quorum sensing as a function of diffusion time, compared for two different local cell concentrations.

6.2 Experiments

Since the modeling from Chapter 5 also shows that surface cell concentrations formed via random or patterned adhesion give similar AHL concentration profiles, all surface localizations were created using the random adhesion method. Bulk cell samples were formed by placing a cell suspension of known population density into a microwell to a depth of 500 μm. Surface cell samples (Figure **6-1**) were formed by harvesting a bulk cell suspension and fixing the population density by dilution in PB medium. The bulk cells were then transferred to a microwell and allowed to settle and adhere to the glass for different times. The remaining non-adhered bulk cells were removed by repeated gentle rinses with fresh PB using slow pipetting.

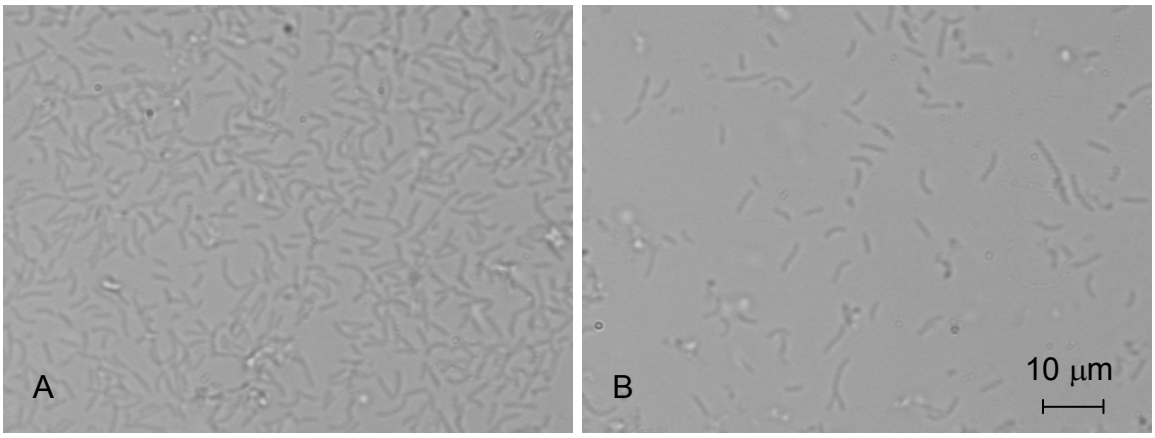

Figure 6-1: Two examples of localized cell populations developed using the procedure described in Section 6.2 and Figure 3-4 and used to collect the data in Figure **6-5**. (A) 5-μm cell spacing. (B) 9-μm cell spacing.

Sample depths were maintained at a depth of 500 μm over the course of the experiment by adding drops of fresh medium as necessary. Cell density was quantified with the ImageJ image processing program and verified with a visual direct count of the cells. Luminescence was quantified with a photomultiplier tube (PMT) through the microscope. Luminescence was reported in W/cell; for the emission wavelength 500 nm, there are 2.5×10^{12} photons/s in 1 watt. Further details on the experimental methods are provided in Chapter 3.

6.3 Results

6.3.1 Bulk quorum sensing

Quorum sensing has been traditionally examined in 3-D bulk suspensions of cells. Figure **6-2** presents the data from a recreation of those typical bulk quorum sensing response versus time experiments and matches with what has been presented in the literature (2). The luminescence is not detectable ($< 10^{-23}$ W/cell) until a large enough cell density ($> 3\times10^{7}$ cells/mL) has grown, after which the luminescence greatly and quickly increases.

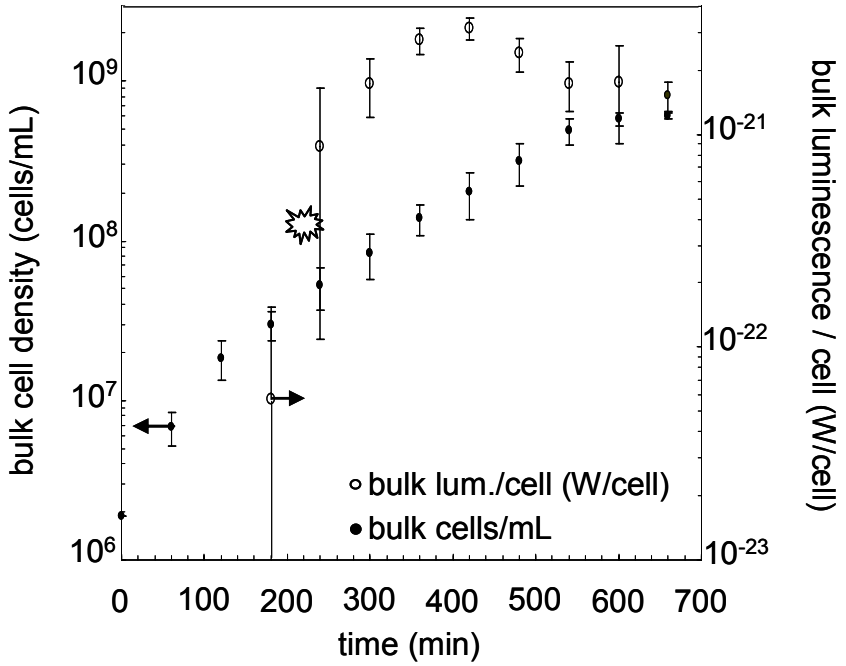

Figure 6-2: The quorum sensing response per cell in 3-D bulk cell samples over time. Each point is the average of five readings and error bars show the 95% confidence level. The bulk cell density on the left axis (black) and the luminescence per cell (W/cell) is on the right axis (white). Both scales are logarithmic. This plot is similar to the first quorum sensing observations by Nealson et al. (2) whose *V. fischeri* experiments were reproduced in experiments presented in this figure. The star-burst demarks I_{QS} (W/cell)– quorum sensing defined in Equation **6.1**.

It is interesting to note that quorum sensing has not been quantifiably defined in the literature in terms of response (only population density). Here it is put forth that "quorum sensing" be defined as the point where the response intensity (e.g., luminescence for the case of *V. fischeri*) reaches 10% of the observed range of intensities beyond the minimum (Equation **6.1**). That is,

$$I_{QS} \equiv 0.1(I_{max} - I_{min}) + I_{min}. \qquad (6.1)$$

Therefore, the case in Figure **6-2** is quorum sensing at 3.7×10^{-22} W/cell (demarked with the star-burst on the plot), which corresponds to the steep increase in response occurs at t = 230 minutes and 5×10^{7} cells/mL on the plot. This quantitative definition of quorum sensing, not based on population density, can facilitate comparisons among quorum sensing experiments.

6.3.2 Localized quorum sensing

To investigate the effect signal diffusion time on quorum sensing, local samples of cells on surfaces, instead of bulk suspensions of cells, are examined. Although the production time for AHL is accessible in bulk bacterial suspensions, the time for signal *diffusion* ($\sim L^2/D$) becomes experimentally accessible when examining a monolayer of cells, on the order of minutes rather than hundredths of seconds as in bulk samples. This is because in the bulk the longest distance without a bacterium is roughly L, but at a surface the longest distance without a bacterium is the height of fluid above the surface (in our case, ~500 μm). For example, consider the time for a signal molecule to diffuse between cells in a bulk suspension that is 10^{11} cells/mL (Equation **6.2**).

$$10^{11}\,\text{cells/mL} = 10^{-11}\,\text{mL/cell} = 10\,\mu\text{m}^3/\text{cell} = 2.15\,\mu\text{m/cell} = 0.05\,\text{seconds} \qquad (6.2)$$

For a bulk suspension of 10^{11} cells/mL, diffusion distance L = 2.15 μm, and diffusion time $\tau \sim L^2/D$ = 0.05 seconds (D = 100 $\mu m^2/s$). For a similarly spaced localized population, the average diffusion distance is now much larger than L = 2.15 μm because there are no cells in the z direction (Figure 6-3). For the surface cell, L = 170 μm

(average of the diffusion distances in x (2.15 μm), y (2.15 μm), and z (500 μm) so $\tau \sim L^2/D = 10$ minutes.

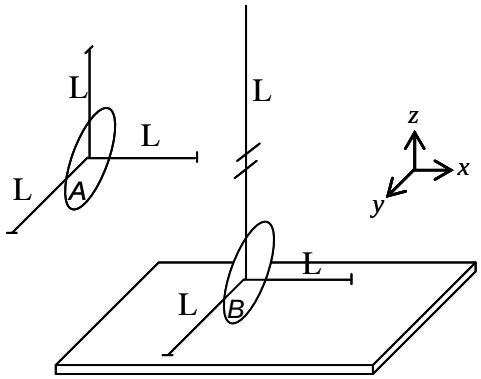

Figure 6-3: Depiction of the larger average diffusion distance (and therefore diffusion time) of 2-D cell samples (B) versus 3-D bulk samples (A).

The two key figures of this thesis, Figure **6-4** and Figure **6-5**, examine localized quorum sensing and the effect of signal diffusion. Figure **6-4** compares the luminescence of various densities of surface cells and bulk suspensions of cells. To compare the two cases, the luminescence on a per cell basis for both the surface and bulk samples versus cell spacing in one dimension (i.e., x or y for the surface samples and x, y, or z for the bulk samples) (Figure **6-4** A) and also the total sample luminescence versus the total number of cells in each sample (Figure **6-4** B) is plotted. Luminescence in both cases was measured at initial time points; bulk samples were measured within one minute of placement into the well and surface samples were measured within one minute of a final transfer of fresh medium into the well.

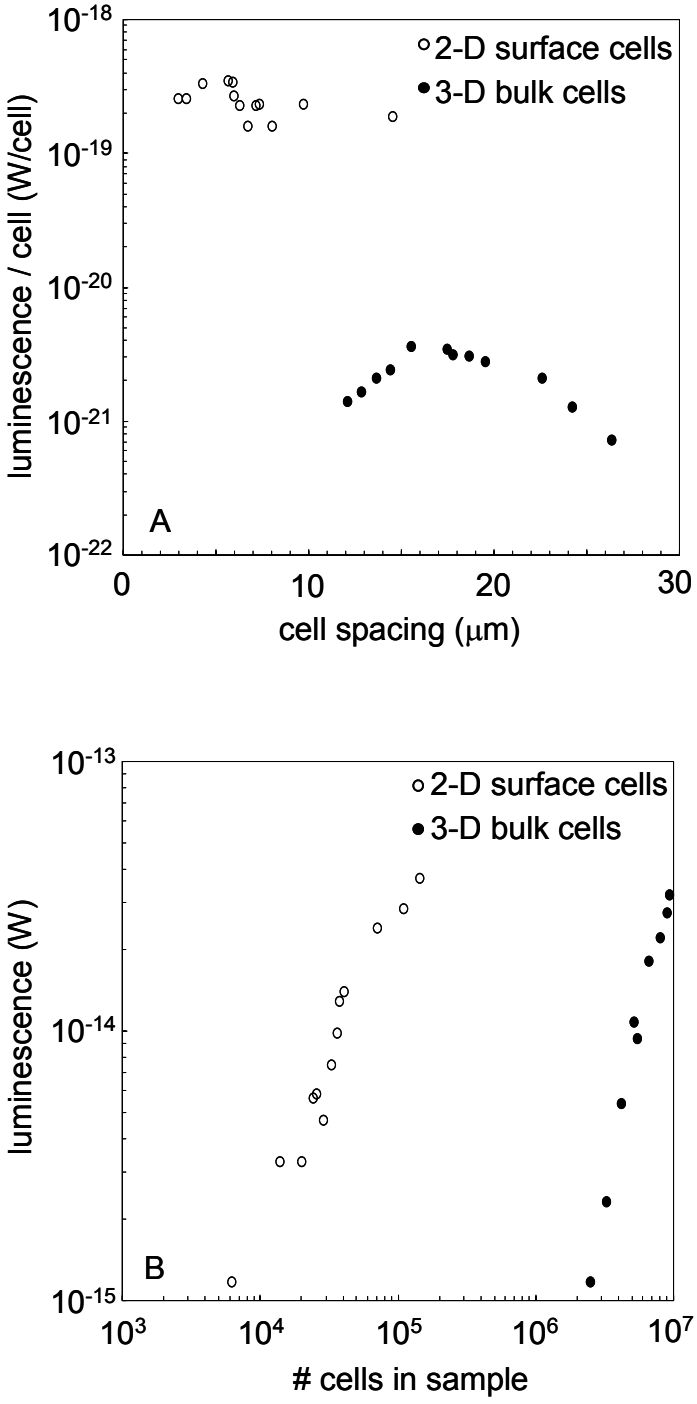

Figure 6-4: The quorum sensing response for 3-D bulk cells (black) and 2-D surface cell samples (white). (A) Luminescence per cell versus cell spacing. (B) Total luminescence versus total cells. Each point represents a separate experiment, each from different batch cultures.

Surface samples, able to contain higher cell densities locally, show 2 orders of magnitude greater luminescence per cell (e.g., 2×10^{-19} vs. 2×10^{-21} W at 14-μm spacing) (Figure **6-4** A). The absolute luminescence values measured are similar, ranging from 1×10^{-15} to 35×10^{-15} W, for both the bulk and localized surface samples, even though the surface samples contain much fewer cells than the bulk samples (Figure **6-4** B). Through this it is shown that quorum sensing does happen locally.

To address the effect signal diffusion time has on quorum sensing, the luminescence of different local surface cell densities (Figure **6-1**) at different time points was monitored (Figure **6-5**).

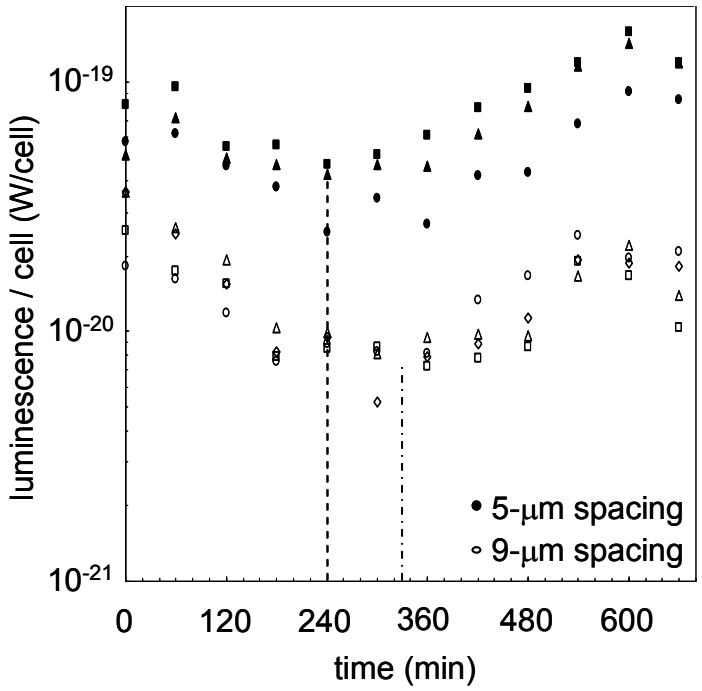

Figure 6-5: The local quorum sensing response per cell in W/cell in 2-D surface cell samples over time for two different cell densities of 5-μm cell spacing (black) and 9-μm cell spacing (white) (Figure **6-1**). Repeat runs for each cell density are represented by varying shapes. The time the luminescence starts to increase for each concentration is demarked by the dashed lines.

The t = 0 point was taken within one minute of a final transfer of fresh medium into the well (refer to the Experimental Section 6.2). Quorum sensing response (luminescence) starts to increase at a slightly earlier time for the higher local concentration case (t = 240 min for an initial surface density set by 5-μm cell spacing, versus t = 330 min for 9-μm cell spacing), as indicated by the dashed lines (Figure **6-5**). After those time points, the rate of increase of the luminescence per cell is 5 times faster in the high surface cell density samples than in the low cell density samples. This rate increase is not visually obvious with a glance at Figure **6-5** because of the log scale.

6.4 Discussion

Quorum sensing has most often been described only in terms of population density (3-5) and measured in 3-D bulk cell samples. The use of 2-D surface cell samples allows signal diffusion time effects to be examined at experimentally reasonable time scales ($\tau \sim$ minutes, rather than hundredths of seconds in 3-D samples). The diffusion time of signals to neighboring cells localized on a surface is accessible because AHL can also diffuse into the bulk, greatly increasing the time required for significant buildup of AHL concentration around a cell.

Some other experiments may come to mind to test diffusion time in quorum sensing. A batch sample of cells starting at an initial cell density that does not exhibit quorum sensing can be monitored over time and eventually quorum sensing will be detected. This is exactly the experiment presented in Figure **6-2**, similar to the first *V. fischeri* quorum sensing tests by Nealson et al. (2). The time variable, however, is

effectively growth time and diffusion time cannot be accessed. A chemostat (a device for continuous culture of bacteria) is capable of independently controlling growth rate and population by adjusting flow rate and nutrient concentration (6). This sounds useful for examining diffusion time in quorum sensing, however, the constant flow of fresh medium in and overflow cells out prohibits quorum sensing studies because signals are being transported out of the culture vessel.

Without an experimental design that allows for signal diffusion time considerations, it is easy to see how quorum sensing came to be understood on a population basis only. We put forth a definition of quorum sensing based not on population density, but rather on response intensity, to avoid the omission of signal diffusion time considerations to allow for comparisons among quorum sensing experiments. Figure **6-4** shows that quorum sensing can happen locally with surface samples of cells, as is evident through the significant 100-fold greater level of luminescence in the surface cells than in the bulk cells.

Figure **6-5** suggests that both population density and signal diffusion time affects quorum sensing. Localized samples of cells spaced 5 μm apart begin quorum sensing 90 minutes sooner than surface cells spaced 9 μm apart. The initial decrease in the response signal in Figure **6-5**, however, makes it difficult to draw strong conclusions. The initial decrease in the response signal in Figure 6-5 has also been noted in previous experiments of bulk *V. fischeri* quorum sensing (2, 7, 8). This "eclipse" (2) phenomenon has been hypothesized to be due to the dilution of substrates necessary for bioluminescence (7) or the presence of an inhibitor that needs to be metabolized (7, 9-12) upon transfer into fresh media. Another explanation to the initial decrease in luminescence in Figure **6-5** is that

there is a carry-over of luminescence from the concentrated bulk samples used to form the local surface samples, which is possible because there are degradation rates associated with proteins used in bioluminescence (13). The decrease is not due to quorum sensing effect *per se*, since any signaling molecules were transferred out of the sample, but luminescence itself. It is advisable for future experimenters investigating the diffusion of quorum sensing signals to use a medium that is pre-conditioned with proper substrates or devoid of luminescence inhibitors to fix eclipsing problems and/or to altogether avoid eclipsing by using a different system with shorter half-life luminescent proteins.

It should also be noted that although the local cell samples used in Figure **6-5** initially lacked cells in the bulk, the eventual reproduction of the surface cells caused an increase in bulk cell concentration. The bulk cell concentration was monitored over the course of the experiment. At the critical time points where quorum sensing begins (demarked by the dashed lines in Figure **6-5**) the bulk concentration in both samples was below quorum sensing level (5×10^6 cells/mL for the low surface density (9-μm spacing) and 2×10^7 cells/mL for the high surface density (5-μm spacing)). For points in Figure **6-5** where the bulk cell density surpassed quorum sensing bulk cell density level of 4×10^7 cells/mL, a corresponding bulk luminescence was subtracted out of the reading, based on the data in Figure 6-2. However, since the bulk concentration of both samples was negligible at the onset of quorum sensing in the local surface experiments, the observation that the high surface density sample started quorum sensing faster than the low sample is real.

The modeling of cells as point sources of AHL demonstrates that quorum sensing can occur with small numbers of cells, as long as enough signal diffusion time is allowed to pass and a certain "true quorum" cell number is met (curves in Figure 5-3). The experiments presented here, however, are best represented by the infinite plane source solution (black squares in Figure 5-3) because the samples were contained in 1.3-cm diameter wells and the cell lawns were allowed to extend to the walls of well. The *V. fischeri* experiments do not allow for testing of a "true quorum" because the luminescence, although detectable in local samples of surface cells, is still measured as a bulk response. Preliminary work has been done (A.1) to create a quorum sensing system with a green fluorescent protein (GFP) reporter in *E. coli* to use in "true quorum" experiments where small (not infinite) isolated areas of surface cells at various densities are monitored over time. GFP, and thus quorum sensing, can be detected in individual cells so the system will allow for the determination of a "true quorum"– a number of cells necessary to elicit a response under a given set of conditions (signal diffusion time *and* cell spacing (density)).

With quorum sensing now implicated in the formation (14), maturation (15), and stability (16) of biofilms for various species, local quorum sensing is especially important. Local surface populations exist naturally in biofilms and the biofilm matrix affects diffusion (the effective biofilm diffusion coefficient relative to water is 0.4) (17). If the "true quorum" number is met then even a small localization of cells on a surface could act as a biofilm seed with enough diffusion time.

6.5 Conclusion

Signal diffusion time, population density, and population number all affect quorum sensing. This experimental work was able to access diffusion in quorum sensing through localizations of cells in 2-D surface samples. Previously studied 3-D quorum sensing samples leave diffusion effects out because 3-D diffusion times are on the order of hundredths of seconds, rather than minutes. Quorum sensing was shown to happen locally in luminescing *V. fischeri* surface samples and a comparison between two different local cell densities suggested diffusion time has an influence on quorum sensing. To better compare among quorum sensing experiments a definition was formed based on response intensity rather than population density, which is not the only variable involved. The diffusion modeling of Chapter 5 shows that under any given set of conditions of signal diffusion time *and* cell spacing (density), there exists a "true quorum"– a number of cells necessary to elicit a response. Experimental evidence of a true quorum may be garnered by detecting fluorescence in quorum sensing *E. coli* on an even more local scale of individual cells arranged in small isolated areas. The data in this thesis demonstrate that *localized* quorum sensing and the influence of cell density, cell number, and signal diffusion time are necessary to consider, which is especially important in biofilms (naturally local cell populations), where local pockets of quorum sensing could kick-start biofilm development.

6.6 References

1. Pappas, K.M., C.L. Weingart, and S.C. Winans. 2004. Chemical communication in proteobacteria: biochemical and structure of signal synthases and receptors required for intercellular signaling. *Molecular Microbiology* 53:755-769.
2. Nealson, K.H., T. Platt, and J.W. Hastings. 1970. Cellular control of the synthesis and activity of the bacterial luminescent system. *Journal of Bacteriology* 104:313-322.
3. Miller, M.B., and B.L. Bassler. 2001. Quorum sensing in bacteria. *Annual Review of Microbiology* 55:165-199.
4. Fuqua, C., and E.P. Greenberg. 2002. Listening in on bacteria: acyl-homoserine lactone signaling. *Nature Reviews Molecular Cell Biology* 3:685-695.
5. Waters, C.M., and B.L. Bassler. 2005. Quorum sensing: cell-to-cell communication in bacteria. *Annual Review of Cell and Developmental Biology* 21:319-346.
6. Madigan, M.T., J.M. Martinko, and J. Parker. 2000. Chapter 5 Microbial Growth. In Brock Biology of Microorganisms, Ninth Edition. Prentice-Hall, Upper Saddle River.
7. Eberhard, A. 1972. Inhibition and activation of bacterial luciferase. *Journal of Bacteriology* 109:1101-1105.
8. Ruby, E.G., and K.H. Nealson. 1976. Symbiotic Association of *Photobacterium fischeri* with the marine luminous fish *Monocentris japonica*: A model of symbiosis based on bacterial studies. *Biological Bulletin* 151:574-586.
9. Holzman, T.F., and T.O. Baldwin. 1983. Reversible inhibition of the bacterial luciferase catalyzed bioluminescence reaction by aldehyde substrate: Kinetic mechanism and ligand effects. *Biochemistry* 22:2838-2846.
10. Eberhard, A., A.L. Burlingame, C. Eberhard, G.L. Kenyon, K.H. Nealson, and N.J. Oppenheimer. 1981. Structural identification of autoinducer of *Photobacterium fischeri* luciferase. *Biochemistry* 20:2444-2449.
11. Reeve, C.A., and T.O. Baldwin. 1981. Luciferase inactivation in the luminous marine bacterium *Vibrio harveyi*. *Journal of Bacteriology* 146:1038-1045.
12. Haygood, M.G., and K.H. Nealson. 1985. Mechanisms of iron regulation of luminescence in *Vibrio fischeri*. *Journal of Bacteriology* 162:209-216.
13. Andersen, J.B., C. Sternberg, L.K. Poulsen, S.P. Bjorn, M. Givskov, and S. Molin. 1998. New unstable variants of green fluorescent protein for studies of transient gene expression in bacteria. *Applied and Environmental Microbiology* 64:2240-2246.
14. Huber, B., K. Riedel, M. Hentzer, A. Heydorn, A. Gotschlich, M. Givskov, S. Molin, and L. Eberl. 2001. The *cep* quorum-sensing system of *Burkholderia cepacia* H111 controls biofilm formation and swarming motility. *Microbiology* 147:2517-2528.
15. Davies, D.G., M.R. Parsek, J.P. Pearson, B.H. Iglewski, J.W. Costerton, and E.P. Greenberg. 1998. The involvement of cell-to-cell signals in the development of bacterial biofilm. *Science* 280:295-298.

16. Tomlin, K.L., R.J. Malott, G. Ramage, D.G. Storey, P.A. Sokol, and H. Ceri. 2005. Quorum-Sensing Mutations Affect Attachment and Stability of *Burkholderia cenocepacia* Biofilms. *Applied and Environmental Microbiology* 71:5208-5218.
17. Stewart, P.S. 2003. Diffusion in Biofilms. *Journal of Bacteriology* 185:1485-1491.

Chapter 7

Engineered Biofilm Development in *P. aeruginosa*

7.1 Introduction

Given the influence of biofilms in the world: industrial surface biofouling (1), medical implant infection (2), and use in bioremediation (3), it is desirable to control biofilm formation. It is understood that the first step in biofilm formation is initial bacterial adhesion (2); however it is difficult to generalize bacterial adhesion mechanisms to all biofilm scenarios because it varies across different niches (4) and there is no one particular external aspect (e.g., LPS (5) or humic acid (6, Chapter 4)) that affects adhesion. After adhesion, bacteria increase extracellular polymeric substance (EPS) production to form biofilms of cells embedded in an EPS matrix. Friedman and Kolter find that genes involved in EPS polysaccharide production, like the *P. aeruginosa psl* gene, are needed in proper biofilm formation (7). Additionally, quorum sensing is necessary for proper *P. aeruginosa* biofilm formation (8) and is implicated as regulating specifically EPS synthesis (9).

The literature establishes that EPS and quorum signaling are necessary for biofilm formation. It would be valuable to know if it was the diffusion of these molecules that affects biofilm formation. Quorum sensing is most often regarded as population density controlled, but the localized (two-dimensional) quorum sensing results from Chapters 5 and 6 reveal that signal diffusion also has an effect. It is easy to extend this concept

from the *V. fischeri* luminescent cells to *P. aeruginosa* biofilm cells; a biofilm is naturally a localized cell density due to its surface association. The goal in this chapter is to determine the influence of cell number, density, and time (n, L, and τ – parameters shown in Chapters 5 and 6 to control quorum sensing) on biofilm development. Biofilms were engineered in controlled manners using laser trapping and random adhesion. Subsequent biofilm development and adhesion forces were quantified with image analysis and shear stress tests. The results presented stem from three main sets of experiments:

1. Compare biofilm development among differently sized (n and L) small engineered biofilms formed via laser trap placement of cells on a surface and measured with image analysis at different time points.
2. Compare biofilm adhesion force changes with time among differently sized (n and L) small engineered biofilms formed via laser trap placement of cells on a surface in a parallel plate flow chamber.
3. Compare adhesion forces in larger (n), but still local, engineered biofilms formed via random cell adhesion to the surface in a parallel plate flow chamber between two local surface cell densities at different times.

7.2 Experiments

The experimental methods are detailed in Chapter 3. As a brief overview though, *P. aeruginosa* PAO1 was grown in LB and harvested at the mid-exponential phase of growth. Engineered biofilms were formed by one of two methods: laser trapping cells

from bulk suspensions to bring into contact with the surface or allowing cells from bulk suspensions to randomly adhere to the surface.

Nanofabrication of the surfaces was also used to form engineered biofilms. However, Chapter 5 details modeling that shows concentration profiles of molecules diffusing from localized cells are similar for both patterned and random adhesion. Therefore, the simpler method of random adhesion was adopted. Incidentally, the nanofabricated patterned surfaces were inconsistent (Figure **7-1**), also motivating the switch to random adhesion. As in Chapter 6, the experiments here aim to access the effect of diffusion, now on biofilm development. Forming initial biofilms via random adhesion is a sound way to do so.

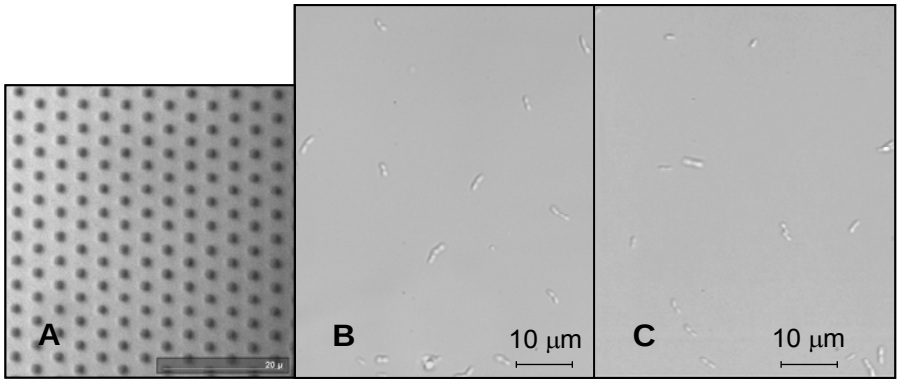

Figure 7-1: Image A shows an example of one of the nanofabricated photomasks used to make patterned patches on glass for preferential cell adhesion. An example of the resulting bacterial "pattern" (B) is not very different from C, a random adhesion example.

Once the engineered biofilms were formed, development was monitored under no flow with a low concentration (10^6 cells/mL) in the bulk above the local surface cells. Adhesion force experiments were set-up, also under no flow, but also with only sterile media in the bulk. After a set time each sample was exposed to a flow program of increasing applied force and detachment was monitored.

7.3 Results

7.3.1 Isolated engineered biofilms

7.3.1.1 Biofilm development measurements

Small arrays of bacteria were patterned onto glass surfaces via laser trap placement. A 1×1 array biofilm development was compared with that of a 2×2 array by imaging at different time points and calculating the growing cluster size (Figure **7-2**). The 1×1 array size does not increase over the 150-minute time period, but the 2×2 array approximately doubles (108% size gain).

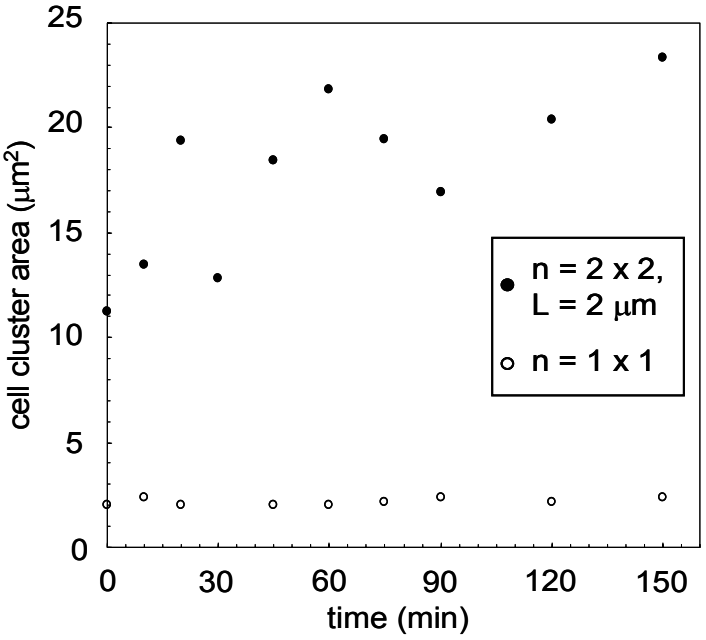

Figure 7-2: Cell cluster size versus time for two different sized arrays formed through laser trap placement. The white circles represent a 1×1 array and the black circles represent a 2×2 array that had a spacing L = 2 μm.

7.3.1.2 Biofilm adhesion force measurements

Adhesion forces for various small laser trap patterned bacteria arrays were calculated. Taking into account the 95% confidence intervals, the adhesion forces do not show an increasing trend for the 1×1 array or the 2×2 array with spacing L = 20 μm (Figure **7-3** A and B). However, the smaller spaced 2×2 array with L = 2 μm does show an increasing adhesion force trend (Figure **7-3** C).

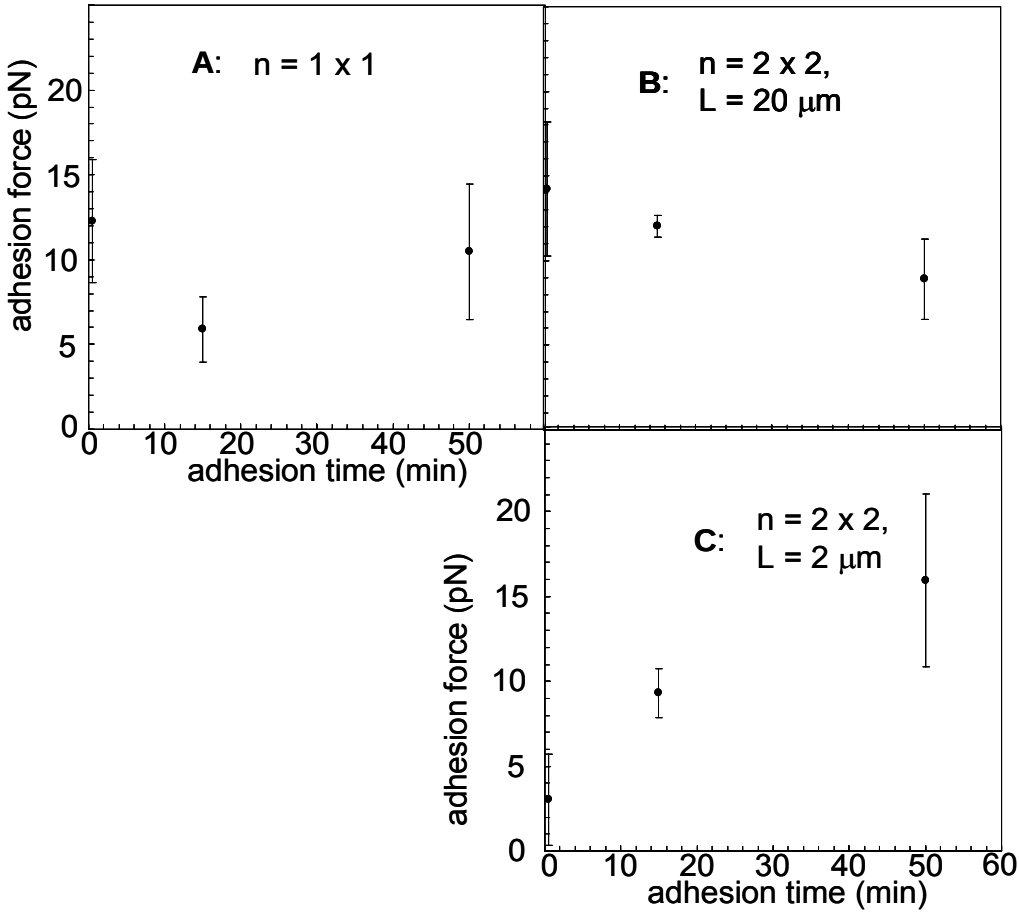

Figure 7-3: The adhesion forces for the small patterned bacterial arrays formed via laser trapping. Plot A is for a 1×1 array, B for a 2×2 array with spacing L = 20 μm, and C for another 2×2 array but with L = 2 μm. The adhesion force is calculated as the average force necessary to detach all the cells in the array. Each point is the average of 3-4 different arrays and error bars represent the 95% confidence interval.

7.3.2 Infinite engineered biofilms- adhesion force measurements

Biofilms formed through the random adhesion technique were allowed to form for various times, after which a series of increasing forces was applied by flowing media through at increasing flow rates for about 4 seconds at each setting. The number of cells that remained attached through the course of the flow program was monitored (Figure **7-4**).

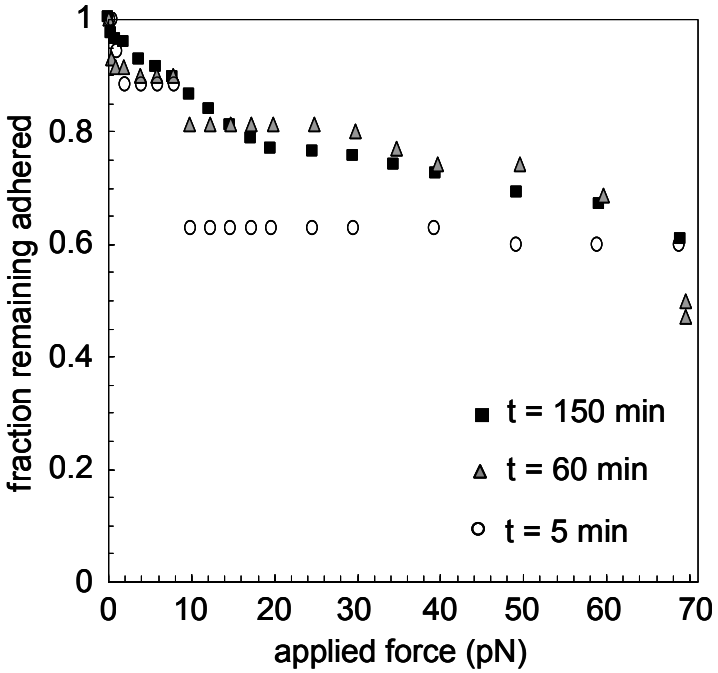

Figure 7-4: The adhesion results for biofilms formed from random adhesion with "effective" cell density = 9.5×10^6 cells/mL. ("Effective" cell density is calculated by taking the depth of fluid above the cells on the surface into account with the surface cell density.) The black squares are for a biofilm adhered 150 minutes, gray triangles– t = 60 minutes, and white circles– t = 5 minutes.

For an adhesion time of 5 minutes, the attached cell percentage quickly drops to 89% after 2 pN of applied force and remains steady until 10 pN are applied, when it drops to 63%. There is no further detachment from the surface. The 60-minute adhesion time

also shows this step-wise decrease in cells at 10 pN, but it is not as pronounced as the 5-minute case (drop to 80% remaining versus 63% remaining). The 150-minute adhesion time trial does not show a step-wise decrease in surface cells, but rather a gradual decrease. The steady decrease in attached cells is more rapid initially, dropping to 77% attached after 20 pN of applied force, beyond which the detach slope lessens. All adhesion time trials end with 50-60% of the cells remaining attached to the surface.

7.4 Discussion

The biofilm development image analysis results suggest that larger *n* biofilms have a head-start on biofilm development. One may hypothesize that the surface cells are merely serving as sticky anchor points to which incident bulk cells inevitably attach. However, if this were the case, an increase in both samples, regardless of initial size, would be expected. A control experiment using non-living surface cells or cell wall components on the surface rather than the live cells would eliminate doubt, but these data (Figure **7-2**) suggests initial biofilm size (*n*) influences biofilm formation.

Adhesion forces of the small laser trap-formed biofilms showed there was only a trend with time for the small *L* 2×2 case (Figure **7-3** C). This could be attributed to shielding, however, the arrays were formed in random alignments with the flow, and flow rates were applied in alternating directions.

These isolated biofilms allow for testing of the "true quorum" concept introduced in Chapter 5. The isolated biofilm experiments pre-dated the diffusion modeling so this was not the original intention of this work. However, a look back at the data from

Section 7.3.1 suggests that there is a "true quorum"– a number of cells necessary to elicit a response for a given diffusion time and cell spacing. In Figure **7-3** B, where L = 20 μm, n = 4 does not constitute a "quorum" to form a biofilm after 1 hour. In Figure **7-3** C, where L is 1/10 of what it was in B, n = 4 may meet the quorum requirements to seed a biofilm, observed in the increased adhesion.

The infinite biofilm adhesion measurements (Figure **7-4**) suggest that 50-60% of the *P. aeruginosa* population is "sticky", (i.e., remain adhered with forces > 70 pN (the maximum measurable force) regardless of adhesion time). Time effects are still observed in the other part of the population though. More cells are weakly attached after 5 or 60 minutes, but not 150 minutes, as exemplified by the sudden detachments that occur in the shorter time samples for applied forces < 10 pN. For applied forces beyond 20 pN, the 60 and 150 minutes trials match, suggesting a possible "saturation" for t > 60 minutes. But perhaps a more sensitive biofilm assay is necessary. Biofilms are by nature difficult to quantify due to the heterogeneous structure (10) and varying developmental stages (11). Adhesion forces are a good measure of the initial stage (attachment). An EPS assay (e.g., with FTIR (12)) may better determine diffusion and population effects in the next stage of EPS production and microcolony formation (Figure 2-3).

This chapter aimed to measure the physical effects of diffusion and population (therefore quorum sensing) on biofilm formation. Previously, quorum sensing effects on biofilms were only seen through genetic analyses and in later stages of biofilm development (8, 13). It is understandable that quorum sensing is involved in mature biofilms due to the high cell densities and diffusion limited conditions present. However, it is not as immediately obvious that quorum sensing is also involved in earlier stages.

This chapter along with Chapters 5 and 6 make the case that quorum sensing can occur on local scales and that both surface population density, surface population number, and diffusion time affect biofilm formation.

7.5 Conclusion

The influence of local (two-dimensional) population density and number as well as signal or EPS diffusion on biofilm development was examined. Adhesion force tests with infinite biofilms showed more cells more weakly attached (< 10 pN adhesion force) at shorter time points, suggesting diffusion controlled biofilm development. Isolated engineered biofilms suggested that a larger number of localized cells or a larger density of localized cells increased biofilm development as measured through cluster sizes and adhesion forces at different time points. The isolated biofilms also brought in the concept of the existence of a "true quorum"– a number of cells necessary to elicit a response. For conditions of L = 2 μm and t = 60 minutes, n = 4 cells was possibly sufficient for a "quorum", as observed through increased adhesion forces. "True quorums" can be thought of as biofilm seeds.

7.6 References

1. Flemming, H.-C. 1997. Reverse osmosis membrane biofouling. *Experimental Thermal and Fluid Science* 14:382-391.
2. Costerton, J.W., P.S. Stewart, and E.P. Greenberg. 1999. Bacterial biofilms: a common cause of persistent infections. *Science* 284:1318-1321.

3. Mohammed, N., R.I. Allayla, G.F. Nakhla, S. Farooq, and T. Husain. 1996. State-of-the-art review of bioremediation studies. *Journal of Environmental Science and Health* A31:1547-1574.
4. Bakker, D.P., B.R. Postmus, H.J. Busscher, and H.C.v.d. Mei. 2004. Bacterial strains isolated from different niches can exhibit different patterns of adhesion to substata. *Applied and Environmental Microbiology* 70:3758-3760.
5. Jones, J.F., J.D. Feick, D. Imoudu, N. Chukwumah, M. Vigeant, and D. Velegol. 2003. Oriented adhesion of *Escherichia coli* to polystyrene particles. *Applied and Environmental Microbiology* 69:6515-6519.
6. Parent, M.E., and D. Velegol. 2004. *E. coli* adhesion to silica in the presence of humic acid. *Colloids and Surfaces B: Biointerfaces* 39:45-51.
7. Friedman, L., and R. Kolter. 2004. Two genetic loci produce distinct carbohydrate-rich structural components of the *Pseudomonas aeruginosa* biofilm matrix. *Journal of Bacteriology* 186:4457-4465.
8. Davies, D.G., M.R. Parsek, J.P. Pearson, B.H. Iglewski, J.W. Costerton, and E.P. Greenberg. 1998. The involvement of cell-to-cell signals in the development of bacterial biofilm. *Science* 280:295-298.
9. Stoodley, P., K. Sauer, D.G. Davies, and J.W. Costerton. 2002. Biofilms as complex differentiated communities. *Annual Review of Microbiology* 56:187-209.
10. Lewandowski, Z., and H. Beyenal. 2003. Biofilm monitoring: a perfect solution in search of a problem. *Water Science and Technology* 47:1251-1256.
11. Sauer, K., A.K. Camper, G.D. Ehrlich, J.W. Costerton, and D.G. Davies. 2002. *Pseudomonas aeruginosa* displays multiple phenotypes during development as a biofilm. *Journal of Bacteriology* 184:1140-1154.
12. Parikh, S.J., and J. Chorover. 2005. FTIR spectroscopic study of biogenic Mn-Oxide formation by Pseudomoans putida GB-1. *Geomicrobiology Journal* 22:207-218.
13. Branda, S.S., J.E. Gonzalez-Pastor, E. Dervyn, S.D. Ehlich, R. Losick, and R. Kolter. 2004. Genes involved in the formation of structured multicellular communities by *Bacillus subtilis*. *Journal of Bacteriology* 186:3970-3979.

Chapter 8

Conclusions & Future Work

8.1 Conclusions

The main goal of this thesis was to address what occurs during the *early stages of biofilm formation* by investigating two processes that lead to biofilms– bacterial adhesion and quorum sensing. I will recap the four aims stated in Chapter 1.2 and describe the conclusions drawn from each.

1. Measure bacterial adhesion orientation and forces in the presence of various humic acid concentrations.

The adhesion of *Escherichia coli* to model soil matter (0.9-μm silica spheres or borosilicate glass capillaries) coated with varying concentrations of humic acid did not have an affect on the adhesion orientation, occurrence, nor force. Humic acid adsorption was verified using zeta potential measurements and ATH tests. Video microscopy showed the number of silica-bacterium couplets increased slightly with adsorbed humic acid. Similarly, adhesion forces measured with differential electrophoresis showed just a slight increase on a humic acid surface. Preferential end-on adhesion was observed for all humic acid coatings and there was no relationship between humic acid concentration and adhesion orientation. Humic acid therefore plays a small role in bacterial adhesion. It is suggested that other biological factors, like metabolism or stress responses, have an effect.

2. Model the diffusion of quorum sensing signals from bacteria arranged on a surface in two dimensions.

The signal diffusion model shows that both population density *and* diffusion can impact quorum sensing. This was tested for two-dimensional samples of cells localized on a surface, modeled both as continuous point sources and an infinite plane source. The signal concentration profiles are similar regardless of the localization method (patterned or random). The existence of a "true quorum" was realized. For a given diffusion time τ and population density (set by spacing L), there exists an actual number of cells n that is necessary to achieve the threshold concentration of signals for quorum sensing.

3. Determine if quorum sensing can occur locally in space and time.

Two-dimensional surface samples of *Vibrio fischeri* cells were used to examine the effects of both population density and signal diffusion on quorum sensing. Past literature has only considered three-dimensional bulk suspensions of cells in quorum sensing experiments, which allowed for the exposition of only population density effects because the very short (hundredths of seconds) diffusion times remained masked. Diffusion becomes an accessible parameter in two-dimensional surface samples, where the diffusion time is on the order of minutes. The surface samples were formed via random adhesion, based on the modeling results, and *V. fischeri* luminescence was measured as the gauge for quorum sensing. A quantitative definition of quorum sensing, based on response intensity rather than population density, was formulated. Localized quorum sensing occurred and a comparison between two different surface densities' luminescence over time showed diffusion does influence quorum sensing; the lower surface density exhibited slower quorum sensing.

4. Determine if biofilm formation can occur locally in space and time.

Experiments analogous to those in the third aim examined the influence of population density, cell number, and diffusion time, now on biofilm development. *Pseudomonas aeruginosa* biofilms were engineered either in infinite arrays via random adhesion or isolated arrays via laser trapping. Adhesion force tests with infinite biofilms showed more cells more weakly attached (< 10 pN adhesion force) at shorter time points, suggesting diffusion controlled biofilm development. Isolated biofilms showed that a larger number of localized cells or a larger density of localized cells increased biofilm development as measured through image analysis of cluster sizes and adhesion forces in a flow chamber at different time points. The isolated biofilms also got at the concept of the existence of a "true quorum"– a number of cells necessary to elicit a response. For a set diffusion time of 60 minutes, $n = 4$ showed increased adhesion at a population density based on $L = 2$ μm, but not $L = 20$ μm. Although adhesion forces are not necessarily direct, specific, and sensitive measurements of quorum sensing or biofilm development, and the presence of EPS or signals was not verified, these biofilm experiments bring to light the importance of diffusion in biofilm formation. Even a small localization of cells on a surface can act as a biofilm seed if given enough diffusion time, as long the quorum number is met.

8.2 Future work

I would like to see the work in this thesis continue in two regards. The "true quorum" concept should be tested using quorum sensing *E. coli* that fluoresce in

response. These cells, *E. coli QSg*, have already been engineered and preliminary experiments have been started in collaboration with Dr. Patrick Cirino (A.1). *E. coli QSg* will allow for quorum sensing to be observed in individual cells and they come with the added benefit of containing a short half-life green fluorescent protein (GFP) (60 minutes), which will aid in unmasking true quorum sensing signal diffusion effects. Care should be taken to avoid masking quorum sensing in the eclipse effect discussed in Section 6.4 by conditioning the medium with proper substrates (and removing inhibitors) for the bioluminescence reaction.

A second avenue of research should be the continued testing of quorum and diffusion sensing in biofilm formation. The *P. aeruginosa* experiments presented in Chapter 7 should be repeated and expanded to cover larger isolated arrays ($n > 4$), denser infinite arrays ($> 9.5\times10^6$ cells/mL), and longer times ($t > 150$ minutes). Isolated cell localizations do not need to be formed using laser trapping nor nanofabrication. Random adhesion is still valid and can be isolated using a nebulization of dilute cells suspensions on the surfaces. The second biofilm developmental stage beyond bacterial adhesion, which is increased EPS production and microcolony formation, should be assayed. Nuclear magnetic resonance (NMR) and Fourier transform infrared (FTIR) spectroscopy may be useful techniques to assay EPS production (1) or diffusion in biofilms (2), or image biofilms (3), and their applications have been discussed with potential collaborators on the Penn State campus (4, 5).

I foresee more distant future applications of this work emerging as genetically engineered bacteria for enhanced *in situ* bioremediation, new antibiotic treatments based

on the disruption of the diffusion of quorum sensing signals, and high sensitivity biosensors (either detecting bacterial quorum sensing or exploiting it).

8.3 References

1. Parikh, S.J., and J. Chorover. 2005. FTIR spectroscopic study of biogenic Mn-Oxide formation by Pseudomoans putida GB-1. *Geomicrobiology Journal* 22:207-218.
2. Vogt, M., H.-C. Flemming, and W.S. Veeman. 2000. Diffusion in *Pseudomonas aeruginosa* biofilms: a pulsed field gradient NMR study. *Journal of Bacteriology* 77:137-146.
3. Hoskins, B.C., L. Fevang, P.D. Majors, M.M. Sharma, and G. Georgiou. 1999. Selective imaging of biofilms in porous media by NMR relaxation. *Journal of Magnetic Resonance* 139:67-73.
4. Mueller, K. 2006. Personal communication on NMR for biofilms. In Penn State Department of Chemistry.
5. Stapleton, J. 2006. Personal communication on FTIR for biofilms. In Penn State Materials Research Institute.

Appendix A

Localized Quorum Sensing in Fluorescent *E. coli*[*]

A.1 *E. coli* QSg

Quorum sensing *E. coli* cells that responded to quorum sensing with green fluorescent protein (GFP) expression were genetically engineered using the facilities available in Dr. Ming Tien's laboratory (Penn State Department of Biochemistry and Molecular Biology, University Park, PA). Plasmid DNA was purified from *E. coli* cells harboring genes for LuxI, LuxR, GFP, or kanomycin antibiotic resistance using Qiagen Spin Miniprep Kit (Qiagen Inc., Valencia, CA). All biological "parts" (i.e., promoters, ribosome binding sites, coding sequences, and transcriptional terminators) were obtained from BioBricks (MIT, Cambridge, MA). The isolated DNA was cleaved at specific recognition sequences using restriction enzymes in a restriction digest step. The cut plasmids were purified in an agarose gel using electrophoresis. The pieces were then removed from the gel and combined to allow for ligation of the DNA resulting in a vector containing all parts of functional genes for LuxI, LuxR, GFP, and kanomycin resistance. This product was transformed into chemically competent E. coli, which was then grown on plates containing kanomycin to select the desired cells. These cells, *E. coli* QSg,

[*] The work described in this appendix was conducted in collaboration with Patrick Cirino and Lane Weaver.

produce AHL with LuxI and bind AHL with LuxR, which activates the transcription of GFP (Figure **1-1**)

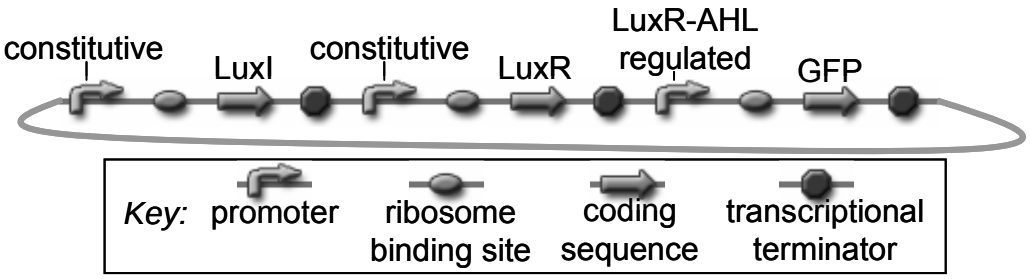

Figure 1-1: Schematic of the major parts of the *E. coli* QSg plasmid.

For experiments, *E. coli* QSg was grown in M9 minimal media with 0.2% glycerol as the carbon source, 0.1% yeast extract (a reduced concentration to avoid fluorescence background), and kanomycin. Single colonies were revived at 30°C on a shaker table at 200 rpm until the stationary phase of growth. Then, the cells were diluted in a transfer into fresh M9 minimal media and grown at the same conditions (30°C and 200 rpm shaking) until harvest time.

A.2 Bulk scale experiments

Several variations on *E. coli* QSg were engineered (for example containing weak, medium, or strong ribosome binding sites) and compared. Figure **1-2** shows some of these variations' fluorescence measurements (Tecan fluorometer) taken at different points during batch growth. There was increased fluorescence at high population densities for samples 16, 23, and 32, but with varying maximal intensities. Sample 8 behaved similarly to the control samples, with constant base level fluorescence, suggesting its

particular genetic variation was not ideal. The positive control constitutively expresses GFP and the negative control contains LuxR-AHL regulated GFP, but no LuxI.

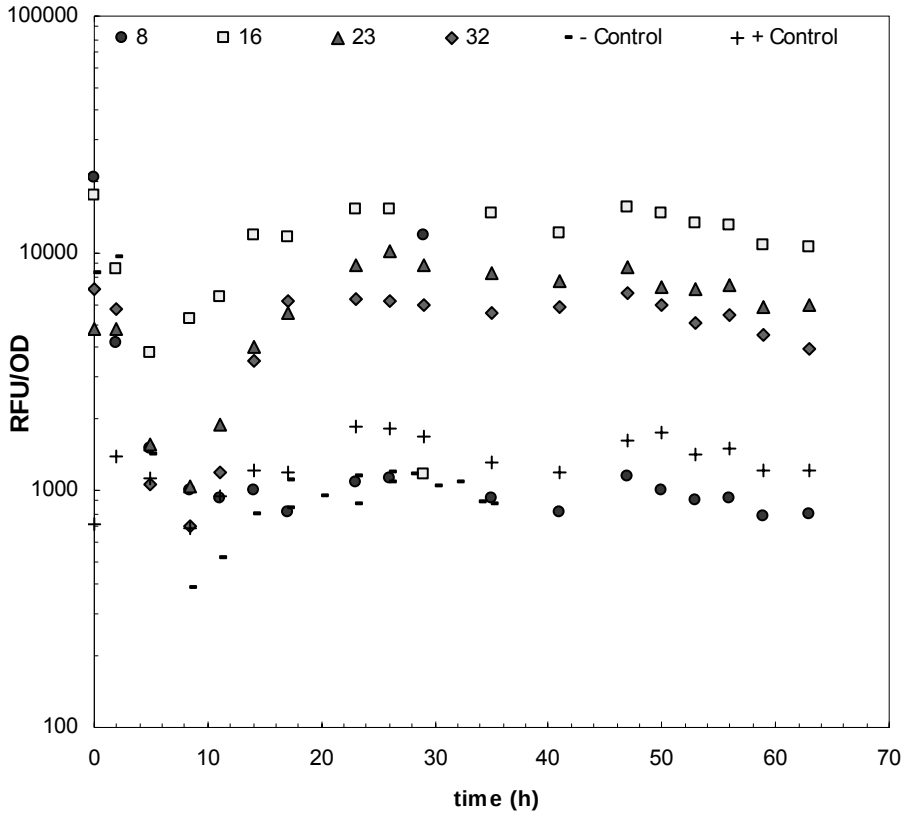

Figure 1-2: Relative fluorescence units per optical density (RFU/OD) for different *E. coli* QSg samples and controls. Samples 8, 16, 23, 32 represent *E. coli* QSg samples containing slight variations in their quorum sensing genes (e.g., weak or strong ribosome binding sites). The positive control constitutively expresses GFP and the negative control contains LuxR-AHL regulated GFP, but no LuxI.

The observed increase in fluorescence at high population densities is how quorum sensing is typically thought of in bulk suspensions such as these. To get at diffusion effects, local samples need to be created. Figure **1-3** gives an example image of the fluorescence that can be seen in individual cells through fluorescent microscopy. This

can be utilized to test for signal diffusion effects in quorum sensing on a local scale and determine “true quorums”.

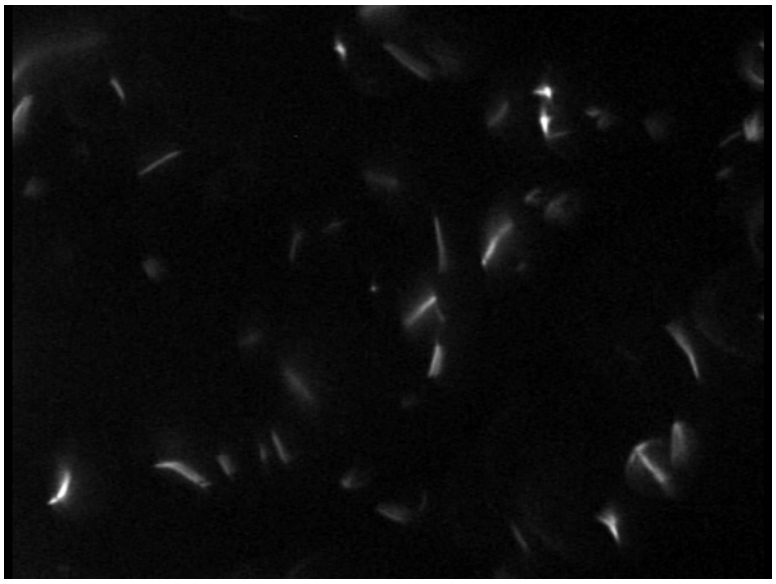

Figure 1-3: Fluorescent microscopy image of *E. coli* QSg in a bulk sample.

Appendix B

Standard Operating Procedures

Safety and sterility while working with bacteria

A. Safety first

1. Standard personal protection equipment
   a. safety glasses
   b. latex or nitrile gloves- rinse with ethanol or change frequently
   c. closed-toe shoes
2. Special personal protection equipment
   a. Orange autoclave gloves for removing bins from the autoclave and other hot items
   b. Blue cryogenic gloves- necessary for prolonged exposure with the cryogenic liquid N_2 tank.
3. Spill procedures
   a. For small drops clean with 70% ethanol in DI water solution.
      NOTE: Ethanol solution is extremely flammable. Do not store ethanol bottle near flame. Make sure all surfaces in the vicinity of flames are dry (free of ethanol), including hands and gloves.
   b. For major spills clean with 10% bleach
4. General health
   a. Wash hands with soap and water before exiting the lab.
   b. Wipe gloves with ethanol before touching community equipment in the lab (e.g. keyboards, microscopes, pipets.)
   c. Biosafety level 2 organisms (*Pseudomonas aeruginosa* and *Burkholderia cepacia*) affect immunocompromised individuals.
      i. <u>All</u> procedures for BSL2 bacteria must be conducted under the laminar flow. Once BSL2 organisms are contained in a closed sample holder (e.g. capillary or focht chamber) the laminar flow hood is no longer needed.
      ii. Store BSL2 waste under the laminar flow hood.
      iii. Sterilize BSL2 waste frequently.
      iv. BSL1 bacteria (*Escherichia coli*, *Bacillus subtilis*, and *Vibrio fischeri*) may be handled in the designated area on the central laboratory bench denoted by the metal biohazard zone surface.
5. Waste handling
   a. Dispose of liquid bacteria waste in marked bottles. BSL1 bottles are located by the biohazard metal plate on the bench in secondary containment. BSL2 bottles are in the left corner of the laminar flow hood also in secondary containment.
   b. Dispose of solid waste contacting bacteria solutions in the appropriate solid waste containers, by the incubators for BSL1 or again under the laminar flow hood for BSL2. Solid waste includes gloves, Kim wipes, paper towels, pipets, and pipet tips for example. Glass waste in contact with bacteria should be placed in the red biohazard sharps receptacles.
   c. Autoclave and dispose of the waste on a regular basis.

B. Sterilizing and Washing Bacteria Contaminated Glassware and Waste Containers

1.) Carefully pour the contents of the growth flask into the waste containers located in the laminar flow hood (for BSL2 waste) or by the designated biohazard zone on the laboratory bench (for BSL1 waste ONLY). ***Note:** Make sure the waste container is in secondary containment to collect any spills.*

2.) Thoroughly rinse the inside of the growth flask with ethanol (70:30 Vol% Ethanol: DI water). Swirl the ethanol in the flask in order to kill and remove bacteria cells. Transfer this waste liquid carefully into the waste container. Do not forget to recap the waste bottle.

3.) With the Distilled Water bottle, fill the growth flask 1/3 to 1/2 full and place the cap back on the flask. Make sure to fill to a level above original bacteria solution's level.

4.) Place the water-filled flask(s) in an autoclave bin. Do not crowd the bin; use multiple bins if necessary. Transport the bin and flasks to the autoclaves which are located on the second floor of Wartik and Fenske. Loosen the caps on the flasks until they rest gently on the top of the flask.
5.) Place the bin(s) in the autoclave and secure the door as tight as possible. Set the autoclave to the liquid cycle setting and sterilize time for 20 min. Start the autoclave.
6.) After 20 min, plus about 10 min to depressurize, remove the flasks and bin with the orange insulated gloves. (The autoclave will buzz for a few minutes after the cycle is finished. After the buzz stops, the door can then be opened.)

Caution Make sure the pressure gauge for the autoclave is resting at **zero** before opening the door. Always stand behind the door and open the door slowly and **carefully** to avoid a potential steam burn. When removing the autoclave bin, wear the orange autoclave gloves and be **careful** not to touch the inside of the autoclave or serious burns may result.

7.) Secure the caps on each flask. Then transport back to the lab for further washing.
8.) Place the bin beside the lab sink, uncap each flask, and **carefully** empty the **hot** liquid in the flasks down the drain with a continual flow of running water.
9.) Wash the inside and outside of each flask and cap with Alconox, rinse with tap water, and then rinse thoroughly with DI water. Any remaining residues could harm the next growth batch. Drain excess water from flasks.
10.) Securely fasten each cap, place in the autoclave bin, and transport for the last autoclave cycle. Place the bin and flasks in the autoclave, secure door, and autoclave for 20 min. on the dry cycle setting.
11.) Remove the bin and flasks, and finally wipe the outside of each flask with a paper towel to remove excess moisture. Store the sterile growth flasks in a dark, closed cabinet.

Glass Beaker Sterilizing and Washing

*Follow steps 1-9; however, use an aluminum foil cover in place of a cap. Also, the second autoclave cycle is not necessary.

Biohazard Waste Bag & Sharps Container Sterilization

1.) When the large or small Biohazard waste bags are full, twist closed and wrap autoclave tape tightly around the twisted end to ensure the bag remains closed.
2.) When either the large or small sharps containers are full, cap the lid and seal with autoclave tape to ensure the lid remains closed.
3.) Place in the large autoclave bin, and then autoclave for 20 min. on the liquid cycle setting. *Wartik's autoclaves sterilize most efficiently.*
4.) Remove the bin and bag **carefully** from the autoclave and place in the white Biohazard Waste can near the autoclave machines. ***Note cautions above for autoclave use.***

Biohazard Liquid Waste Sterilization

1.) When the Liquid Waste container is 3/4 full (not completely full or else the waste will boil over and the sterilizing process will not be as efficient), secure lid and place the container in the autoclave bin.
2.) Transport to autoclave and loosen the waste container lid to prevent an explosion or cracking in the container from the pressure build-up.
3.) Autoclave for 20 min. on the liquid cycle setting. *Wartik's autoclaves sterilize most efficiently*
4.) Remove the bin and waste container **carefully** from the autoclave. ***Note cautions above for autoclave use***
5.) Transport the bin and waste container back to the laboratory sink. Turn on the faucet for a steady flow of water. With the orange insulated gloves still worn, unscrew the waste container cap and pour the waste contents down the drain. Rinse the waste container with tap water from the faucet and then secure the cap and place the container back in a secondary bin for use.

C. Aseptic technique

"Louis Pasteur observed that once a medium is sterilized, it remains sterile unless contaminated from an external source. He used this observation to reject spontaneous generation but it also lays the foundation for sterile (or aseptic) technique. (1)"

1. Sterilize work surfaces
    a. Wipe surfaces with 70% ethanol and Kim wipes before and after use. This includes work benches but also bottles, caps, pipettors, and gloved hands.

   b. UV-sterilize the laminar flow hood regularly. Leave the UV lamp on for about 20 min with the sash fully closed. NOTE: UV sterilization only works at the surface level. Closed container contents will not be sterilized.
2. Use sterile instruments and media
   a. Use instruments (pipets, pipet tips, plates, etc.) that come sterile, or autoclave (20 minutes on liquid cycle), or flame sterilize (dip in ethanol and burn in flame). Mark autoclaved tips with autoclave tape.
   b. Follow the sterilizing and wash procedure for growth flasks and other glassware for bacteria procedures (e.g. test tubes for serial dilutions).
   c. Only autoclave containers that are less than ¾ full.
3. Keep containers closed
   a. Only open pipets and place tips on pipettor immediately before use. Set pipettor volume prior to tipping.
   b. Only keep pipet tip boxes open long enough to place tip on pipettor.
   c. Store media in the refrigerator and only open under the laminar flow hood for only the shortest time possible. (Recap before transfer.)
4. Do not lay down sterile objects
   a. Flame sterilize tweezers and glass spreaders before and after use. Do not lay these instruments during procedures.
   b. Avoid laying media bottle caps down.
   c. Do not lay sterile pipets down. If you touch a pipette to anything other than what you are working with, discard it.
5. It is recommended to use flame sterilization to ensure sterility
   a. Flame the opening of media bottles before and after transfers.
   b. Quickly flame pipet tips before use.
   c. Flame growth flask openings just before and making transfers.
6. Minimize drafts- no breathing, coughing, or talking over sterile materials and avoid fast movements and working in high traffic areas.
7. Think and prepare
   a. Mentally review the procedure and make sure you have everything you need before you start working. This prevents you from having to get up and prevents the agitation of the air surrounding your work area.
   b. Loosen all caps and arrange materials to ensure they are easily accessible.
8. Use the laminar flow hood.

D. CDC Description of Biosafety Level 1 and 2 and Necessary Precautions
http://www.cdc.gov/od/ohs/biosfty/bmbl4/bmbl4toc.htm

Biosafety Level 2 is similar to Biosafety Level 1 and is suitable for work involving agents of moderate potential hazard to personnel and the environment. It differs from BSL-1 in that (1) laboratory personnel have specific training in handling pathogenic agents and are directed by competent scientists; (2) access to the laboratory is limited when work is being conducted; (3) extreme precautions are taken with contaminated sharp items; and (4) certain procedures in which infectious aerosols or splashes may be created are conducted in biological safety cabinets or other physical containment equipment. The following standard and special practices, safety equipment, and facilities apply to agents assigned to BSL 2:

1. Standard Microbiological Practices
   a. Access to the laboratory is limited or restricted at the discretion of the laboratory director when experiments are in progress.
   b. Persons wash their hands after they handle viable materials, after removing gloves, and before leaving the laboratory.
   c. Eating, drinking, smoking, handling contact lenses, and applying cosmetics are not permitted in the work areas. Food is stored outside the work area in cabinets or refrigerators designated for this purpose only.

d. Mouth pipetting is prohibited; mechanical pipetting devices are used.

e. Policies for the safe handling of sharps are instituted.

f. All procedures are performed carefully to minimize the creation of splashes or aerosols.

g. Work surfaces are decontaminated on completion of work or at the end of the day and after any spill or splash of viable material with disinfectants that are effective against the agents of concern.

h. All cultures, stocks, and other regulated wastes are decontaminated before disposal by an approved decontamination method such as autoclaving. Materials to be decontaminated outside of the immediate laboratory are placed in a durable, leak-proof container and closed for transport from the laboratory. Materials to be decontaminated off-site from the facility are packaged in accordance with applicable local, state, and federal regulations, before removal from the facility.

i. An insect and rodent control program is in effect.

2. Special Practices

a. Access to the laboratory is limited or restricted by the laboratory director when work with infectious agents is in progress. In general, persons who are at increased risk of acquiring infection, or for whom infection may have serious consequences, are not allowed in the laboratory or animal rooms. For example, persons who are immunocompromised or immunosuppressed may be at increased risk of acquiring infections. The laboratory director has the final responsibility for assessing each circumstance and determining who may enter or work in the laboratory or animal room.

b. The laboratory director establishes policies and procedures whereby only persons who have been advised of the potential hazards and meet specific entry requirements (e.g., immunization) may enter the laboratory.

c. A biohazard sign must be posted on the entrance to the laboratory when etiologic agents are in use. Appropriate information to be posted includes the agent(s) in use, the biosafety level, the required immunizations, the investigator's name and telephone number, any personal protective equipment that must be worn in the laboratory, and any procedures required for exiting the laboratory.

d. Laboratory personnel receive appropriate immunizations or tests for the agents handled or potentially present in the laboratory (e.g., hepatitis B vaccine or TB skin testing).

e. When appropriate, considering the agent(s) handled, baseline serum samples for laboratory and other at-risk personnel are collected and stored. Additional serum specimens may be collected periodically, depending on the agents handled or the function of the facility.

f. Biosafety procedures are incorporated into standard operating procedures or in a biosafety manual adopted or prepared specifically for the laboratory by the laboratory director. Personnel are advised of special hazards and are required to read and follow instructions on practices and procedures.

g. The laboratory director ensures that laboratory and support personnel receive appropriate training on the potential hazards associated with the work involved, the necessary precautions to prevent exposures, and the exposure evaluation procedures. Personnel receive annual updates or additional training as necessary for procedural or policy changes.

h. A high degree of precaution must always be taken with any contaminated sharp items, including needles and syringes, slides, pipettes, capillary tubes, and scalpels.

i. Needles and syringes or other sharp instruments should be restricted in the laboratory for use only when there is no alternative, such as parenteral injection, phlebotomy, or aspiration of fluids from laboratory animals and diaphragm bottles. Plasticware should be substituted for glassware whenever possible.

ii. Only needle-locking syringes or disposable syringe-needle units (i.e., needle is integral to the syringe) are used for injection or aspiration of infectious materials. Used disposable

needles must not be bent, sheared, broken, recapped, removed from disposable syringes, or otherwise manipulated by hand before disposal; rather, they must be carefully placed in conveniently located puncture-resistant containers used for sharps disposal. Non-disposable sharps must be placed in a hard-walled container for transport to a processing area for decontamination, preferably by autoclaving.

iii. Syringes which re-sheathe the needle, needleless systems, and other safety devices are used when appropriate.

iv. Broken glassware must not be handled directly by hand, but must be removed by mechanical means such as a brush and dustpan, tongs, or forceps. Containers of contaminated needles, sharp equipment, and broken glass are decontaminated before disposal, according to any local, state, or federal regulations.

i. Cultures, tissues, specimens of body fluids, or potentially infectious wastes are placed in a container with a cover that prevents leakage during collection, handling, processing, storage, transport, or shipping.

j. Laboratory equipment and work surfaces should be decontaminated with an effective disinfectant on a routine basis, after work with infectious materials is finished, and especially after overt spills, splashes, or other contamination by infectious materials. Contaminated equipment must be decontaminated according to any local, state, or federal regulations before it is sent for repair or maintenance or packaged for transport in accordance with applicable local, state, or federal regulations, before removal from the facility.

k. Spills and accidents that result in overt exposures to infectious materials are immediately reported to the laboratory director. Medical evaluation, surveillance, and treatment are provided as appropriate and written records are maintained.

l. Animals not involved in the work being performed are not permitted in the lab.

3. Safety Equipment (Primary Barriers)

a. Properly maintained biological safety cabinets, preferably Class II, or other appropriate personal protective equipment or physical containment devices are used whenever:

i. Procedures with a potential for creating infectious aerosols or splashes are conducted. These may include centrifuging, grinding, blending, vigorous shaking or mixing, sonic disruption, opening containers of infectious materials whose internal pressures may be different from ambient pressures, inoculating animals intranasally, and harvesting infected tissues from animals or embryonate eggs.

ii. High concentrations or large volumes of infectious agents are used. Such materials may be centrifuged in the open laboratory if sealed rotor heads or centrifuge safety cups are used, and if these rotors or safety cups are opened only in a biological safety cabinet.

b. Face protection (goggles, mask, face shield or other splatter guard) is used for anticipated splashes or sprays of infectious or other hazardous materials to the face when the microorganisms must be manipulated outside the BSC.

c. Protective laboratory coats, gowns, smocks, or uniforms designated for lab use are worn while in the laboratory. This protective clothing is removed and left in the laboratory before leaving for non-laboratory areas (e.g., cafeteria, library, administrative offices). All protective clothing is either disposed of in the laboratory or laundered by the institution; it should never be taken home by personnel.

d. Gloves are worn when hands may contact potentially infectious materials, contaminated surfaces or equipment. Wearing two pairs of gloves may be appropriate. Gloves are disposed of when overtly contaminated, and removed when work with infectious materials is completed or when the integrity of the glove is compromised. Disposable gloves are not washed, reused, or used for touching "clean" surfaces (keyboards, telephones, etc.), and they should not be worn outside the

lab. Alternatives to powdered latex gloves should be available. Hands are washed following removal of gloves.

4. Laboratory Facilities (Secondary Barriers)
   a. Provide lockable doors for facilities that house restricted agents (as defined in 42 CFR 72.6).
   b. Consider locating new laboratories away from public areas.
   c. Each laboratory contains a sink for hand washing.
   d. The laboratory is designed so that it can be easily cleaned. Carpets and rugs in laboratories are inappropriate.
   e. Bench tops are impervious to water and are resistant to moderate heat and the organic solvents, acids, alkalis, and chemicals used to decontaminate the work surfaces and equipment.
   f. Laboratory furniture is capable of supporting anticipated loading and uses. Spaces between benches, cabinets, and equipment are accessible for cleaning. Chairs and other furniture used in laboratory work should be covered with a non-fabric material that can be easily decontaminated.
   g. Install biological safety cabinets in such a manner that fluctuations of the room supply and exhaust air do not cause the biological safety cabinets to operate outside their parameters for containment. Locate biological safety cabinets away from doors, from windows that can be opened, from heavily traveled laboratory areas, and from other potentially disruptive equipment so as to maintain the biological safety cabinets' air flow parameters for containment.
   h. An eyewash station is readily available.
   i. Illumination is adequate for all activities, avoiding reflections and glare that could impede vision.
   j. There are no specific ventilation requirements. However, planning of new facilities should consider mechanical ventilation systems that provide an inward flow of air without recirculation to spaces outside of the laboratory. If the laboratory has windows that open to the exterior, they are fitted with fly screens.

Preparing bacteria for experimentation

A. Revive bacteria

(*Overnight cultures should be grown only from a previously-tested bead or glycerol stock that was grown from a single colony or from a single colony on a fresh plate.*)from culture bead:

1. Transfer 30 mL growth media into 50-mL autoclaved flask with sterile pipet.
2. Raise cane of cryogenic vials from storage vessel. Use blue cryogenic glove if necessary. Vials of culture beads are labeled. Set vial on hood surface.
3. Sterilize tweezers over gas flame.
4. Take a culture bead out of its vial and drop it into the flask of media with the sterilized tweezers.
5. Securely seal the vial and place back in storage. Do not allow thawing.
6. Cap & label the flask and place on incubated shaker overnight (~16-20 hours) at proper growth temperature and 150 rpm.
7. Sterilize tweezers again.

from glycerol stock, replace bead steps 1 – 7 with:

3. Set vial from cryogenic storage vessel on hood surface and let the frozen stock melt. Rubbing the vial between hands makes this happen faster.
4. Transfer 600 μL of the liquid stock into the 30 mL of media using an autoclaved pipet tip.
5. Dispose of the vial in a biohazard container.

from glycerol stock, another alternative is to replace bead steps 1 – 4 with:

1. Transfer 2 mL growth media into 15-mL sterile growth tube with sterile pipet.
2. Raise cane of cryogenic vials from storage vessel. Vials of culture beads are labeled. Set vial on hood surface.
3. Uncap the frozen liquid stock and scrape a small amount of ice from the surface of the culture using a sterile pipet tip.
4. Place the pipet into the culture tube or streak out onto a prepared plate.

*Note: The thaw method is often intended for glycerol working stocks from -20 °C storage while the scrape method is more intended for glycerol reserve stocks from -80 °C.
from a single colony on a fresh agar plate, replace bead steps 1 – 5 with:

1. Transfer 2 mL growth media into 15-mL sterile growth tube with sterile pipet.
2. Open lid to plate and carefully scrape a colony off the agar surface using an autoclaved pipet tip.
3. Drop the tip into the media.

B. Grow bacteria

(*Cells revived overnight are in late log - stationary phase. Cells for experiments should be in mid-log phase to ensure that all cells are dividing so a transfer is necessary.*)

1. Transfer 100 mL media into 250-mL autoclaved flask with sterile pipet.
2. Temper the broth for 15 – 30 minutes by placing in the incubator.
3. Add 1 mL of revived cells using autoclaved pipet tip or 1 mL sterile pipet.
4. Place flask on incubated shaker table at 150 rpm and harvest at mid-exponential time (concentration ≅ 10^8 cells/mL).

Media preparation

Procedure Time: 1 h + cooling time

1. Measure out appropriate mass of powdered broth.
2. Pour into a media bottle (either orange or purple capped).
3. Fill the bottle with DI water to the appropriate volume.
4. Cap tightly and mix thoroughly by shaking and inverting vigorously. (It helps to have some water in the bottom of the bottle before adding the dry powder to avoid clumping and sticking to the bottom.)
5. Place a piece of autoclave tape on the bottle.
6. Immediately after preparing, autoclave on liquid cycle for 20 minutes with the cap loosened.
7. Remove from autoclave and allow it to cool a bit under the flow hood before storing in the refrigerator with tightened cap and labeled.
8. Important notes:
    a. Never fill the media bottle more than ¾ full (adjust masses accordingly) for effective autoclaving.
    b. Avoid contamination. Always store autoclaved media in refrigerator and only open under laminar flow hood to keep sterile. Only place sterile pipets and pipet tips into media. Keep cap in hand or set top down if necessary. The bottle should be uncapped only for the minimum amount of time possible. For added sterility, flame the opening of the bottle before and after inserting a pipet.
    c. Before use, check for contamination of the media by gently swirling and watching for cloudiness. It is also a good idea to incubate a tube of only media during growth as a contamination control.
    d. Concentrated solutions of media (or media ingredients) can be made and then diluted before autoclaving. This is especially helpful when small masses are required. Just remember that with PBS, diluting 100mM IS PBS solution to 10mM PBS is not a simple dilution. A 10x 10mM PBS solution needs to be made for a direct dilution.

C. Wash & load bacteria

(*The cells are washed before experimentation to replace the growth medium with fresh growth media, a salt solution with no nutrients to arrest growth, or a buffered solution to control pH. Cell concentration can also be adjusted at this time.*)

1. Harvest cells at the mid-exponential point of growth, as determined by growth curve.
2. Wash the cells in the appropriate suspending medium (e.g., PBS)
    a. Place a given volume of bacteria broth solution in centrifuge tube by pipetting from culture flask and cap. NOTE: For BSL 2 bacteria (***B. cepacia*** and ***P. aeruginosa***), all opening of containers and transfer of liquid must be done under laminar flow hood. Bacteria of BSL 1 can be worked with on a bench top.
    b. Turn on and open centrifuge and remove metal cover.
    c. Place tube in centrifuge, being sure to balance the centrifuge.
    d. Replace centrifuge cover, close centrifuge, and begin centrifuging (5000 rpm (= 3,000 g) for 10 minutes).

e. At end of cycle, remove centrifuge tube carefully, making sure to not disrupt the pellet that has formed. Pipet the supernatant out into biohazard liquid waste container, again being careful not to disrupt the pellet. NOTE: If BSL 2, this is done under the laminar flow hood.
f. Pour fresh media into the tube and cap.
g. Vortex tube until the pellet is resuspended.
h. Repeat steps c-g twice more.
i. Resuspended bacteria solution is now ready for experimental use.

3. To load an electrophoresis cell, first make sure the cell has been appropriately cleaned (sonicated, acid soaked, and rinsed with deionized water) and contains no leaks.
   a. Check that the valves on the cell are closed and fill both sides of electrophoresis cell with bacteria solution to about the middle of the ground glass fittings.
   b. Carefully place appropriate electrodes (one by one) into ground glass fittings creating an airtight fit. Catch excess bacteria solution that may escape from cell as the electrodes are inserted by holding a paper towel to the openings. Clean any surfaces or gloves with ethanol afterwards.
   c. The loaded cell is now ready for experimentation. Now that it is sealed, it is safe to work with outside the laminar flow hood.
4. To load a capillary, first make sure it is properly cleaned (sonicated in a beaker with Alconox and deionized water solution, acid soak, and rinsed with deionized water) and secured to microscope slide with silicone sealant or paraffin wax.
   a. Pipet roughly 30 μL of bacteria solution at the edge of one capillary opening. Allow capillary action to draw the fluid into the capillary. Add more solution, if necessary, to fill capillary completely.
   b. Wipe any excess solution from slide.
   c. Capillary cell is now ready for experimentation.
   d. Dispose of slides in biohazard sharps container.
5. Other possible experimental holders are the focht chamber, well-plates and test tubes.

Cryopreservation

(*In cryopreservation, cells are preserved by cooling to low sub-zero temperatures at which biological activity stops. The use of a cryoprotectant is necessary to avoid cell damage by ice formation upon freezing.*)

A. Initial notes
   1. Reserve or working stock bacteria solutions of *Escherichia coli, Bacillus. subtilus, Burkholderia cepacia*, and *Pseudomonas aeruginosa* may be obtained from the Logan lab in the Sackett Building (Civil and Environmental Engineering). The *Vibrio fischeri* stock originated from the ATCC.
   2. Prepare a frozen stock of newly acquired or created strains as soon as possible.
   3. Overnight cultures (grown to late-log / early stationary phase) should be grown only from a single colony on a fresh plate or from a previously-tested glycerol stock that was grown from a single colony.
   4. Always prepare more than 1 vial of frozen stock. To ensure the genetic stability of a culture, the number of passages from the original must be minimized.
   5. Use aseptic technique. You do not want to your stocks contaminated!
   6. The level of liquid nitrogen in the LN2 tank must be checked every week. If the level is low, then order more through the open account with Messer.
   7. If not storing in liquid nitrogen but rather a sub-zero freezer, first flash freeze the vials of cells in liquid nitrogen before placing in the freezer. Sub-zero freezers are also available for use in the Cirino laboratory.

B. Culture bead preparation
   1. The Microbank storage vials are located in the Extra Bio Supplies cabinet underneath the primary laboratory bench in Rm. 178.
   2. With a marker, label the vials as desired (one organism per vial): organism, date, and initials. While labeling, avoid exposing the vials to direct light sources for any length of time.
   3. Other than labeling, all other handling of the vials should be completed under the sterile laminar flow hood to avoid contamination.

4. Prepare an overnight culture of the desired organism.
5. Unscrew the cap of a vial and transfer about 850 μL of bacteria cells from the growth flask with a sterile pipet into the vials (enough to fill the vial).
6. After transfer, close the vial tightly, and gently invert 4-5 times to emulsify the organism. **Do not vortex**. At this stage, the cells should be attached to the porous beads.
7. Next, unscrew the vial cap, and then with a pipet fitted with a sterile tip, remove all the liquid present in each vial. Excess liquid causes clumping when the vials are frozen. Dispose of excess liquid in a waste container.
8. Repeat steps 5-9 if making multiple vials.
9. Tightly secure the vial caps and store in the liquid nitrogen tank.

C. Glycerol stock preparation

(*Most strains of bacteria can be stored for one to two years in glycerol solution at -20 °C. At -80 °C they can be stored almost for life time. It is preferred to store working stocks at -20 °C and archives at -80 °C.*)

1. Prepare glycerol
    a. To measure out 100% glycerol, use a syringe, the balance, or heat and pipet.
    b. Autoclave (20 min liquid cycle) a glycerol solution that is no more than 80% glycerol in DI water. Solutions greater than 80% are viscous and difficult to work with.
    c. Allow to cool.
    d. Dispense the sterile glycerol solution into sterile cryovials using a sterile pipet tip. An alternative is to dispense non-sterile glycerol solution into non-sterile vials and autoclave together. The final glycerol concentration after adding cells should be 20%.

*Note: Vials of sterilized glycerol can be prepared in batches ahead of time and stored at room temperature until required.

2. Label the vials.
3. Pipet the necessary volume of an overnight culture of cells into each vial to achieve the 20% glycerol concentration. Mix by pipetting a few times.

    *Note: some protocols recommend using overnight cultures while others suggest to check the absorbance of the overnight culture and adjust to 0.4 – 0.6 by diluting and growing up for at least 20 minutes more so that the cells are in the exponential phase of growth yet have a high enough concentration for good revival.
4. Cap and vortex each vial after adding the cells to evenly disperse the glycerol.
5. Allow the cells to equilibrate with the glycerol at least 15 minutes but no more than 45 minutes. The vials can also be labeled during this time.

*Note: some protocols omit this equilibration step.

6. Freeze.

Growth Curves

(*Growth curves are performed to determine the mid-exponential phase growth time for each organism under specific growth conditions*)

Procedure Time: 4+ h (end at start of stationary growth phase)

1. Start an overnight culture of cryopreserved cells in the appropriate medium.
2. After the cells are revived, transfer 1 mL into 100 mL fresh, tempered media and incubate the flask at the appropriate growth temperature and shaking at 150 rpm. This is the start of the growth curve.
3. Zero the spectrophotometer with a cuvette of fresh, tempered media. (λ = 600nm, or the wavelength where maximum absorbance is achieved in the spectra.)
4. Every 20 minutes transfer a sample of growing cells into a cuvette using aseptic technique to avoid contamination. Record the time and absorbance. Return the sample to flask to avoid loosing too much volume.
5. Continue absorbance measurements until the exponential phase of growth ends. This is the point on the growth curve (log abs (or abs on a log scale) versus time) where the linear exponential phase steadies out .
6. To determine the mid-exponential time, find the start and end of the exponential phase, calculate the middle time, and add the lag phase time to obtain the total time to mid-exponential growth phase time.

7. To determine the doubling time, divide the log of 2 by the slope of the linear exponential phase.

Actual cell counts

(*A viable count or microscopy total count is necessary to determine the number of cells the absorbance at mid-exponential growth phase time actually represents.*)

A. Plate count (viable count)

Procedure Time: 4 h prep + 1 h after incubation to read plates

1. Prepare agar plates
    a. Prepare media and add 15 g agar / L media before autoclaving.
    b. After autoclaving, set the media bottle under the flow hood and allow it to cool to the point where you are just able to touch it. Do not allow the agar to solidify (below 40 ^{o}C).
    c. Pour the media into plates (100x15mm) so that they are about 1/3 full (35-40 mL). Only lift the plate cover slightly above the plate.
    d. Recover and allow the plates to set.
    e. After the plates are set, if there is condensation on the agar surface, place the plates upside-down, tilted and resting on their covers, to allow the condensation to evaporate faster.
    f. Extra plates can be stored in the refrigerator. (Temper before use.)
    g. Rinse the media bottle right after it is emptied, before solidification.
    h. Label the bottoms of the plates with the desired identifications.
2. Prepare serial dilutions of the cell suspension
    a. Place 900 μL salt solution (PBS or NaCl or KCl) into small glass test tubes and autoclave covered with foil (or just make sure both are sterile).
    b. Add 100 μL of cells to the first test tube.
    c. Add 100 μL from the first tube into the second tube, and continue the serial 1/10 dilutions.
3. Prepare spread plates
    a. Pipet 100 μL of the desired dilution onto the center of one plate. For proper statistical analysis, plates containing between 30 and 300 colonies will give the most accurate results. It is recommended to plate the 3 dilutions that might achieve this and in triplicate.
    b. Flame sterilize a glass spreader by dipping into ethanol then passing through a flame to burn off the alcohol. Cool the spreader in the air or by touching it to the edge of the plate.
    c. Spread the inoculum over the surface gently with the cooled glass spreader. Be careful not to jab into the surface.
    d. Allowed the cells to be absorbed by the medium.
    e. Invert the plates and incubate upside-down (to avoid condensation from getting on the agar surface) at the necessary growth temperature.
    f. Incubate at least 24 hours and check for colonies. Incubate further until colonies have formed.
4. Count colonies
    a. Only count plates that contain 30 – 300 colonies. You can mark each colony with a marker to keep track of those counted.
    b. Each colony represents 1 colony forming unit (CFU), therefore 1 cell.
    c. Calculate #/mL the CFU, sample volume, and sample dilution.

B. Microscopy total count

Procedure Time: 2 h

(*Absorbance is also considered a “total count” since it does not discriminate between live and dead cells. This microscopic total count can be turned into a live count with the use of Live/Dead BacLight, a fluorescent product that stains live and dead cells differently.*)

1. Load cells into a capillary or hemacytometer.
2. Allow the cells to settle.
3. Observe under the microscope and count the cells in the frame.
4. Determine the number of cells / mL.

a. If using the hemacytometer, refer to the paperwork to find the size of the marked divisions
b. If using a capillary, use a micrometer image to determine the size of one frame and the capillary height is given on its container.

Acid cleaning of glass for use with bacteria experiments

1. Sonicate glassware in a beaker containing Alconox solution prepared with deionized (DI) water for 10 min.
   *Note: Do not allow sonicator bath water to enter the beaker. Use a larger beaker (1 or 2 L for the large sonicator) filled with DI water as secondary containment if necessary.
2. Rinse thoroughly with copious amounts of DI water. If cleaning capillaries, run water through capillaries.
3. Sonicate in 50% ethanol as described in step 1.
4. Rinse with DI water as described in step 2.
5. Soak in 6 M hydrochloric acid for at least 1 hour.
   * Note: Always pour acid into water, not water into acid.
6. Rinse in DI water as described in step 2.
7. Clean glassware can be stored in DI water until use.
8. Set cover slips on Kim wipes under the flow hood to dry. To dry capillaries, touch one end to a Kim wipe and pinch until all the water is wicked out.

Piranha etch of glass or silicon wafers

(*Respect Piranha. You must first be trained in its use and know the emergency procedures detailed in section E of this document. Emergency contacts are: EH&S (**5-6391**) (after hours **3-1111**) and **911**.*)

A. Preparation

1. Make sure substrates are clean and dry prior to placing in the Piranha bath.
   *Note: Piranha is to be used to remove **only** residual contamination and to hydroxylate the substrate surface.
2. Sonicate the substrates in a 1:1 mixture of ethanol and DI water for 5 minutes and thoroughly dry with either air or N_2.
3. Set up the Pyrex dishes that will contain the Piranha. These must be under the acid fume hood inside of a square Pyrex dish as secondary containment.
4. Label all these dishes clearly stating they contain Piranha.
5. Make a caution sign stating Piranha is in use under the hood, sign and date it, and tape it to the sash.
6. Determine exactly how much Piranha you will need and do not make extra.
   a. Use a Piranha solution of 3:1 (v:v) sulfuric acid (H_2SO_4) and hydrogen peroxide (H_2O_2).
   b. **Never** make a Piranha solution with more than 50% hydrogen peroxide since a severe explosion could occur.
   c. Only make as much Piranha as you will use. **Do not store**. Dispose of excess properly (see section C).
   d. Avoid making large volumes of Piranha. If the substrates are Petri dish bottoms then it is recommended to just etch the bottoms and not the entire dish.
7. Wear the proper personal protection equipment- **lab coat, acid apron, acid gloves, and acid goggles**.

B. Etching

1. Measure out the sulfuric acid and pour it into the Piranha container you will be doing your substrate cleaning in. Sulfuric acid is located under the acid fume hood.
2. Measure out the hydrogen peroxide and pour it into the sulfuric acid. Hydrogen peroxide is in the large refrigerator. **Always** add hydrogen peroxide to acid.
   *Note: An exothermic reaction immediately takes place (you will see gas emitted and the solution becomes hot). Always keep the hood sash down so it is between you and the solution.
3. Immediately place the substrate in the Piranha and leave it uncovered for 30 min.
4. After cleaning remove the substrate from the solution with tweezers and place in a DI water bath. Rinse very well with DI water.

C. Clean-up and waste disposal

1. The Piranha solution should not be hot after 30 minutes but be careful in case it is. If it feels warm then let it sit open until it cools.
2. Pour the solution into the bottle kept in the back left corner of the fume hood labeled Piranha waste. Use a funnel and keep the bottle in the back corner overnight **uncovered**.
3. Place the containers in a water bath and thoroughly rinse with DI water.
4. The next day pour the Piranha waste into the official waste bottle (labeled and located in the back left corner in the bottom of the hood). Overnight the Piranha should have finished giving off any gas, but do not tightly cap this official waste bottle, just in case.
   *Note: **Only** put acid Piranha waste in the acid Piranha waste container. Do not add any other acid waste or vary the sulfuric acid: hydrogen peroxide ratio greatly.
5. Do not fill the Piranha waste bottle into the neck of the bottle. Start another container and alert the safety officer (or EHS directly) to get a pick-up of the filled container.

D. Further notes
   1. The 3:1 sulfuric acid: hydrogen peroxide solution used for 30 minutes is a standard Piranha protocol.
      a. Other ratios can be used for different lengths of time and different temperatures.
      b. **Never** exceed 50% hydrogen peroxide.
      c. A heated base Piranha solution can be used (3:1 ammonium hydroxide: hydrogen peroxide). Store waste separately!
   2. If any other solutions (water, acids, bases, acetone, alcohol, or other organics) splash or spray into the Piranha the exothermic reaction will accelerate. Be very careful and do not leave wash bottles in the fume hood.
   3. Only make as much Piranha solution as necessary.
      a. Do not store Piranha.
      b. Dispose of excess as stated above.

E. Emergency steps for exposure
   1. Have someone contact EH&S (**5-6391**) (after hours **3-1111**) and **911**.
   2. Skin contact-
      a. Leave the area and go under a safety shower.
      b. Remove all contaminated clothing and rinse skin at least 15 min.
   3. Eye contact-
      a. Irrigate eyes for at least 15 minutes at the eyewash keeping eyelids apart and away from eyeballs.
      b. Place ice pack on eyes until reaching emergency room.
   4. Inhalation burns the upper respiratory tract but symptoms may be delayed (coughing and/or tightness in chest).
      a. If conscious, get assisted into an area with fresh air and seek medical attention.

Focht chamber (Bioptechs' parallel plate flow chamber)

A. Assembly (refer to Focht chamber diagram on next page)
   1. Turn the top of the chamber (white) upside-down. Place the upper gasket (.75mm thick) into the recess while aligning the perfusion clearance holes with the perfusion tubes.
   2. Place the micro-aqueduct slide on the upper gasket so that it is aligned with perfusion tubes (grooved side up). Do not force the slide down on the tubes.
   3. Place the lower gasket (0.1mm - 1.0mm thick) onto the micro-aqueduct slide and press around the perimeter creating a seal. These gaskets can be ordered with custom shapes. A convenient one has the following rectangular geometry: 0.25 mm high × 3.0 mm wide × 22 mm long.
   4. Perfuse some media through the perfusion port producing a bead on the surface of the slide to displace air trapped in the line.
   5. Lower the cover slip (40 mm diameter) onto the bead until it is resting on the gasket.
   6. Place the closure assembly on top of this stack while aligning the black electrical connector with the oval slot in the chamber top. Maintain a gentle pressure while turning the chamber over so that it is right side up then can observe as the four paws engage the top through the depressions about the perimeter. Turn the large knurled ring counter-clockwise until tight (yes, lefty-tighty in this case). This will symmetrically tighten and seal the chamber.

B. Mounting
1. The chamber can now be mounted onto the microscope adapter and setting in place with the screw.
2. Place on the microscope stage, fitted with the special chamber stage plate.
3. Attach perfusion tubing to the inlet and outlet ports of the chamber. Bioptechs recommends 1/16" Tygon #2275 tubing for best biocompatibility and ease of use. Generic silicone tubing is fine.
4. Check for bubbles & leaks when initially flowing sample through. It may be necessary to reconnect tubing if bubbles do exist or to take apart & repeat assembly if leaking.
5. The vertical portion of the drain tubing which extends down from the stage if using a waste receptacle will create a siphon and form negative pressure in the chamber. This negative pressure will cause the cover slip to flex. This can be eliminated by breaking the siphon at a point equal to the height of the specimen with a "T" fitting.
6. Keep the pump as close to the chamber as possible and tubing lengths as short as possible. Also locate at or slightly above the level of the chamber. Tape down tubing so it remains steady.

C. Break-down
1. Remove assembly from the microscope stage and its adapter plate. Replace the custom stage plate with the regular slide plate.
2. Rotate the large knurled ring in the base of the chamber clockwise (yes, righty-loosey) until it stops. This will release and disengage the chamber top.
3. If using temperature control, hold the white portion of the chamber while simultaneously (using thumb and forefinger) rotating CCW the two smaller knurled nuts located on either side of the black electrical contact unit. This will remove the black portion which contains sensitive electronics so that they can remain dry.
4. Remove the rest of the component.

D. Clean-up
1. The closure assembly (metal part) and power/sensor connector do not come into contact with the specimen and should only be cleaned with a damp cloth or alcohol wipe. DO NOT immerse either one in liquid.
2. Cover slips and gaskets should be hand cleaned and short-cycle autoclaved before use. Do not use alcohol on gaskets.
3. The white plastic (Delrin) portion of the FCS2 will be in fluid communication with the specimen and can be autoclaved at 120°C for 15 minutes.
4. Tubing and fittings can be autoclaved as well.

Microscope Use Instructions

(*The Nikon manual is also a good reference for microscope use.*)

1. Turning on the microscope:
1. Flip the power switches “ON” which are found on the two grey power supplies located near the microscope. One is power to the microscope and the other to the stage.
2. Make sure the power adapter for the camera is plugged in.
3. Press the power buttons on both the television and DVD player if intending to view the images on a monitor.
4. Push in the dia-illumination switch (white button on left side) for the light bulb to turn ON.
5. Rotate the brightness adjustment dial, located under the dia-illumination switch (white button), clockwise until the optimum brightness for viewing is reached.

2. Placing a sample on the stage and focusing:
1. Tilt the upper half of the microscope (condenser, dia-illuminator) back to easily maneuver the sample on the stage by loosening the knob which is located on the back of the microscope in the middle of the arm that extends upward.
2. Turn the turret which holds the objectives until the desired objective is directly under the stage and locked into the optical path.
3. If using an objective requiring oil or water, carefully place one drop of oil or water on the lens. If necessary, use lens paper to wipe off excess liquid without touching the lens.
4. Take the prepared slide and invert it before placing it into the designated indentation on the stage plate and fastening with the spring-loaded clamp.

5. Use the joystick to position the objective below the desired viewing section on the slide.
6. Use the coarse focus knob to lower the stage in order to roughly focus the slide image. If using the objectives requiring a liquid, lower the stage until the liquid touches and noticeably disperses on the slide.
7. Move to section 3 if the microscope's field of view is not adjusted correctly.
8. Then, on the right side of the remote control pad, adjust the fine focus knob until the sample is clearly visible.
9. Adjust the brightness to properly brighten the image
10. With the joystick, move the stage to view the entire sample. The black vertical button to the left of the joystick adjusts the maximum stage speed. Pressing once reduces the speed to 25% of the maximum, pressing a second time increases to 50% of the maximum, and a third time returns to 100% speed. This cycle can be repeated by continually pressing the button.

3. Kohler Illumination:

(*Kohler Illumination is important to achieve uniformly bright images without glare. If using DIC, fluorescence, or laser trapping, Kohler Illuminate first.*)

1. While looking into the eyepiece tube, turn the optical path switch-over dial located on the right side until some light is seen through the eyepiece (Port 1 is the eyepiece and Port 5 is the camera).
2. Center the condenser by lowering the field diaphragm lever (F-stop) on the dia-illuminator until the field diaphragm image, which appears as a stop sign, is in view.
3. Adjust the condenser focus knob to bring the "stop sign" image into focus.
4. Then, turn the two condenser centering screws to center the field diaphragm image in the field of view.
5. Adjust the condenser aperture diaphragm by moving the lever just above the condenser to the left or right. Narrowing (to the left) decreases illumination and brightness while increasing contrast and depth of focus.
6. Finally, move the field diaphragm lever on the dia-illuminator until the field diaphragm image is the same size as the view field.
7. Return to Section 2, Step 8.

4. Using Differential Interference Contrast Attachment (DIC):

(*Differential interference Contrast illuminates transparent subjects through the generation of different levels of light intensity which create a 3-D effect.)*

1. Follow microscope use steps 1-3 first.
2. In the microscope parts and accessories drawer near the microscope, locate the DIC prism (known as Wollaston or Nomarski prisms) which corresponds to the objective in use: 100x, 40x, 20x, etc.
3. Remove the plastic spacer which rests beneath objective, a part of the turret. Fully insert the DIC prism into the turret beneath the desired objective.
4. Next, adjust the DIC module which is attached to the condenser turret which is located directly above the condenser lens. Rotate the module until it clicks into place at the appropriate module setting. (When not using DIC, the module setting will be set at A.) The module setting depends upon the objective numerical aperture. For the 100x Oil Immersion Objective, the ∞ H module setting is used. For the 40x, 20x, and 10x objective, the ∞ M module setting is used (H denotes high magnification and M medium magnification).
5. Then, beneath the objective turret, directly above the right port, fully slide the T-A analyzer until it reaches the second click stop position in order to bring the analyzer into the optical pathway. The vibration direction lever, on the far right end of the T-A analyzer, should be centered. On the old microscope this is kind of hidden below the filter holder slider on the right side below the objective turret.
6. Finally, slide the polarizer (just above the condenser) fully to the left. The polarizer rotation lever may be adjusted to further fine tune the contrast of the illuminated subject. Lining up the dot mid-way between the left-most mark and the center mark is usually good.

5. Shut Down

1. Push in the dia-illumination switch (white button on the left side) for the light bulb to turn OFF.

2. Tilt the upper half of the microscope (condenser, dia-illuminator) back to easily remove the sample from the stage by loosening the knob which is located on the back of the microscope in the middle of the arm that extends upward.
3. Use the coarse focus knob to lower the stage until fully lowered to prevent scratching of the lens when removing the slide.
4. Press the spring-loaded clamp to release the slide from the designated indentation on the stage plate and remove the slide. Dispose of the slide in the broken glass container, or if bacteria was used, in the Biohazard Sharps container.
5. If using an oil objective, use lens paper to clean the excess oil. Be careful to avoid touching the lens of the objective.
6. Restore the upper half of the microscope from the tilted position and tighten the knob on the back of the middle arm of the microscope.
7. Flip "OFF" the power switches on the two grey power supplies located near the microscope. One is power to the stage and the other to the microscope.
8. Press the power buttons on the television and DVD player to turn off.
9. When the microscope has cooled, place the microscope cover carefully over the microscope to prevent dirt and dust from affecting the scope.
10. Make sure any filters used for DIC, fluorescence, or laser trapping are removed.

6. Lens cleaning
    1. Occasionally the camera lens (or other) will have to be cleaned. Cleaning will help eliminate spots on images.
    2. Blow with dust free air from a can.
    3. Fold lens paper to create a folded edge that is a little longer than the size of the optic.
    4. Put 100% ethanol or acetone onto the paper swab.
    5. Wipe with one continuous motion.
    6. Repeat and apply pressure to remove stubborn spots.
    7. Gently dry with air can, aiming short gentle bursts away from the surface and only around the outer casing.
    8. Call Nikon for further cleaning. Routine servicing should be scheduled each year.
7. Image capturing
    1. Scion image
        a. Open Scion image. Select the LG camera if on the old microscope.
        b. Go to "Special" and select "Start Capturing".
        c. The light may need to be turned up.
        d. To save a single frame
            i. Go to "File" and "Save as" to save the current frame.
            ii. Alternatively, go to "Edit" and "Select all" and then go to "".
        e. To save a stack of frames
        f. To integrate an image over some time
    2. DVD
        a. Turn on the TV and DVD recorder.
        b. Insert a DVD (+R for the new microscope, -R for the old microscope).
        c. Select the desired recording quality by scrolling through the record times.
        d. On the remote press "Monitor" if on the new microscope or "Return" if on the old microscope to get the camera feed.

            *Note: Occasionally the feed channel needs to be set on the DVD recorder on the new microscope. To do so, press "monitor" then press the channel up button until CAM1 is selected.
        e. Hit record on the DVD recorder.
        f. Press pause to pause recording or stop to end a chapter on the DVD.
        g. New chapters can be added to DVDs that are not filled for subsequent experiments.
        h. To be able to play the DVD in a computer it must first be finalized. Descriptive names can be assigned to chapters before this. Once finalized, no more recording can be done on the DVD.

3. Making a clip from a DVD using Dazzle Movie Maker
    a. Turn on the TV and DVD recorder and insert the desired DVD.
    b. Make sure Dazzle is plugged in.
    c. Open Movie Star. There is an icon on the desktop.
    d. Click on the still camera image on the right of the window if taking 1 frame, or the video camera image if taking a clip.
    e. Movie Star should now show what is playing on the TV. If not, then restart the computer.
    f. Click the camera on the desired frame, or the record and stop button on the desired frames.
    g. Copy the clip from Movie Star's directory on the left of the window.

8. Stage controller commands and programming

(*The Prior manual gives good details starting on p 33 on using general commands and programming the stage controller*)

1. Open the stage controller program prior.ht with the stage on. The icon is on the desktop.
2. Useful commands (commands and arguments are separated using a space, comma, semi-colon, tab, equals, colon, or equals):
    a. Carriage return <cr>- reports the stage position in x,y,z
    b. O speed% <cr>- sets the stage speed. Enter speed percentage values 1-100.
    c. O no argument <cr>- reports the joystick speed. Includes button speed (see step 10 in the focusing section) so that if the button speed is at 50% and O is set to 50 then a value of 25 is reported.
    d. G x,y,z <cr>- "Go" moves the stage to an absolute position x,y,z. Z is optional.
    e. GR x,y,z <cr>- "Go relative" moves the stage by the amount specified by x,y,z (in microns). Z is optional.
    f. K <cr>- an emergency stop. Mechanical inertia may result.
3. Programming the stage
    a. COMP 0 <cr>- sets the controller compatibility mode to standard.
    b. MACRO <cr>- starts recording program code
    c. GR x,y,z <cr>- Go relative, in microns
    d. WAIT t <cr>- stage movement pauses for time in milliseconds
    e. Continue program
    f. MACRO <cr>- runs through the program one time
    g. Using the SOAK command rather than MACRO will repeatedly loop the program and report the number of complete cycles on each pass. Stop a SOAK program by entering an action. The current cycle will complete and then stop.

Laser trap alignment

(*The laser can damage the eyes and skin. Wear the green laser goggles at all times while the laser power is up. Close the all shades and doors and warn others in the lab that the laser is on and to put on goggles. Do not place hands in the laser path.*)

1. Set up the laser on the optical table behind the microscope.
2. Turn the key on the power supply to the laser ¼ turn to the right and allow to warm-up.
3. During warm-up, turn on the microscope and Kohler illuminate with the 40× objective in place (no DIC).
4. Remove the 40× objective.
5. Tilt the condenser arm up.
6. Pull out the dichroic filter by pulling out the filter holder on the right under the objective turret on the old microscope to the "DK" position or by turning the wheel on the left just below the objective turret and behind the yellow filter holder cover to position #1.
7. Make sure that the epi-port is open, either by removing the tape (old microscope) or moving the lever under the objective turret from C to O (new microscope).
8. Make sure the eyepiece port is closed and 100% of the light is entering the camera.
9. Turn on the laser (push in the red "on/off" button on the power supply).

10. Bring power up to 60 mW (7.9% total power) by slowly turning the knob on the power supply. The power will go up slowly at first and then faster as it gets higher. With the camera feed going to the TV, the laser spot should become visible (if almost centered).
11. Center the laser by adjusting it left and right (by hand) and up and down (by turning the knob on its stand.
12. If having troubling aligning, use the photosensitive cards. First hold the card up to the epi-port and make sure the laser is entering centered. Once properly adjusting the laser, then hold the card to the objective hole and make sure the laser spot circular and centered. Continue with increasingly larger magnification objectives.
13. Put the beam expander on the optical table in between the laser and the back of the microscope. Gently tighten the screws that clamp down on it. Align it to maximize the spot on the monitor. Again, use the photosensitive cards to make sure the beam expander is aligned by holding the cards up to the entrance of the beam expander, the epi-port, the objective hole, and finally objectives, adjusting the beam expander at each step.
14. Insert the filter in the camera port during experimentation to save the life of the camera.
15. After experimentation, turn down the laser power and turn off with the red button.
16. Leave the power supply on for 10 extra minutes to allow for cool-down. Then turn the key ¼ turn to the left to completely shut down.
17. Remove the beam expander and recap everything so the lenses do not get dusty or scratched.
18. Close the epi-port and remove the filter from the camera port.

Adherence To Hydrocarbons (ATH) Test

1. Use borosilicate glass test tubes (12 x 75 mm) with caps, cleaned according glass cleaning SOP.
2. Rinse the test tubes with the media of interest. The results will vary depending on ionic strength so use the same conditions you have in your experiments, e. g. 100mM PBS.
3. Suspend your colloidal sample (cells or particles) in media to the desired concentration and pipet 1.3 mL into each test tube.
4. Add 0.3 mL of hydrocarbon to each test tube. I use n-hexadecane.
5. Cap the test tubes and vortex each for 2 min on setting 5.
6. Allow the vortexed test tubes to rest for phase separation, about 15 min.
7. After phase separation, prepare your sample for the spectrophotometer.
    - Carefully transfer 1 mL of the aqueous phase (the denser phase) using a long-tipped pipet tip or needle into a cuvette.
    - Dilute with 3 mL of media to fill the cuvette if using large-volume cuvettes.
8. For the blank, use the same concentration of colloids prepared in step 3. Place 1 mL of it into a cuvette and dilute as in step 7 if necessary.
9. Measure absorbance at 600 nm (or the wavelength for maximum absorbance as determined by the spectra) to calculate the fraction of sample removed to the hydrocarbon phase, and thus hydrophobicity.

*Make sure all substances are at the same temperature.

*This protocol may be modified, but the key is to be consistent between batches. Results will vary with colloidal concentration, aqueous volume, hydrocarbon volume, and vortexing.

Laminar flow hood use

(*"The most important part of a laminar flow hood is a high efficiency bacteria-retentive filter. Room air is taken into the unit and passed through a pre-filter to remove gross contaminants (lint, dust etc). The air is then compressed and channeled up behind and through the HEPA filter (High Efficiency Particulate Air filter) in a laminar flow fashion. That is, the purified air flows out over the entire work surface in parallel lines at a uniform velocity. The HEPA filter removes nearly all of the bacteria from the air. (2)" *) Laminar flow hoods:

1. provide clean air to the working surface area.
2. provide a constant flow of air out of the work area to prevent room air from entering.
3. remove contaminants introduced into the work area by personnel by suspending in air flow out from the hood.

are <u>not</u> to be used as a fume hood since exhaust goes into the room.

1. Leave the hood on. If turned off for any reason, it should be on for at least 30 minutes and thoroughly cleaned before reusing.
2. Rinse gloved hands with 70% ethanol before entering the hood. It is also recommended to wear long sleeves to minimize the shedding of skin into the work area. Open cuffs allow the entrapment of contaminated air between the wrist and forearms and the inside sleeves, which can then be introduced into the work area. Avoid abrupt movements or wear fitted cuffs.
3. Clean the hood before use by wiping with alcohol. (The plastic sides and glass sash should also be cleaned periodically.) To UV sterilize, turn on the UV lamp with the sash down for about 20 min.
4. Place desired objects into hood
    a. Wipe down all objects to be placed under the hood to remove excess dust.
    b. Keep instruments at a comfortable distance from the opening of the hood.
    c. Wait 5 min before beginning work under the hood to allow sufficient time for the ultra-clean air passing over the work area to remove airborne contamination, especially particulate matter from the newly introduced items.
    d. Outer pouches and wraps should be removed at the edge of the work area as the sterile contents are pulled into the work area. Do not set the wrappings down in the flow hood.
5. Perform work under the flow hood carefully
    a. Make sure the hood is uncluttered and that nothing obstructs the vents
    b. The bottom of the sash should be at armpit level.
    c. Conduct work as far into the work area as possible, at least 4" from the front grill.
    d. Keep hands within the cleaned area of the hood as much as possible. Do not touch hair, face or clothing.
    e. Do not allow hands to obstruct airflow around the openings of sterile containers.
    f. Avoid disruptive air currents
        i. Make sure you have everything you need before you start working to avoid repeatedly getting up.
        ii. Keep coughing, quick movements, talking, etc. to a minimum.
        iii. Try to keep the working area away from drafts, traffic, and excessive activity.
        iv. Avoid the use of an open flame inside the cabinet, as it disrupts the air.
6. Clean up after yourself
    a. Remove items and make sure it is not left cluttered.
    b. Wipe down with ethanol.
    c. Leave flow hood on.

1. Fankhouser, D. 2001. Sterile technique: Delivery of liquids by pipet. In University of Cincinnati Clermont College.
2. McAuley, D. 2005. Aseptic technique. In Global RPH.

Appendix C

Magnetic Separation for *In situ* Environmental Remediation of Polycyclic Aromatic Hydrocarbons*

This study examines the use of polymer coated magnetic particles to sequester polycyclic aromatic hydrocarbons (PAH) from the environment for subsequent removal via magnetic interactions. Polystyrene particles were able extract only 5% of a 0.1 mole fraction non-aqueous solution of naphthalene in hexadecane. Removal of magnetic particles from columns of PBS liquid media using a neodymium magnet showed very good agreement with a model of the magnetic removal that predicted positive particle velocities down to a depth of 4.6 cm. Particle removal decreased from 91% in a PBS column to 57% in sand. Particle removal from sand was improved by insertion of an iron rod into the column. This magnetic well assisted technique resulted in 65% particle removal. Another modification coined magnetic barrier assisted particle removal employed a steel wool filter in the sand column. The steel wool filter alone achieved 59% particle removal. If the steel wool filter was magnetized by application of the magnet, removal increased to 93%. With such modifications, *in situ* remediation via magnetic separation could be a viable technology.

* Parent comprehensive project.

1. Introduction

Polycyclic aromatic hydrocarbons (PAHs) are a group of compounds that enter the environment through the combustion of organics from both natural events (such as brush fires) and human activities (such as fuel combustion)[1]. PAHs have been detected in air, soil, sediments, water, and foods. Data detailing the effects of human exposure to a single pure PAH are limited. However, many different PAHs cause cancer to exposed laboratory animals and extrapolated estimates suggest the compounds are also human carcinogens[2]. Although direct human exposure to PAHs from aquatic and soil sources is not a major concern, PAHs accumulate in the food chain and are released into the atmosphere during clean-up activities. Freshwater amphipod survival is reduced from 100% in a sand control to 0% in East River, New York sediments, due to PAH contamination[3]. PAH remediation costs and time can range from $75/t soil for 4 months with soil washing (a New Jersey Superfund site), to $340/t soil for 18 months with thermal desorption (a Michigan Superfund site), to $14/1000 gal water at an on-going operation using pump-and-treat technology, (US DOE Kansas City plant)[4].

Due to the hydrophobic nature of PAHs, the contaminants tend to accumulate in sediments and soils, deposited there either from the air or from sources leaking petroleum[1]. PAHs partition to hydrophobic soil particles and pores and non-aqueous phase liquids (NAPLs) from which removal is difficult. Certain bacteria and fungi are able to degrade PAHs, but because of the contaminant's affinity for natural sequestration it has a low bioavailability[5].

To increase the bioavailability of PAHs and thus render the persistent environmental contaminant degradable, we investigate the use of polymer encapsulated magnetic particles to sequester and remove PAHs from soils and waters with a magnetic separation technique. Magnetic separation is a technology that has been implemented since 1970 when it was first applied in the ceramics industry to remove mineral impurities from kaolin slurry[6]. Since then

magnetic separations have been considered for the removal of radioactive elements[7], toxic metals[8], phosphates[9], and viruses[10] from waste streams.

High-gradient magnetic separation (HGMS) is the magnetic separation technique most commonly studied for use in contaminant collection. The high processing rates and simplicity HGMS offers has made it an attractive approach[11]. Briefly, in HGMS a waste stream flows through the bore of a magnet (an electromagnet[6] or a permanent magnet[12]) that is packed with a large pore volume magnetic matrix (such as stainless steel wool[6]) where contaminants collect via attractive magnetic forces. It is the magnetic matrix that causes the high gradients in the applied magnetic field. If HGMS is applied to polluted soil then the soil must first be transported to the processing plant and suspended in an aqueous phase (and subsequently recovered from the aqueous phase after treatment)[13]. If the contaminant is not naturally magnetic then the waste stream is first seeded with magnetic carriers to which the contaminants sorb[13]. The matrix material needs to be cleaned intermittently at which point the magnetic carriers can be recycled[14].

In addition to the essential magnetic separation items– the magnetic carrier and the magnet, magnetic separations for soil or water remediation would also require excavators and transportation machinery to transport the contaminated soil or water to an off-site processing plant, suspension and recovery of the soil in an aqueous phase, and processing equipment such as tanks, mixers, and pumps. Excavation costs alone can total $\$150/yd^3$ for site preparation, excavation, transportation, and backfilling[15]. Removal also disrupts the local ecosystem and causes contaminant loss to the atmosphere[3]. In situ magnetic separation for remediation of soil or water would avoid these disadvantages, but does not exist and has never been applied. We investigate the possibility of implementing magnetic separations for in situ remediation of PAHs from soil and water both as a stand-alone process and also in conjunction with other in situ remediation technologies currently in use. Specifically, permeable reactive barriers and

recirculation wells seem amenable to being combined with or modified to include magnetic separations for enhanced remediation.

We begin by measuring the ability of polymer encapsulated particles to adsorb the PAH naphthalene from a non-aqueous phase. We then address three in situ magnetic separation schemes: 1) stand-alone magnetic particle removal from water and from soil, 2) magnetic well assisted magnetic particle removal, and 3) magnetic barrier assisted magnetic particle removal. Ultimately these techniques could serve to increase PAHs bioavailability for enhanced in situ bioremediation and to remove PAHs without excavation for further treatment off-site.

2. Materials and Methods

2.1. Naphthalene sequestration from a non-aqueous phase

Particle solutions containing 0, 10^6, or 10^8 particles/mL were made in 10 mM phosphate buffered saline (PBS) of pH 7.3. The particles were carboxyl hydrophobic polystyrene microspheres of 3.2-μm diameter (Interfacial Dynamics). Solutions with a 0.1 mole fraction of naphthalene in hexadecane were made by heating to 50^{o}C to fully dissolve the naphthalene. A maximum mole fraction of 0.17 can be achieved with naphthalene dissolved in hexadecane[16] so an intermediate mole fraction of 0.1 was chosen. Five milliliters of the naphthalene solution were added to 15 mL of aqueous particle solution in glass vials, which were then capped and agitated at 150 rpm. Removal of naphthalene from hexadecane by the particles was measured by sampling the hexadecane phase at different times, filtering to remove any particles, and measuring absorbance with a UV-visible light spectrophotometer (Helios) at λ = 317.5 nm. A calibration was conducted by obtaining absorbance measurements for dilutions of the 0.1 mole fraction naphthalene solution with 0 set as pure hexadecane. Each sample's absorbance was compared to the original 0.1 mole fraction naphthalene in hexadecane solution to calculate the fraction of naphthalene removed.

2.2. Soil column preparation

White quartz sand particles (Sigma-Aldrich #274739) 210-300 μm in diameter were used as model soil. The sand was prepared by sonicating in deionized (DI) water for 1 h, rinsing every 10 min. It was then soaked in 10% sulfuric acid on a 180 rpm shaker for 3 h after which it was rinsed with copious amounts of DI water. The porosity θ, which is the ratio of the void volume to the total volume in a column of soil, was measured as $\theta = 0.44 \pm 0.02$ by filling a graduated cylinder with dry sand to 7 mL, adding 10 mL water, and measuring the total volume.

The sticking coefficient α, which is the ratio of the number of times a particle attaches to a sand grain to the number of times a particle comes into contact with a sand grain, was calculated as $\alpha << 0.01$, based on the DLVO theory[17].

$$\alpha = 2a_p\kappa \exp\left(\frac{-\psi_{\max}}{k_B T}\right) \qquad (1)$$

a_p is the particle radius, κ is the inverse Debye length, ψ_{max} is the potential energy at the secondary minimum based on the DLVO theory, k_B is the Boltzman constant, and T is temperature. The Hogg-Healy-Fuerstenau formula for spheres was used to calculate the electrostatic potential and the Lifshitz theory for the van der Waals potential to determine ψ_{max}. The sticking coefficient was also verified experimentally. The clean sand was pipetted into a 10-mL plastic syringe to a height of 5 cm. After rinsing the column with 10 mL 10 mM PBS media, 10 mL of the 10^6 particles/mL solution was pumped at a flow rate of 4 mL/min into the column and the effluent was collected for analysis. The sand was also sampled at 1-cm depths and sonicated to remove any attached particles. After allowing the sand to separate by gravity the samples were observed using a Nikon TE 300 Eclipse inverted optical video microscope with a 20× objective. Images were captured with a CCD camera and Scion Image Acquisition Software

(Scion Corporation). After settling through the 200-μm high capillary holder, particles were counted and averaged over 10 frames that were 282 × 212 μm.

These measurements (Figure 1) allowed for calculation of N/N_o (the number of particles exiting a length of the column over the number of particles initially entering the column), and thus the sticking coefficient α based on the Rajagopalan and Tien (RT) model of particle transport through porous media[18].

$$\alpha = \frac{-2\ln\left(\frac{N}{N_o}\right)a_c}{3(1-\theta)L\eta_{RT}} \qquad (2)$$

The soil radius is represented by a_c, the column length by L, and η_{RT} is the collector efficiency, which is a function of the particle diffusion, interception, and settling[19].

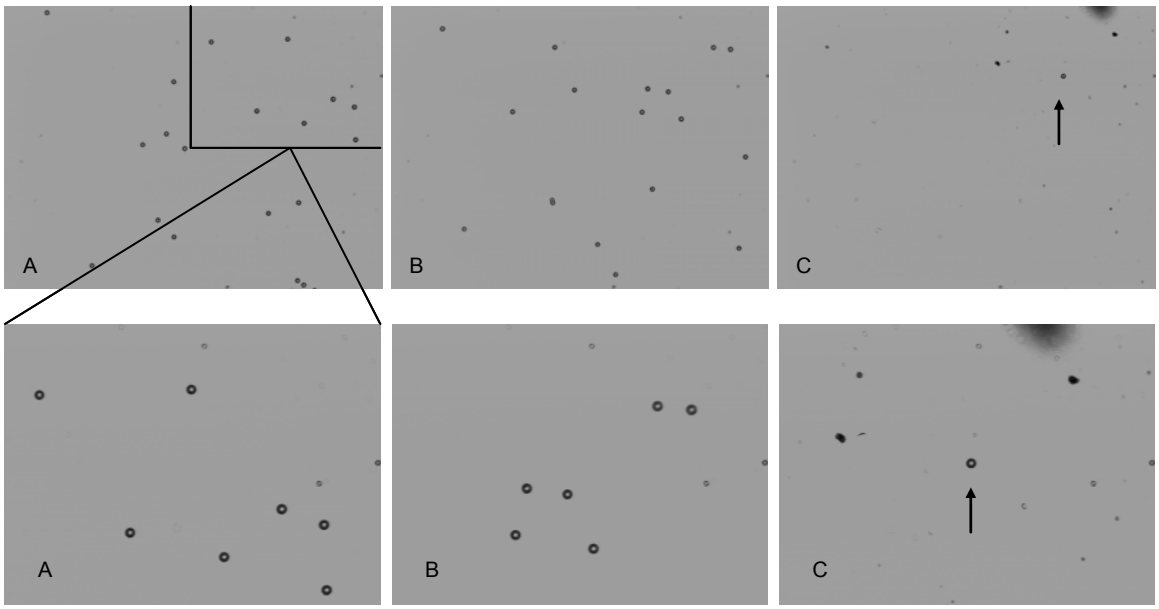

Figure 1. Sample images captured to calculate N_o from the initial particle solution (A) and N from the particles in the effluent (B). Also shown is an image of particles that remained in the column attached to the sand at a depth of 5 cm that were removed by sonication for analysis (C). The lower images are cropped to show only the upper right quarter of one frame. The entire frames show N/N_o = 18/19 and the 1 particle that remained in the column (at arrow) as well as a few debris particles from the sand. These are 1 of 10 frames taken for each the influent, effluent, and sand samples for this particular run.

2.3. Magnetic removal of particles

Polymer encapsulated spherical superparamagnetic particles of 2.8-μm diameter, 11.4% magnetite, and 1200 kg/m^3 density were purchased from Bangs Laboratories. A 10^6 particles/mL solution of these magnetic particles in 10 mM PBS was transferred to a 100-mL graduated cylinder to heights of 2, 5, 10, 15, and 20 cm. A neodymium (Nd) cylindrical magnet (K & J Magnetics) 25.4 mm in diameter and 25.4 mm in length was covered with tape so that any magnetic particles attracted to the magnet could be easily removed. The magnetic field of this magnet at a distance of 5 cm is 100 G, as measured by a gaussmeter (AlphaLab). The magnet was placed in the graduated cylinder at a depth where it was just in contact with the particle solution. After 5 min the magnet was removed and the particle solution was mixed and sonicated. The decrease in particle concentration was determined with a UV-visible light spectrophotometer and verified with a direct count under 20× magnification as described above.

Magnetic particle removal from PBS was also measured on a microscopic scale in a capillary with dimensions 2 × 0.2 × 68 mm. The capillary was cut to a length of 68 mm to accommodate the constraints of the microscope stage plate. Once filled with a 10^6 magnetic particles/mL solution, the capillary was secured in a vertical position and the Nd magnet was placed on top. After 30 min the magnet was removed and the capillary was carefully transferred to a glass slide where particle concentration at each centimeter was determined under 20× magnification as described above.

The magnetic removal of particles from the sand column was tested by filling a 10-mL plastic syringe that was cut to a height of 5 cm with the prepared sand and then 10^6 particles/mL solution. The Nd magnet was placed on the top of the column for 30 min. Afterwards, the sand was sonicated to remove any attached particles and allowed to separate by gravity. The solution was imaged under 20× magnification and the particles were counted as described above. The

magnetic well condition involved inserting an iron nail into the syringe before filling with the sand. For the magnetic barrier condition, the sand column was placed horizontally rather than vertically. The syringe was cut in half length-wise to make a trough. A magnetic filter of steel wool was placed centrally and the column was filled with the sand. The 10^6 particles/mL solution was pumped in at 4 mL/min, either with the Nd magnet placed on the steel wool or without the magnet, until the column was full. The 2 cm before, at, and after the filter were sampled and analyzed as described above.

3. Results and discussion

3.1. Contaminant sequestration

The contaminant sequestration experiments did not show a large removal of naphthalene from the non-aqueous phase using polystyrene particles (Figure 2). After 76 h the particles were able to remove 5% of the naphthalene.

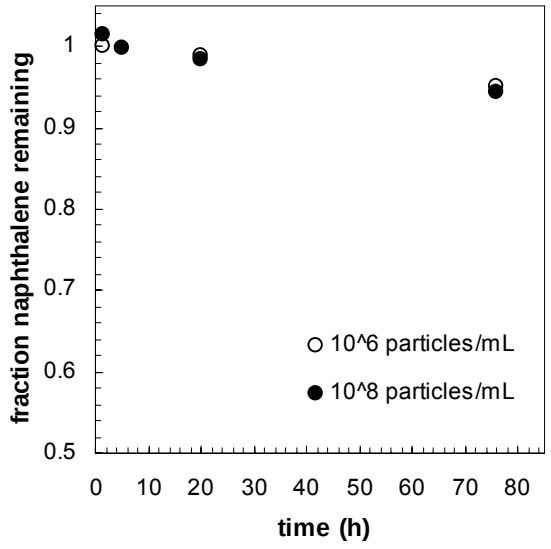

Figure 2. Removal of naphthalene from the non-aqueous phase (hexadecane). Samples of a 0.1 mole fraction of naphthalene in hexadecane solution were added to aqueous particle solutions of varying concentration (10^6 particles/mL– open circles, 10^8 particles/mL– closed cirlces) and allowed to shake for varying time. The 0 particles/mL data are not shown because there was not enough phase separation after shaking to sample and analyze the non-aqueous phase.

The overall concentration of naphthalene in the sample was over 10,000 ppm by mass. Menzie et al. compile data on environmental PAH concentrations from literature and monitoring programs and report a median PAH concentration of 1.4 ppm by mass in sediment[20]. The sequestration experiment should be repeated with lower naphthalene concentrations to test particle saturation limits. In special cases however, PAH contamination can be orders of magnitude larger. The PAH concentration at a Superfund site in Brainerd/Baxter, Minnesota was measured as 70,633 ppm by mass[1], a concentration that these particular polystyrene particles would not be able to remove. The original idea was that naphthalene would sequester to the polystyrene via hydrophobic interactions. The actual hydrophobicity of the particles needs to be determined, which can be accomplished using an adherence to hydrocarbons (ATH) test, a technique previously used by our group[21].

A few authors have recently focused on developing novel techniques to sequester PAHs using various substances such as aspen wood fiber[22], cyclodextrins[23], and amphiphilic polyurethane[24,25]. Functionalizing magnetic particles with these substances should be investigated for effective sequestration of PAHs and subsequent magnetic removal. Magnetic particles can be synthesized with various coatings such as titania and polystyrene[26,27], and silica[28], so we are not limited by the types of particles offered commercially.

3.2. Magnetic removal of particles

The forces acting on a particle in a column with a magnet are a magnetic force F_M, a gravitational force F_G, and a hydrodynamic force F_H.

$$F_M + F_G + F_H = 0 = \frac{2a_m{}^3 \chi_p \mu_f m^2}{\pi d^7} - \frac{4}{3}\pi a_p{}^3 (\rho_p - \rho_f) g - 6\pi\eta a_p U \qquad (3)$$

a_m represents the radius of the magnetic material in the particle (not to be confused with the total particle radius a_p), χ_p is the magnetic susceptibility of the particle's magnetic material, μ_f is the

magnetic permeability of the media, m is the magnetic moment of the Nd magnet, d is the distance between the Nd magnet and the particle, ρ_p and ρ_f are the densities of the particle and of the media, g is gravitational acceleration, η is media viscosity, and U is particle velocity. The expression for the magnetic force was derived from Maxwell equations[29]. Velocity can be determined as a function of d since all other parameters are known constants based on the experimental set-up. Gathering the constant terms in the magnetic force expression, $F_M = C/d^7$ and $C = 9.2\times10^{-24}$ Nm^7. Based on this value, the distance where particle velocity is zero is calculated as 4.6 cm. *U(d)* can be used to calculate particle displacements from various distances for different magnet interaction times (Figure 3).

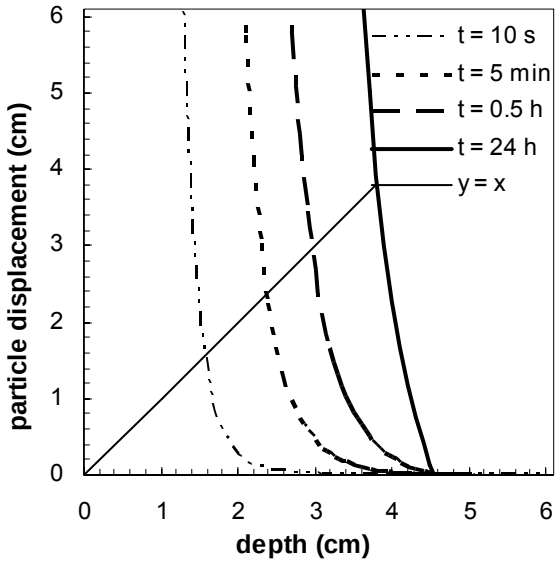

Figure 3. Model of particle ($\chi_p = 20$) movement from various depths in a column with a magnet (m = 12 J/T) held at 0 cm. The intersection of the y = x and model curves represents the depth above which particles are fully removed.

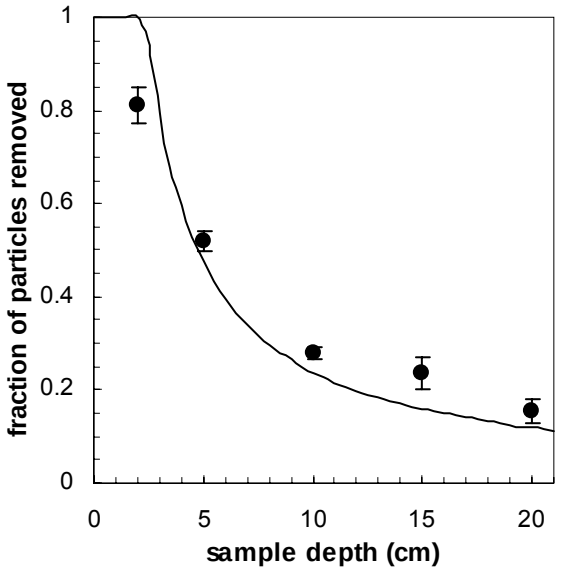

Figure 4. Removal of the polymer encapsulated magnetic particles from PBS media in a 100 mL cylinder using an Nd magnet for 5 min. The sample depth indicates the height of the column of solution (and thus the farthest distance of a particle from the magnet). Each point is the average of three repeats and error bars indicate standard error. The solid line represents the results based on the model calculations described above and is not a fitted curve.

The magnetic removal of particles was measured on both a bulk scale (Figure 4) and a microscopic scale (Figure 5). It should be noted that these two measurements are not exactly analogous and the axes on Figures 4 and 5 have slightly different meanings. For the bulk experiments, (Figure 4), a sample depth of 2 cm refers to a column of particle solution that was 2 cm deep, a sample depth of 5 cm refers to a column of particle solution that was 5 cm deep, and so on. The fraction of particles removed in the bulk experiments was measured from the total solution. The bulk experiment results show slightly better removal than predicted by the model (Figure 4), suggesting the estimated magnetic force constant *C* is actually slightly larger.

The capillary experiments (Figure 5) measured the fraction of particles removed from a particular depth in column, not from the total sample.

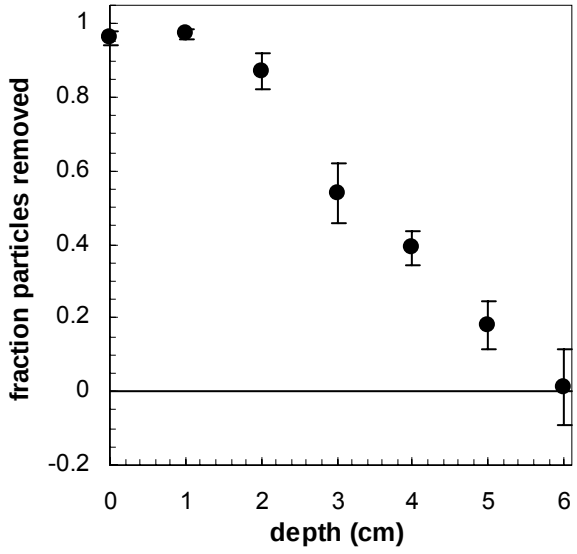

Figure 5. Removal of the polymer encapsulated magnetic particles from PBS media in a 27 μL capillary using an Nd magnet for 30 min. Each point is the average of four repeats and error bars indicate standard error.

It is expected that Figure 5 show a dip to 0 particles removed at the d = 4.6 cm point based on the model calculations (U = 0 at 4.6 cm). This is not seen, but removal was not measured at that exact depth and also that trend may be hidden in the averaging. It is possible for the fraction of particles removed to be less than 0 as is seen in the 6 cm point error bars (Figure 5). At depths greater than 4.6 cm, particle velocity is negative meaning particles are falling. The particle concentration can therefore increase at the bottom of the column, which is manifested in a negative removal fraction.

To test the applicability of magnetic separation for in situ remediation, the removal of magnetic particles from sand columns was examined and compared over five cases (Figures 6, 7).

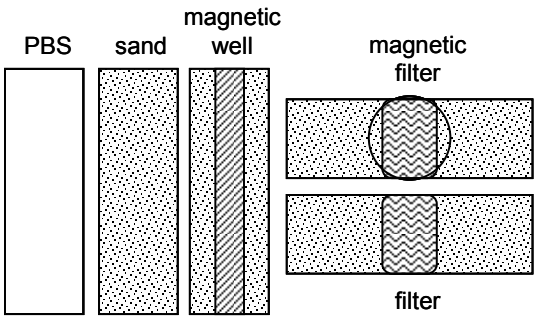

Figure 6. Depiction of magnetic removal techniques. There are two stand-alone magnetic particle removal methods, from either PBS or sand columns. Magnetic well assisted particle removal uses an iron rod inserted down the depth of the column of sand. The filter conditions have horizontal flow through steel wool, with out and with the magnet placed on top of the steel wool filter.

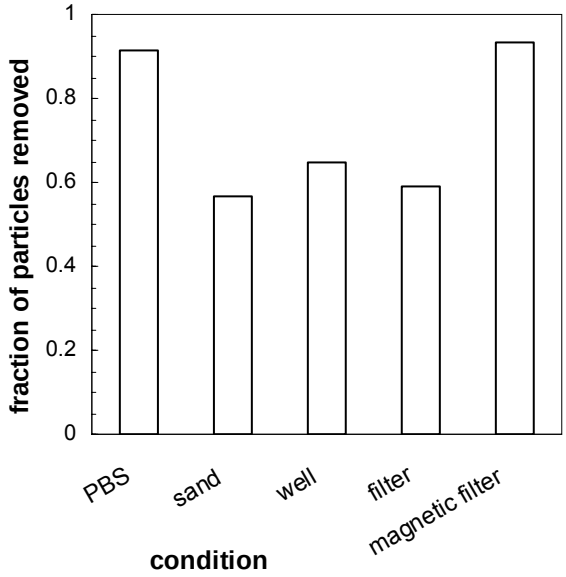

Figure 7. Comparison of magnetic removal techniques. The first three bars use vertical columns 5 cm deep with 30 min Nd magnet application. The filter conditions have horizontal flow of magnetic particles through the steel wool filter at 4 mL/min until the column is filled. Particle concentration is 10^6 particles/mL for all methods. The results are based on one run and repeats need to be conducted for statistics.

Particle removal decreases from 91% in PBS to 57% in sand (Figure 7). An explanation is hindered particle transport through soil. Transport through the soil was modeled based on the RT model (Equation 2). The sand used in the experiment is categorized between medium and fine sized, so for our 2.8-μm diameter particles the model predicts an *N/No* between 0.92 and

0.96, implying most of the particles should be able to freely transport through the column. The model parameters used to calculate *N/No* may be incorrect. Also, the RT model does not take into account tortuosity, which may affect transport.

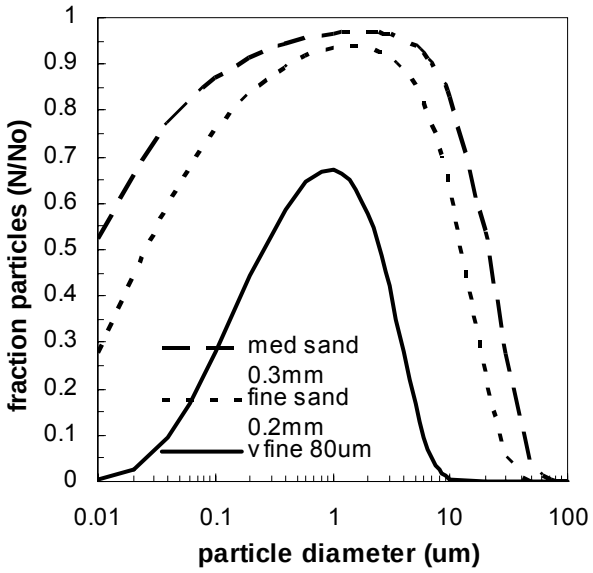

Figure 8. Model of particle transport through very fine (full line), fine (small dashes), and medium (large dashes) sized sand. The results are based on model parameters that match the experimental conditions.

The insertion of an iron rod to act as a magnetic well shows an 8% improvement in particle removal from the pure sand column (Figure 7). A larger improvement might be expected, but a quick test of the magnet and rod revealed the magnetic field is strong only axially, and weak transverse to the rod axis. A new rod modified with another magnetic material (such as the steel wool for example) that disrupts the axial magnetic field lines should show improvement, able to gather more particles in the transverse direction. The steel wool filter is able to remove 59% of the incoming particles from the column, but with the addition of an Nd magnet to magnetize the filter, removal improves to 93% (Figure 7).

4. Conclusion

We have hypothesized that polymer encapsulated magnetic particles can be employed for in situ remediation of PAHs. The particles failed to successfully sequester our model contaminant naphthalene, however other particle coatings besides polystyrene have promise. Magnetic removal of the particles was possible from limited distances in both water and soil media. Modifications to the magnetic removal system, such as magnetic well or filter assistance, can improve particle recovery. The technique could be beneficial since it avoids site excavation, improves bioavailability for bioremediation, is amenable to other contaminants via different particle surface modification, and allows for particles reuse after recovery. Particle design, contaminant sequestration, transport through soil, and magnetic interactions must be further considered before this interesting technique could be successfully applied.

Acknowledgement

This research was funded by the National Science Foundation through NSF CRAEMS grant CH3-0089156.

Appendix

Nomenclature

a_c	radius of soil grain (collector) (m)
a_m	radius of magnetic material (m)
a_p	radius of total colloidal particle (m)
d	separation distance of magnet and particle (m)
F_G	gravitational force (N)
F_H	hydrodynamic force (N)
F_M	magnetic force (N)
g	gravitational acceleration (m/s^2)
k_B	Boltzman constant (J/K)
L	length of column (m)
m	magnetic moment of magnet (J/T=J·A·m/N=A·m^2)
N	particle concentration (#/mL)
N_o	initial particle concentration (#/mL)
T	temperature (K)

U	velocity of particle (m/s)
α	sticking coefficient (dimensionless)
χ_p	magnetic susceptibility of particle (dimensionless)
η	viscosity of medium (Pa·s)
η_{RT}	efficiency of collector soil grains (dimensionless)
κ	inverse Debye length (m^{-1})
μ_f	magnetic permeability of medium ($T \cdot m/A = N/A^2$)
θ	soil porosity (dimensionless)
ρ_f	density of medium (kg/m^3)
ρ_p	density of particle (kg/m^3)
ψ_{max}	potential (J)

References

1. Juhasz, A. L., and R. Naidu. 2000. Bioremediation of high molecular weight polycyclic aromatic hydrocarbons: a review of the microbial degradation of benzo[a]pyrene. International Biodeterioration and Biodegradation. 45:57-88.
2. Hertel, R. F. 1998. Selected non-heterocyclic polycyclic aromatic hydrocarbons. World Health Organization, Geneva.
3. Tabak, H. H., J. M. Lazorchak, L. Lei, A. P. Khodadoust, J. E. Antia, R. Bagchi, and M. T. Suidan. 2003. Studies on bioremediation of polycyclic aromatic hydrocarbon-contaminated sediments: bioavailability, biodegradability, and toxicity issues. Environmental Toxicology and Chemistry. 22:473-482.
4. Khan, F. I., T. Husain, and R. Hejazi. 2004. An overview and analysis of site remediation technologies. Journal of Environmental Management. 71:95-122.
5. Hatzinger, P. B., and M. Alexander. 1997. Biodegradation of organic compounds sequestered in organic solids or in nanopores within silica particles. Environmental Toxicology and Chemistry. 16:2215-2221.
6. Oder, R. R. 1976. High gradient magnetic separation theory and applications. IEEE Transactions on Magnetics. 12:428-435.
7. Nunez, L., B. A. Buchholz, and G. F. Vandegraift. 1995. Waste remediation using in situ magnetically assisted chemical separation. Separation Science and Technology. 30:1455-1571.
8. Benjamin, M., et al. 1982. Removal of toxic metals from power-generation waste streams by adsorption and coprecipitation. Journal of the Water Pollution Control Federation. 54:1472.
9. Shaikh, A. M. H., and S. G. Dixit. 1992. Removal of phosphate from waters by precipitation and high gradient magnetic separation. Water Research. 26:845-852.
10. Bitton, G., and R. Mitchell. 1974. The removal of Escherichia coli bacteriophage T7 by magnetic filtration. Water Research. 8:549.
11. De Latour, C. 1973. Magnetic separation in water pollution control. IEEE Transactions on Magnetics. 9:314-316.
12. Ebner, A. D., and J. A. Ritter. 2004. Retention of iron oxide particles by stainless steel and magnetite magnetic matrix elements in high-gradient magnetic separation. Separation Science and Technology. 39:2863-2890.
13. Macasek, F., J. D. Navratil, and S. Dulanska. 2002. Magnetic sorbent for soil remediation- a waste for waste treatment. Separation Science and Technology. 37:3673-3692.
14. Kurinobu, S., J. Uesugi, Y. Utumi, and H. Kasahara. 1999. Performance of HGMS filter and recycling of magnetic seeding material on magnetic seeding method. IEEE Transactions on Magnetics. 35:4067-4069.

15. City of Shelton, Connecticut web site. July 2005. Planning level remediation cost estimate- soil removal- Farmer's Market. <http://www.cityofshelton.org/pdf/grant/Techvarletter%20Att2%20Costs.pdf>.
16. Bernardez, L. A. and S. Ghoshal. 2004. Selective solubilization of polycyclic aromatic hydrocarbons from multicomponent nonaqueous-phase liquids into nonionic surfactant micelles. Environmental Science and Technology. 38:5878-5887.
17. Pontius, F. W., ed. 1990. Water Quality and Treatment, 4th ed. McGraw-Hill, New York. Chapter 6.
18. Rajagopalan, R. and C. Tien. 1976. Trajectory analysis of deep-bed filtration with the sphere-in-cell porous media model. AICHE Journal. 22:523-533.
19. Yao, K., M. T. Habibian, and C. R. O'Melia. 1971. Water and waste water filtration: concepts and applications. Environmental Science and Technology. 5:1105-1112.
20. Menzie, C. A., B. B. Potocki, and J. Santodonato. 1992. Exposure to carcinogenic PAHs in the environment. Environmental Science and Technology. 26:1278-1284.
21. Parent, M. E. and D. Velegol. 2004. E. coli adhesion to silica in the presence of humic acid. Colloids and Surfaces B. 39:45-51.
22. Boving, T. B. and W. Zhang. 2004. Removal of aqueous-phase polynuclear aromatic hydrocarbons using aspen wood fibers. Chemosphere. 54:831-839.
23. Badr, T., K. Hanna, and C. de Brauer. 2004. Enhanced solubilization and removal of naphthalene and phenanthrene by cyclodextrins from two contaminated soils. Journal of Hazardous Materials. B112:215-223.
24. Kim, J., C. Cohen, and M. L. Shuler. 2000. Use of amphiphilic polymer particles for in situ extraction of sorbed phenanthrene from a contaminated aquifer material. Environmental Science and Technology. 34:4133-4139.
25. Tungittiplakorn, W., L. W. Lion, C. Cohen, and J. Kim. 2004. Engineered polymeric nanoparticles for soil remediation. Environmental Science and Technology. 38:1605-1610.
26. Guo, H., X. Zhao, G. Ning, and G. Liu. 2003. Synthesis of Ni/Polystyrene/TiO2 multiply coated microspheres. Langmuir. 19:4884-4888.
27. Leun, D. and A. K. Sengupta. 2000. Preparation and characterization of magnetically active polymeric particles (MAPPs) for complex environmental separations. Environmental Science and Technology. 34:3276-3282.
28. Bruce, I. J., J. Taylor, M. Todd, M. J. Davies, E. Borioni, C. Sangregorio, and T. Sen. 2004. Synthesis, characterization and application of silica-magnetite nanocomposites. Journal of Magnetism and Magnetic Materials. 284:145-160.
29. Jackson, J. D. 1999. Classical Electrodynamics, 3rd ed. Wiley, New York.

VITA

Mary Elizabeth Parent

EXPERIENCE

Pennsylvania State University, University Park, PA, Ph.D. May 2007
Thesis in Chemical Engineering: "From Bacterial Adhesion to Biofilm Formation: Impact of Humic Acid and Quorum Sensing"

- Determined effect of humic acid on bacterial adhesion to silica.
- Modeled the diffusion of quorum sensing signals from bacteria.
- Determined if quorum sensing can occur locally in space and time.
- Determined if biofilm formation can occur locally in space and time.
- Techniques: bacterial cell culture and maintenance, microscopy, optical laser trapping, pN force measurements, nanofabrication.

Comprehensive Project, December 2005

- Created a novel *in situ* remediation technique using magnetic polymer particles to sequester and then remove hydrocarbon contaminants from environmental sites.
- Modeled magnetic removal and particle transport and then tested at lab-scale.
- Showed the design is not practical as a stand-alone method.

Publications & Presentations

- Parent & Velegol. Colloids and Surfaces B: Biointerfaces, 39:45-51 (2004).
- Oral presenter: ACS 232 & 229, ISABB 3, ECSS 9 & 8, MAPS 02/01/06.
- Poster presenter: GRC (Bacterial Cell Surfaces 2004), Grad Exhibit 19, ECSS 7.

Teaching Assistantships

- Design of Chemical Plants (CHE 470), Spring 2006.
- Chemical Engineering Lab (CHE 480), Spring 2004.

Energen, Inc., Billerica, MA, Engineering Internship, Summer 2001

- Implemented magnetostrictive technologies to design flow valves. This involved performing fluid mechanic calculations and creating AutoCAD drawings.
- Conducted force and displacement experiments to test magnetostrictive materials.

NAVC, Boston, MA, Fuel Cell Study Internship, Summer 2000

- Assisted in writing Future Wheels I, a publication on the use of fuel cells for transportation applications, submitted to DARPA.
- Developed a fuel cell information web page for the NAVC web site.

Rensselaer Polytechnic Institute, Troy, NY, B.S. in Chemical Engineering, May 2002

AWARDS

1st place presenter- PSU Environmental Chemistry Student Symposium, Spring 2006
Women in Engineering Program Travel Grant, Spring 2005
Gordon Research Conference Travel Award, Spring 2004
Harvey & Geraldine Brush Graduate Fellowship, Fall 2002-Spring 2003
GE Faculty for the Future Fellowship, Fall 2002-Spring 2003
Rensselaer Medal and Scholarship for Math and Science, Fall 1998-Spring 2002